DURABILITY ASSESSMENT OF JOINT ASSEMBLY FOR FIBERGLASS RESIN COATED CONCRETE CYLINDER PIPES

BY

MOHAMMED MOHAMMED HUSSEIN AL-THOLAIA

A Thesis Presented to the
DEANSHIP OF GRADUATE STUDIES

KING FAHD UNIVERSITY OF PETROLEUM & MINERALS
DHAHRAN, SAUDI ARABIA

In Partial Fulfillment of the
Requirements for the Degree of

MASTER OF SCIENCE

In

CIVIL ENGINEERING

JUNE, 2010

KING FAHD UNIVERSITY OF PETROLEUM & MINERALS
DHAHRAN 31261, SAUDI ARABIA

DEANSHIP OF GRADUATE STUDIES

This thesis, written by **MOHAMMED MOHAMMED HUSSEIN AL-THOLAIA** under the direction of his thesis advisor and approved by his thesis committee, has been presented to and accepted by the Dean of Graduate Studies, in partial fulfillment of the requirements for the degree of **MASTER OF SCIENCE** in **CIVIL ENGINEERING.**

Thesis Committee

Prof. Abul Kalam Azad (Advisor)

Prof. Muhammed H. Baluch (Member)

Dr. Shamshad Ahmad (Member)

Dr. Hussain J. Al-Gahtani
(Department Chairman)

Dr. Salam A. Zummo
(Dean of Graduate Studies)

11/6/10
Date

وقل رب زدني علما

DEDICATED

TO MY FATHER, MOTHER, AND MY

CHILDREN AND TO MY BROTHER AND SISTERS

ACKNOWLEDGMENT

Praise and thanks a lot God Almighty, for giving me the health, knowledge and patience to complete this work. I acknowledge the financial support given by Thamar University and by KFUPM's Civil Engineering Department during my graduate studies.

My sincerest gratitude goes to my advisor Prof. Abul Kalam Azad. I am also grateful to my Committee Members, Prof. Muhammed Hussein Baluch, Dr. Shamshad Ahmad, for their constructive guidance and support. Thanks are also to the department's Chairman Dr. Husain J. Al-Gahtani and his secretary for providing aid, and to other staff members of the department especially the lab supervisor, Dr. Essa, and the technicians: En.Muhitur Rahman, Emran, Mr. Mukaram, and Mr. Omar, for their help.

Special thanks and appreciate to the sponsor company, Ameron Saudi Arabia, Ltd, for their financial support with the specimens and corresponding needed fund during the entire process of this work.

Deep thanks are to the research institute team, the supervisor Prof. Mohammed Maslehuddin, and the researchers: Shameem, Bary, and Abdul Qadoos, for their help and supplying with needed instruments.

My heartfelt gratitude is given to my beloved father, mother, and my children, who always support me with their love, patience, encouragement and constant prayers. I would like to thank brother, sisters, and all members of my family in Yemen.

TABLE OF CONTENTS

LIST OF TABLES

LIST OF FIGURES

THESIS ABSTRACT

NAME: **MOHAMMED MOHAMMED HUSSEIN AL-THOLAIA**

TITLE: **DURABILITY ASSESSMENT OF JOINT ASSEMBLY FOR FIBERGLASS RESIN COATED CONCRETE CYLINDER PIPES.**

DEPARTMENT: **CIVIL ENGINEERING**

DATE: **June, 2010**

The durability performance is the most important subject that distinguishes the good material characteristics from the bad ones, particularly under aggressive environmental conditions. Concrete cylinder pipes (CCP) consisting of steel rebar wrapped steel shell, lined with cement mortar inside and outside the pipes, are manufactured in Saudi Arabia to transport water and other fluids. They are used above and underneath the soil and are often subjected to chemical attack when exposed to aggressive environmental conditions.

Durability of CCP is therefore a prime concern to users and producers. For protection, fiberglass resin coating (FRC) is used on the exterior surface of CCP. However, it cannot be applied on the joint, which creates a potential weakness, because of the necessity to make it flexible and easy to construct at site. The assembled joint typically consists of a Bell and Spigot system in which a steel plate is used covered by diaper-wrapped lean cement mortar for protection.

For the protection of steel plate at the joint, three different types of primer coatings: red oxide, zinc primer, and epoxy coating, were considered in this study. A qualitatively assessment of durability was carried out for the assembled joint using the three types of coatings to select the best performing one and the role of electrical resistance of fiberglass resin coating, mortar lining, and coating on steel plates, in the overall effective electrical resistance of main CCP section and assembled joint sections was also qualitatively assessed.

A total of sixteen prototype assembled joint pipe specimens were used; eight for wet-dry cycle test in sabkha solution and eight for thermal cyclic test, for six months exposure. In parallel, test specimens using coated steel plates with three different coatings and bare steel plates were used in three different tests: natural corrosion process test (specimens of 150*75*58 mm subjected to hot and humid environment for 74 days), high chloride exposure (specimens of 300*300*58 mm ponded with 10% NaCl solution for 160 days), and accelerated corrosion test (specimens of 150*75*58 mm subjected to 4 volts for two durations of 4 and 8 days), total of 40 test specimens were used for the three planned tests. For the electrical resistance test, twelve specimens with coated (epoxy paint, red oxide and zinc primer) and uncoated steel strips of 180*20*8 mm were used.

Epoxy paint coating was found to be the best performance one under such tests as it delays the corrosion initiation time significantly and has the highest electrical resistance value comparing to red oxide coating and zinc primer coating as well as the mortar lining at the joint assembly.

However, the fiberglass resin coating has the highest electrical resistance value comparing to all the three coatings (epoxy paint, red oxide and zinc primer coatings) and to the mortar lining of the main body of the pipes. The polyethylene diaper/mortar lining at the joint assembly showed good performance under both the wet-dry cyclic test and thermal cycling test.

MASTER OF SCIENCE DEGREE
KING FAHD UNIVERSITY OF PETROLEUM AND MINERALS
DHAHRAN, SAUDI ARABIA

ملخص الرسالة

الإســــــــــم : **محمد محمد حسين الثلايا**

عنوان الرسالة : **تقييم متانة نقطة التجمع للأنابيب الأسطوانيه الخرسانيه المطليه بالياف راتنج الفيبرجلاس**

التخصـــــص : **الهندسة المدنية**

تاريخ التـخرج : **يونيو 2010م**

يعتبر أداء المتانة الموضوع الأهم الذي يميز سمات المواد الجيدة من السيئة ، لا سيما في ظل الظروف البيئية العدوانية . الأنابيب الخرسانية الاسطوانية (CCP) تتألف من القضبان الفولاذية التي تلف اسطوانة الصلب من الخارج حيث يتم التبطين الداخلي والخارجي باستخدام مونه اسمنتيه هذا ويتم تصنيعها في المملكة العربية السعودية لنقل الماء والسوائل الأخرى. وهي تستخدم فوق وتحت التربة مما يجعلها تتعرض لهجوم كيماوي عندما تتعرض لظروف بيئية عدوانية. وعلى هذا تكون متانة الـ(CCP) مصدر قلق رئيسي للمستخدمين والمنتجين على حد سواء. لغرض الحمايه, الياف راتنج الفيبرجلاس (FRC) يستخدم على السطح الخارجي للجسم الرئيسي للانابيب. لكن لايمكن استخدامه في نقطة التجمع وذلك للحاجه لجعلها مرنه وسهلة في التنفيذ في الواقع لهذا فأنها تعتبر منطقة ضعف. تتكون نقطة التجمع من نظام (Bell and Spigot), لوحين من الصلب الذين يتم تغطيتهما بالمونه الاسمنتيه داخليا وخارجيا حيث تكون المونه الاسمنتيه الخارجيه ملفوفه بالبوليثيلين للحمايه.

لحماية مسطحات الصلب في نقطة التجمع ، ثلاثة أنواع مختلفة من الطلاء التمهيدي تم اعتبارها في هذة الدراسه(أكسيد الحديد الأحمر ، طلاء الزنك ، وطلاء الإيبوكسي) حيث أجري تقييما نوعيا للمتانة لنقطة التجمع باستخدام الثلاثة الأنواع من الطلاء لتحديد ايهم افضل كما تم التقييم النوعي لدور المقاومة الكهربائية لكل من: (FRC) ، مونة البطانه الاسمنتيه والطلاء على ألواح الصلب، في المقاومة الكهربائية الشاملة للانابيب الخرسانيه الاسطوانيه المطليه بألياف راتنج الفيبرجلاس وكذلك نقطة التجمع.

اجمالي ما مجموعه 16 عينة نموذجية لنقطة التجمع تم استخدامها ، ثمانية لاختبار دورة الرطب - الجاف في محلول سبخة وثمانية لاختبار دورة الحرارة والتبريد ، وذلك لمدة ستة أشهر متواصلة . وفي موازاة ذلك ،

استخدمت عينات معمليه صغيرة الابعاد وذلك باستخدام ألواح الصلب المطلي مع الثلاثه الانواع المختلفه من الطلاء السابق ذكرها بالاضافه الى ألواح الصلب الغير مطليه جميعها مخفيه في المونه الاسمنتيه في ثلاثة اختبارات مختلفة : اختبار عملية التآكل الطبيعية (عينات من 150 * 75 * 58 ملم مكونه من NaCL 12%-مونه اسمنتيه تم تعريضها لبيئة حارة ورطبة لمدة 74 يوما) ، التعريض لنسبه عالية من الكلورايد (عينات من 300 * 300 * 58 ملم تم غمرها في محلول كلوريد الصوديوم بنسبة 10 ٪ لمدة 160 يوما) ، واختبار التآكل المتسارع (عينات من 150 * 75 * 58 ملم تم تعريضها لـ 4 فولت لمدتين هما من 4 و 8 أيام) ، باجمالي 40 عينه للاختبارات الثلاثة المخطط لها .لاختبار المقاومة الكهربائية تم استخدام اثني عشر عينه مع الطلاء(مطليه بالـ: الايبوكسي ، الزنك التمهيدي, واكسيد الحديد الاحمر) وغير المطليه بابعاد 180 * 20 * 8 ملم .

طلاء الايبوكسي امتاز بأفضل أداء في إطار هذه التجارب لأنه يأخر وقت بدء التآكل بشكل كبير وايضا كان له أعلى قيمة للمقاومة الكهربائية مقارنة مع طلاءاكسيد الحديد الأحمر و طلاء الزنك التمهيدي ، وايضا مع مونة البطانه الاسمنتيه عند نقطة التجمع .

طلاء الـ (FRC) كان له أعلى قيمة للمقاومة الكهربائية مقارنة بجميع الانواع الثلاثه للطلاء (طلاء الإيبوكسي ، أكسيد الحديد الاحمر وطلاء الزنك التمهيدي), ومونة البطانه الاسمنتيه من الجسم الرئيسي للأنابيب .وأظهرت (حفاضات البولي ايثيلين / مونة الاسمنت) عند نقطة التجمع أداء جيد في كل من اختباري دورتي الرطب- الجاف والحرارة والتبريد.

درجة الماجستير في العلوم

جامعة الملك فهد للبترول والمعادن

31261 – الظهران

المملكة العربية السعودية

CHAPTER ONE

INTRODUCTION

1.1 General

For use of any industrial products in harsh environmental conditions, (e.g. hot and humid, presence of high levels of chlorides and sulfates), attention must be given to ensure the durability of such products.

The coastal belt of Saudi Arabia is known for its aggressive environment to promote chloride-induced corrosion of steel. Sabkha soil that contains of over 15% Cl^- and 0.5 % $SO4^{--}$ is one of the common soils in the Kingdom of Saudi Arabia. The aggressivity of soil and the environment compounded by hot and humid environment demand outmost consideration of durability of concrete construction.

Concrete cylindrical pipes (CCP) are commonly used in the Kingdom of Saudi Arabia to transport water and other fluids across this vast land. In its current form of construction, a CCP is manufactured by providing a cement-mortar cover to spirally reinforced thin steel shell, which is wrapped by steel reinforcing bars, and then applying a protective coating on top of the mortar to enhance durability and to protect the pipes against moisture and chemical attack[34].

To make connection for these pipes, the bell and spigot joint section entails forged steel element called spigot and hot rolled slitted element called bell, that are welded to the steel cylinders on each side of the joint and then the joint being wrapped in-situ with

polyethylene line grout band (diaper), and secured at the joint. Then lean sand-cement mortar is poured in the ensuring recess thus engulfing all steel with mortar. Cement grout is then internally applied to the joint recess. (Figure 1.1)

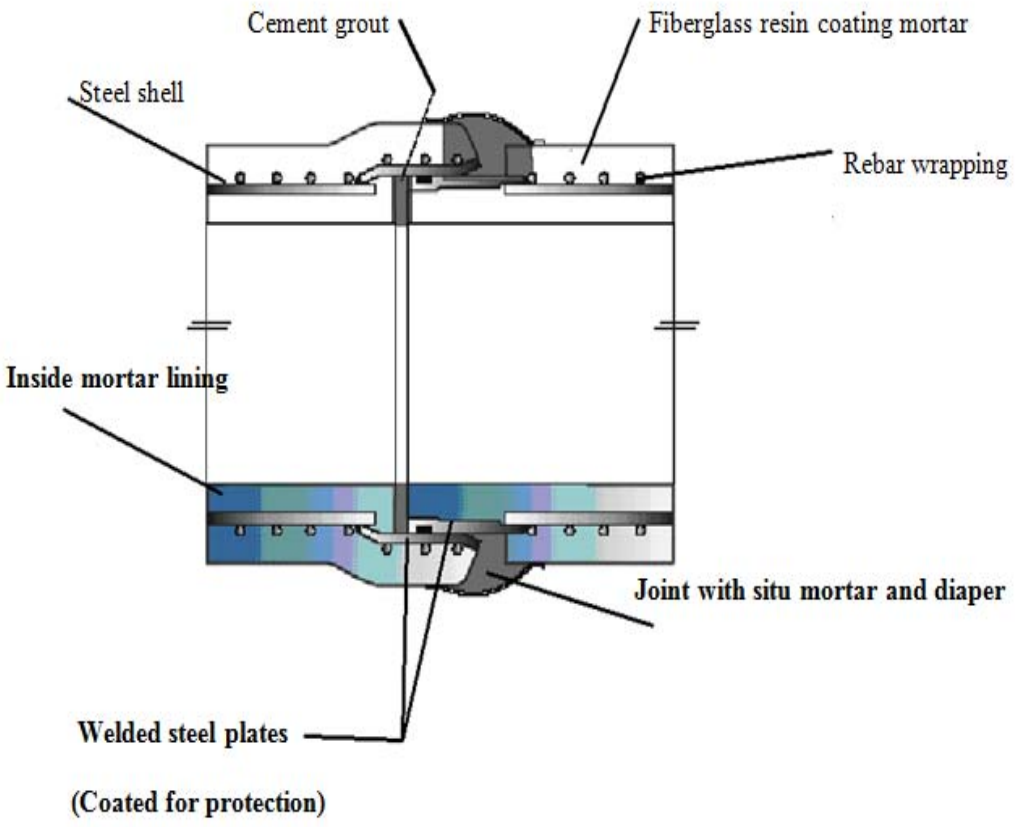

Figure 1.1 Bell and Spigot Assembled Joint FCCP Section [34].

Recently, fiberglass resin coating has been adopted by Ameron Saudi Arabia Ltd (one of the leading manufacturers in the Kingdom) as a protective coating system for the main body of the CCP. Past study [29] has shown that the fiberglass resin coating is an effective protective coating system for CCP pipes due to its excellent adhesion, durability, resistivity, and its ability to provide corrosion protection to pipes by serving as a barrier to ingress of moisture and chloride.

However, the FRC cannot be applied to the assembled joint of the fiberglass resin coated concrete cylinder pipes (FCCP) because of its in situ construction and the need of some joint flexibility.

Three types of primer coatings have been tried by Ameron as coating systems to the steel plate. The three coating systems are: red oxide primer (RP), zinc primer dim 6(ZP), and epoxy paint (EP). This work was a continuation of research funded by Ameron Saudi Arabia to evaluate the durability of the joint system used by the company.

The durability performance of the assembled joint system which consists of: concrete mortar (2 sand: 1 cement) and 0.5 water cement ratio, coatings on steel plates, and the polyethylene diaper band, was assessed using three different coatings on the steel plate.

This assessment was based on using different types of specimens; prototype assembled joint section pipe specimens and small scale (laboratory specimens). For the prototype specimens, the following two tests were carried out:

a) Thermal cycling test.

b) Wet-dry cyclic test.

For the small scale laboratory specimens, three different types of test were conducted:

a) Natural corrosion process test.

b) High chloride exposure.

c) Accelerated corrosion test.

The information gathered from the above tests, was used for the qualitatively assessment of the components of the assembled joint section, the three types of coating to select the best performing one, the assessment of the diaper as a barrier against the ions ingress, and the function of the concrete mortar.

With addition to the durability performance assessment of the joint assembly system components, the electrical resistance assessment of the fiberglass resin coating (FRC) on the main body of the concrete cylinder pipes, and the electrical resistance assessment of the joint assembly component were carried out based on the above tests results as well as the electrical resistance test results and the past work results [29].

By combining all tests results, the role of electrical resistance of the fiberglass resin coating (FRC), mortar lining and coating on steel plates in the overall effective electrical resistance of the main concrete cylinder pipe section and assembled joint section was qualitatively assessed.

1.2 **Significance of the Study**

As mentioned above, the earlier work to evaluate the fiberglass resin coating as an effective protective coating system for the concrete cylinder pipes (CCP) was based only

on the prototype pipes, not the assembled joint section. The assembled joints (connections) create a potential weakness in the pipe system as the connecting plates are vulnerable to chemical attack. The durability of the joint assembly needs to be assessed.

In this research, the durability assessment and the electrical resistance assessment of the assembled joint sections of the CCP were carried out using three different types of primer coatings for the steel plate, red oxide primer (RP), zinc primer dim coat 6 (ZP), and epoxy paint (EP), to identify the best performing coating for the plates.

1.3 **Scope and Objectives**

The work in this research is limited to study the durability performance and the electrical resistance of the assembled joint system components of the fiberglass resin coated concrete cylinder pipes (FCCP) for the three different types of primer coatings (red oxide, zinc primer and epoxy paint) using two different specimens types: prototype pipe assembled joint and small size specimens.

The primary objectives of this study are as follows:

1- Evaluate the durability of the prototype assembled joint pipes under cyclic exposure conditions (wet-dry cycle and thermal cycling test), with the three different coating types applied to the joining plate.
2- Evaluate the durability performance of the assembled joint components (the diaper, the mortar, and the coatings) under the accelerated corrosion test, natural corrosion test, and high chloride exposure.
3- Determine the best-performing coating at the joint.

4- Qualitatively assess the role of electrical resistance of the fiberglass resin coating, mortar lining, and coating on steel plates in the overall effective electrical resistance of main CCP section and assembled joint sections.

1.4 Research Methodology

In order to achieve the above objectives, this research has used a methodology encompassing the following phases:

1. Literature Review
    I. Composite materials
    II. Protective coatings
        a. Fiberglass resin coating
        b. Epoxy-based coating
        c. Red Oxide Coating
        d. Zinc Primer Coating
        e. Other types of coatings
2. Experimental Program
    I. Durability assessment
        a. Test program on assembled joint prototype specimens
            - Thermal cycling test
            - Wet-dry cyclic test
        b. Test program for laboratory scale mortar specimens
            - Natural corrosion process test
            - High chloride exposure test

CHAPTER TWO

LITERATURE REVIEW

2.1 Composite Materials

Composites materials are made up of two main components whose combined physical strength exceeds the properties of either of them separately. Reinforced plastic composite consist of the curing resin in which fibrous reinforcing network embedded. The thermosetting type resin is a plastic that cures from a liquid to a solid through a chemical reaction of its components.

For example, a typical thermosetting epoxy resin has a tensile strength below 10000 psi and is a quite brittle. However, the resulting composite of reinforcing the thermosetting epoxy resin with fiber glass has a tensile strength between 45000 and 50000 psi. This high strength for the relatively low weight is the main reason that makes fiberglass composite is popular [1].

The physical properties of composite are fiber dominant which means that when resin and fiber are combined, their performance remains like the individual fiber properties [1]. There are three types of reinforcing material as following: fiberglass (the most widely accepted and least expensive reinforcement), carbon fiber and Kevlar.

Regarding the resins types, there are many different types of resins like epoxy resins and polyester resins. Epoxy resins are thermosetting resins that can be cured by internally generated heat. Epoxy systems consist of two parts, resin and hardener. When

mixed together, the resin and hardener activate, causing a chemical reaction which cures the material.

Epoxy resins have bonding and physical strength greater than polyester resins [2]. When high adhesion is necessary, ever coat epoxies will bond permanently to fiberglass, metal, concrete and many plastics [2].

2.2 Protective Systems Coatings

Coating is a covering that is applied to an object. The aim of applying coatings is to get better surface properties of a bulk material, a substrate. In general, the description of the coatings can be based on their appearance, e.g. clear, metallic, and by their function like corrosion protective [3].

Another classification for coatings can be classified as organic and inorganic coatings. The organic coatings develop protection either by a barrier action from the layer or from active corrosion inhibition provided by pigments in the coatings [4].

In real life, the barrier properties are limited because all the organic coatings are permeable to water and oxygen to some extent [4].

The coating systems are also described by generic type of binder or resin, and grouped according to the curing or hardening mechanism of that generic type.

Paints are mostly classified as primers and topcoats. Primers are applied directly to the metal surface. They contain pigments of Zinc and perform the main job of corrosion protection. Topcoats are applied over the primer, mainly for the sake of

manifestation. However, they provide diffusion barrier and close the pores in the primary coat [4].

Here is the description of some of the common material used as coating applications [5].

2.2.1 Fiberglass Resin Coating

Fiberglass or glass fiber is material made from very fine fibers of glass. It is used as a reinforcing go-between for many polymer products; the consequential composite substance, properly known as fiber-reinforced polymer (FRP) or glass-reinforced plastic (GRP), is called "fiberglass" in popular practice.[6]

Glassmakers all over history have experimented with glass fibers, but mass manufacture of fiberglass was made possible with the innovation of finer equipment tooling. Incorporating glass fibers with the diameter and texture of silk fibers was exhibited in 1893 by Edward Drummond Libbey at the World's Columbian Exposition.[6]

However, the material which is known today as "fiberglass" was invented in 1938 by Russell Games Slayter of Owens-Corning as a product for the insulation uses. It is marketed under the buy and sell name Fiberglass, which has become a popular trade name. A fairly similar, but more expensive technology used for applications requiring very high strength and low weight is the use of carbon fiber [6].

Glass is in general viewed as an elastic solid in which no significant crystallization has occurred. Thus there is no long-range ordering or unlimited creation of any Bravais lattice. The glass has little crystalline formation, even as a fiber. [7]

The properties of the structure of glass in its softened stage are greatly like its properties when spun into fiber. One definition of glass is "an inorganic substance in a condition which is continuous with, and analogous to the liquid state of that substance, but which, as a result of a reversible change in viscosity during cooling, has attained so high a degree of viscosity as to be, for all practical purposes, rigid."[7]

When a thin filament of silica-based or other formulation glass is extruded into many fibers with small diameters suitable for textile processing, the glass fiber is created. The technique of heating and drawing glass into fine fibers has been known for millennia; however, the use of these fibers for fabric applications is more recent. Until this time all fiberglass had been manufactured as staple.[7]

Silica, SiO2, is the source of textile-grade glass fibers. In its uncontaminated form, it exists as a polymer, $(SiO2)_n$. It has no true melting spot but makes softer at 2000°C, where it starts to debase. At 1713°C, most of the molecules can go around freely. If the glass is reduced heating quickly, they will not form an ordered structure.[8]

Tetrahedron configuration with the silicon atom at the center and four oxygen atoms at the corners, SiO4, is formed in the polymer. By sharing the oxygen atoms, these atoms then form a network bonded at the corners. Because glass has a formless structure, its properties are the same along the fiber and across the fiber [8]. Because the thinner fibers are more ductile, the freshest, thinnest fibers are the strongest [9].

“The viscosity of the molten glass is very important for manufacturing success. The viscosity should be rationally low during drawing, pulling of the glass to reduce fiber

circumference. If it is too high, the fiber will break during drawing. However, if it is too low, the glass will form droplets rather than drawing out into fiber" [6].

"Uses for regular fiberglass include mats, thermal insulation, electrical insulation, reinforcement of different materials, tent poles, sound absorption, heat- and corrosion-resistant fabrics, high-strength fabrics, arrows, bows and crossbows, translucent roofing panels, automobile bodies and boat hulls. It has been used for medical purposes in casts. Fibreglass is extensively used for making FRP tanks and vessels'' [6].

2.2.2 Epoxy-Based Coatings

Epoxy or polyepoxide is a thermosetting polymer which is formed from reaction of an epoxide "resin" with polyamine "hardener". When the epoxy base, polyepoxide, is mixed with a catalyst, the process which is called an exothermic curing process starts. As a result of the exothermic curing process, the epoxy base forms a strong stress tolerant, flexible compound [10].

Nearly all common epoxy resins are obtained from a reaction between Epichorohydrin & Bisphenol A [11]. The first marketable attempts to prepare resins from epichlorohydrin occurred in 1927 in the United States. Recognition for the first synthesis of Bisphenol A based epoxy resins are shared by Pierre Castan of Switzerland and S.O. Greenlee in the United States in 1936. Castan's work was approved by Ciba, Ltd. Greenlee's work was for a company called Devoe-Reynolds of the United States [12].

The availability of the epoxy based coatings in many different application blends is high and these blends contain wide range types of filler materials. Typical filler materials include silica, carbon fiber, composites, fiberglass, polyester, vinyl, alumina,

ester and minerals. In general, epoxies are known for their excellent adhesion, chemical and heat resistance, good-to-excellent mechanical properties and very good electrical insulating properties [13].

A lot of properties of epoxies can be modified (for example silver-filled epoxies with good electrical conductivity are available, although epoxies are usually electrically insulating). Variations offering high thermal insulation, or thermal conductivity combined with high electrical resistance for electronics applications, are on offer [12and13].

Also, the applications of the epoxy based coatings include: epoxy based powder coating, fusion bonded epoxy powder coatings, paints, and paint primer.

Epoxy adhesiveness is a main part of the category of adhesives called "structural adhesives". These high-performance adhesives are used in the construction of aircraft, automobiles, bicycles, boats, golf clubs, skis, and other applications where high strength bonds are necessary [12and14].

In common, epoxy adhesives cured with heat will be more heat- and chemical-resistant than those cured at room temperature. The strength of epoxy adhesives is degraded at temperatures above 350°F [12and14]. Some epoxies are cured by experience to ultraviolet light. Such epoxies are usually used in optics, fiber optics, optoelectronics, and dentistry.

Epoxy resin, mixed with pigment, is used as a painting medium, by pouring layers on top of each other to form a complete picture [12 and15]. Epoxy resin is used in manufacturing rotor blades of wind turbine. The resin is infused in the core material like

balsa wood, foam, and reinforcing media glass fabric. The process is called VARTM, i.e. Vacuum Assisted Resin Transfer Moulding [12].

Because of the excellent properties and good finish, epoxy is most favored resin for composites. Here are some of the epoxy coatings which can be summarized as the following:

- **Fusion-Bonded Epoxy Coatings**

Fusion Bonded Epoxy Coating commonly referred to as FBE coating is an epoxy based powder coating and comes under the category of protective coatings in paints& coating nomenclature [16]. They are used in oil and gas pipeline applications, but are also used fairly in waste and wastewater applications as well.

AWWA C213 covers the material and application requirements for these types of coatings for the inside and outside of steel water pipe, special sections, welded joints, connections, and fittings of steel water pipelines installed underground or underwater under normal construction conditions [5,16and17].

- **Liquid Epoxy Coatings**

There are many types: some are solvent-based and others are 100% solids; some are cured by heat and others cured chemically. The curing agent might be an amine, amine adducts or polyamide; and the epoxy may be modified with coal tar, or others [5].

AWWA C210 covers liquid, chemically cured epoxies for the internal and external of steel water pipe, fittings, and special sections installed underground or underwater[5,18].

Solvent-based epoxies were usually used before as substituسte coating system to cement-mortar in potable water applications for steel pipe. The use of these low solids, solvent-based epoxies has recently decreased because of the problems involved with the use of solvents and VOC air pollution [5].

As a consequence, 100% solids rigid polyurethane and high solids or solvent less epoxy are used instead of the solvent-based epoxies. Liquid coal-tar epoxy coatings have been used as an internal lining system for wastewater or non-potable water pipes of all the three substrates: steel, ductile iron, and concrete. The grouping of both the epoxy and coal-tar unite the good properties of the two supplies to form a good water and saltwater-resistant coating [5,19and20].

2.2.3 Red Oxide Coating

For iron, there are three main oxides one of them is the red oxide (III) and its formula is Fe_2O_3. It is considered as the main source of the iron for the steel industry. It is reddish brown with shape and chemical composition as shown in Figure 2.1.

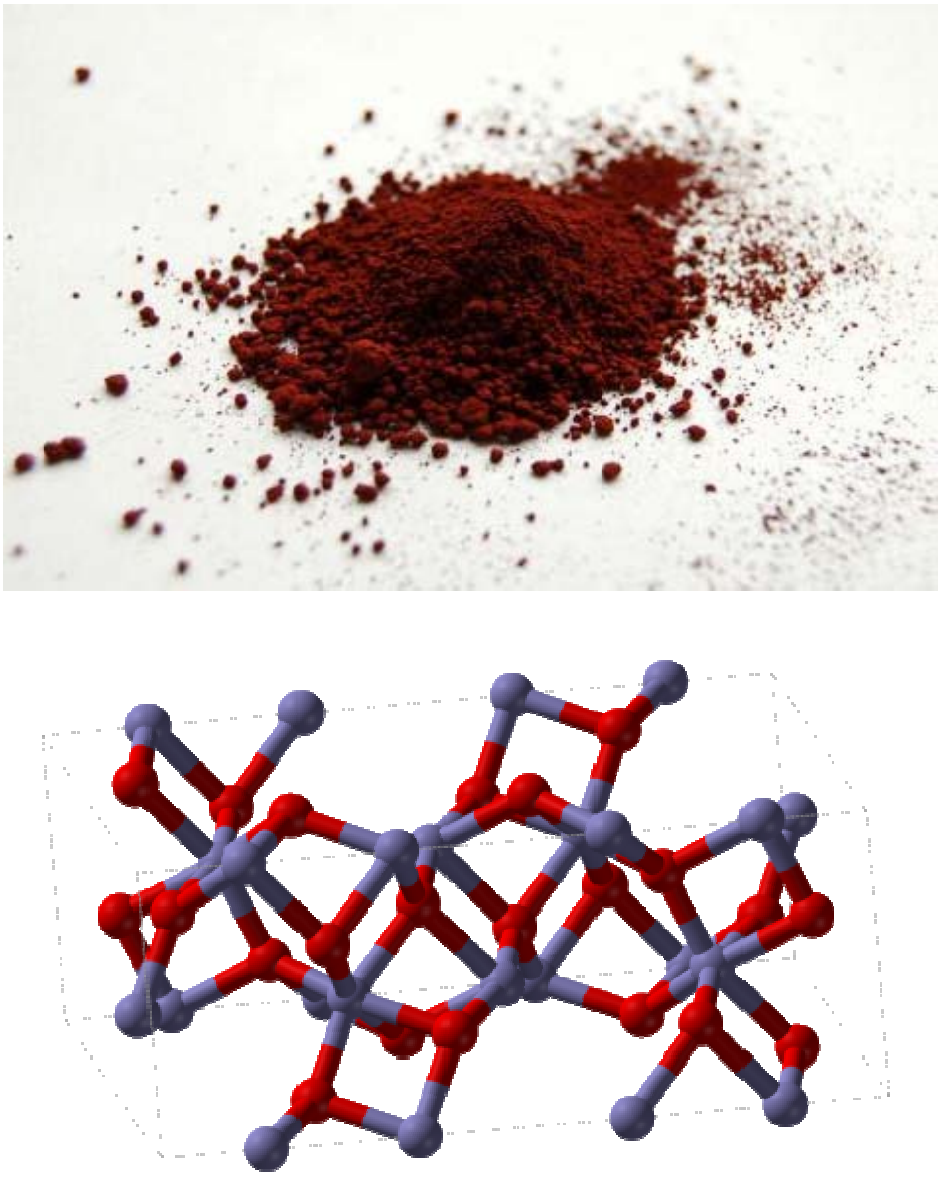

Figure 2.1 Red Oxide Shape and Chemical Composition [21]

The red oxide iron (III) can be produced from the iron oxidation and can be prepared by electrolyzing a solution of sodium bicarbonate, an inert electrolyte with an iron anode, in the laboratory [21].

$$2Fe + 3/2\ O_2 + H_2O \longrightarrow 2FeO(OH)$$

$$2FeO(OH) \longrightarrow Fe_2O_3 + H_2O$$

At 200 ° c, the iron (III) hydroxide changed into Fe_2O_3. Many uses for the red oxide are; iron industry, polishing, pigment and biomedical uses [21].

2.2.4 Zinc Primer Coating

Like any metals, zinc is one of the components of the earth's crust and also it exists in air, water, animals and humans [2.2].

Its ores were used for producing brass before it was discovered in the metallic form and its compounds were used for healing wounds and sore eyes. In India 1374, it was recognized as a new metal. Both zinc oxide and zinc metal were produced from the 12^{th} to the 16^{th} century in India and Zawar. Then, the production of zinc moved to China in the 17^{th} century. In 1546, it was recognized as a separate metal in Europe [22].

It is used as a coating for steel by providing two protections; cathodic action and a physical barrier. In the presence of zinc as coating on steel and the steel at some cut edge or surface scratch exposed to the moisture, the sacrificial loss of zinc in the vicinity of the exposed steel protects steel from corrosion until the zinc has been sacrificed which is known as a protection by cathodic action[23].

As physical barrier, it provides metallic barrier that does not allow moisture to contact steel. However, zinc has eroded gradually because of its slower degradation and therefore the barrier life depends on the thickness of the coating [23].

Many other uses for zinc such as; human body, it is essential with a certain quantity for each age and gender, purifying water, and improving air quality by using zinc-air batteries (zero emission vehicles) [22].

2.2.5 Other Types of Coatings

As it is stated earlier, there are many types of coatings and they are classified based on many parameters which already mentioned. Also with addition to the epoxy-based coatings, the other available coatings can be summarized as the following: etching primer (wash primer), acrylics, alkyd resins, autooxidative Cross-Linking Coatings, bituminous, nitrocellulose, 100% solids rigid polyurethane coatings[24,25], vinyl's, polyesters, phenolics, and silicone, for more information see [26, 27, 28].

As the previous description, there are a lot of types of coatings that can be used as a protective coating system. The fiberglass resin coating system which is adopted as a protective system for the concrete cylinder pipes by Ameron Company was evaluated by the center of engineering research (KFUPM).

Based on the findings from that study[29], the recommendations are: fiberglass resin coating as developed by Ameron Company is highly recommended as an effective protective coating for CCP pipes due to its excellent adhesion, durability, resistivity and its ability to provide corrosion protection to pipes by serving as a barrier to ingress of moisture and chloride.

The coating should be at least 2-3 mm in thickness. It is highly recommended that the coating application to CCP pipes shall be carried out carefully without any construction anomaly. Special care must be exercised to ensure perfect coating at connections.

Based on that study, the Ameron Company tried also system of coating for the assembled joint connection. This work was carried out to assess the proposed connection components; mortar lining, diaper and coatings on steel plates, as shown in Figure 1.1 above with three coating types: Red Oxide primer (RP), Zinc primer Dim Coat 6(ZP), and Epoxy Paint (EP).

CHAPTER THREE

EXPERIMENTAL PROGRAM

In this work, the experimental program that was planned basically consists of two main parts, the durability assessment and the electrical resistance assessment of the FCCP assembled joint components which are: the diaper, the mortar and the three different coatings (epoxy paint, red oxide and zinc primer Dim coat 6). The following are the major operational tasks:

1. Preparing two different types of specimens; prototype assembled joint pipe specimens and small scale, laboratory specimens. Both the prototype and the lab specimens had three different coating for the steel plates namely, epoxy paint, red oxide, and zinc primer Dim coat 6. In addition, bare steel was also used in both types of specimens to serve as control specimens.
2. Subjecting the prototype assembled joint pipe specimens to two different exposure tests; alternating wet and dry cycles and alternating heat and cool cycles, for duration of six months.
3. Subjecting the lab specimens to the following tests: high chloride exposure (10 % NaCl solution), under hot and humid environment (natural corrosion), and accelerated corrosion test under a constant potential of 4 volts for two different periods of time, 4 days and 8 days.
4. Breaking down the corroded specimens to measure the weight loss of the coated and uncoated steel strips for comparison and gravimetric analysis.

5. Extracting concrete powder samples from the prototype specimens after the alternating wet and dry cycles were completed for chemical analysis to determine the water soluble chloride and sulfate concentration.
6. Periodically extracting concrete powder samples from the lab specimens subjected to high chloride exposure test at different depths to determine the water soluble chloride concentration.
7. Periodically measuring the corrosion current densities of the lab specimens subjected to hot and humid exposure test using the linear polarization resistance technique (LPR) to track the corrosion initiation time. Also doing the same measurements for the lab specimens subjected to high chloride exposure test.
8. Measuring separately, without mortar, the electrical resistance of the coated steel strips (epoxy paint, red oxide and zinc primer Dim coat 6 coating) and the uncoated steel strips.

In this chapter, the details of all the above mentioned tasks and all information about the specimen's designations and sizes, preparation, tests procedures, and the tests set ups are covered.

3.1 **Durability Assessment**

The durability assessment of the fiberglass coated cylinder pipes (FCCP) assembled joint section components; the diaper, the mortar and the three different coatings (epoxy paint, red oxide and zinc primer Dim coat 6), was based on the following two different specimens: the prototype assembled joint section specimens and the laboratory (small scale) specimens.

3.1.1 Test Program on Assembled Joint Prototype Specimens

Each specimen has two main parts: (i) the main body of the pipe and (ii) the assembled joint section. The core pipe is manufactured based on AWWA C303 standard requirements with modifications to the process of curing and the application of the cement mortar coating, and consists of: welded steel cylinder, centrifugally cast cement-mortar lining, steel reinforcing bar wrapped at a predetermined stress around the cylinder, a dense cement-mortar coating over the steel cylinder and the wrapped reinforcement and fiberglass coating which is applied at a later stage to the dry surface of the cement-mortar coated pipe [34].

The mortar for lining and coating consists of one part cement to not more than three parts of fine aggregate by weight. Steel cylinder thickness depends on the pipe diameter with a minimum thickness of 1.5 mm and a maximum thickness of 10 mm. Minimum diameter of rod reinforcement is 6.0 mm with a maximum diameter of 14 mm. Minimum area of rod reinforcement is 493 mm2/m of pipe wall or numerically equal to 83.3 % of the pipe diameter in mm. Maximum area of rod reinforcement is 50% of the total steel area. Maximum centre-to-centre spacing of rod reinforcement does not exceed 50 mm. For more information about the manufacturing process see [34].

The bell and spigot, the assembled, joint section (Figure 3.1) entails forged steel element called Spigot and a hot rolled slitted element called Bell, that are welded to the steel cylinders on each side of the joint and then the joint being wrapped in-situ with grout polyethylene lined grout band, diaper, and secured to the ends of the two pipes

(Figure 3.1). Then lean cement mortar is poured in the ensuring recess thus engulfing all steel with mortar. Cement grout is then internally applied to the joint recess.

At the assembled joint section, the Bell and Spigot joint ring and the steel rods were coated with three different types of coatings; epoxy paint, red oxide and zinc primer Dim coat 6, along with uncoated bare steel. Each assembled joint section had a shell diameter of 400 mm and length of 300 mm, as shown in Figure 3.2.

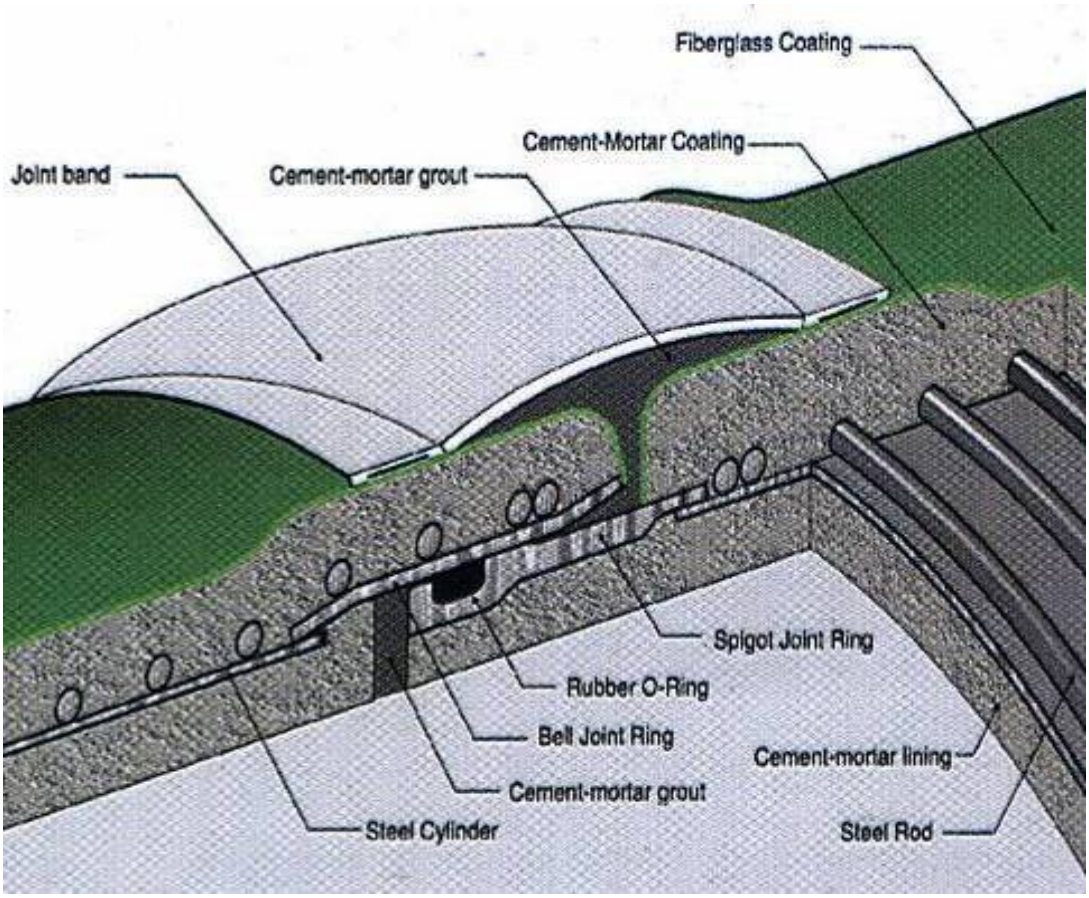

Figure 3.1 Bell & Spigot Assembled Joint FCCP Section

Figure 3.2 Assembled Joint FCCP Section Specimens

Using these specimens, two different types of tests were carried out; thermal cycling test and wet-dry test, for a period of six months. Total of sixteen specimens, eight for the thermal cycling test and eight for the wet-dry cyclic test (as shown in Table 3.1), as in the following:

TABLE 3.1 Required Number of Prototype Specimens for Each Test

Test Type	Number of Specimens
Thermal cycling	$4 \times 2 = 8$
Wet-Dry Cyclic	$4 \times 2 = 8$

a. Thermal cycling test

The purposes of this test were: to find out the effect of thermal cycling on the formation of cracks at the joint assembly and to examine the condition of the diaper and the effectiveness of its adhesion to the pipe.

The thermal cycling test [30] is one of the exposure tests that are used to evaluate and assess the performance of the structure member under the various change temperature conditions. In this work, eight prototypes assembled joint section specimens were used in this test, as shown in Table 3.2 and Figure 3.3, and the specimens were subjected to thermal cycling which was as follows:

Heating for 6 hours at temperature of 70 degrees centigrade and relative humidity (RH) of 90 % and then cooling at room temperature for 18 hours. This test was carried out for 6 months duration.

TABLE 3.2 Bell and Spigot Section for Thermal Cycling Test

Type of Specimen	Types of Coatings	No. of Specimens	Specimen Designation
Bell & Spigot	Bare Steel	2	BS-1T to BS-2T
Bell & Spigot	Epoxy Paint	2	EP-1T to EP-2T
Bell & Spigot	Red Oxide	2	RP-1T to RP-2T
Bell & Spigot	Zinc Primer Dim Coat 6	2	ZP-1T to ZP-2T

Figure 3.3 Thermal Cycling Test Specimens

After the test was completed, the condition of the diaper and its adhesion to the pipe was checked by visual inspection. Then, the diaper was removed to check the effect of the thermal cycling on the formation of cracks at the joint assembly.

b. Wet-Dry cyclic test

The main objective of this test was to evaluate the role of the diaper as a protective element from the salts penetration, chloride ions Cl^- and sulfate ions, from the surrounding environment into the assembled joint section. Also, if there was corrosion, determine the threshold salts limit for the three types of coating, epoxy paint, red oxide and zinc primer coating, on steel plate connection.

The used specimens in this test were eight prototypes assembled joint section pipe specimens with details as described above and as shown in Table 3.3.

TABLE 3.3 Bell and Spigot Section for Wet-Dry Cyclic Test

Type of Specimen	Types of Coatings	No. of Specimens	Specimen Designation
Bell & Spigot	Bare Steel	2	BS-1W to BS-2W
Bell & Spigot	Epoxy Paint	2	EP-1W to EP-2W
Bell & Spigot	Red Oxide	2	RP-1W to RP-2W
Bell & Spigot	Zinc Primer Dim Coat 6	2	ZP-1W to ZP-2W

The specimens were subjected to alternating wet-dry cycles testing consisting of 48 hours of wetting in Sabkha-type chloride and sulfate solution followed by 48 hours of drying at the laboratory temperature, as shown in Figure 3.4 and Figure 3.5, for 6 months.

The Sabkha solution was prepared by adding NaCl, Na_2SO4 and $MgSO_4$ to obtain 15.7% Cl^- and 0.55% SO_4^{--} concentration.

Figure 3.4 Wet-Dry Cyclic Test Specimens in the Sabkha Solution

Figure 3.5 Wet-Dry Cyclic Test Specimens in Dry Condition

Then, powder samples were extracted from immediately underneath the diaper (0.5cm depth and marked as in Table 3.4) close to the diaper and other deeper places as shown in Figure 3.6, to be chemically analyzed for the water soluble chloride concentration and sulfate concentrations.

TABLE 3.4 Powder Samples Extracted From Wet-Dry Test Specimens Designation

Prototype Specimen	Powder Sample	Location of Sample	Prototype Specimen	Powder Sample	Location of Sample
BS1W	BS1WS	A	**RP1W**	RP1WS	A
	BS1W1	B		RP1W1	B
	BS1W2			RP1W2	
	BS1W3	C		RP1W3	C
BS2W	BS2WS	A	**RP2W**	RP2WS	A
	BS2W1	B		RP2W1	B
	BS2W2			RP2W2	
	BS2W3	C		RP2W3	C
EP1W	EP1WS	A	**ZP1W**	ZP1WS	A
	EP1W1	B		ZP1W1	B
	EP1W2			ZP1W2	
	EP1W3	C		ZP1W3	C
EP2W	EP2WS	A	**ZP2W**	ZP2WS	A
	EP2W1	B		ZP2W1	B
	EP2W2			ZP2W2	
	EP2W3	C		ZP2W3	C

Note. **BS**-Bare Steel, **EP**-Epoxy Paint, **RP**-Red Oxide, **ZP**-Zinc Primer and **W**-Wet dry test specimen

A: 0.5 cm underneath the diaper at the joint, **B**: 1-2 cm underneath the diaper at the joint, and **C**: 1-2 cm underneath the FRC at main body of pipe

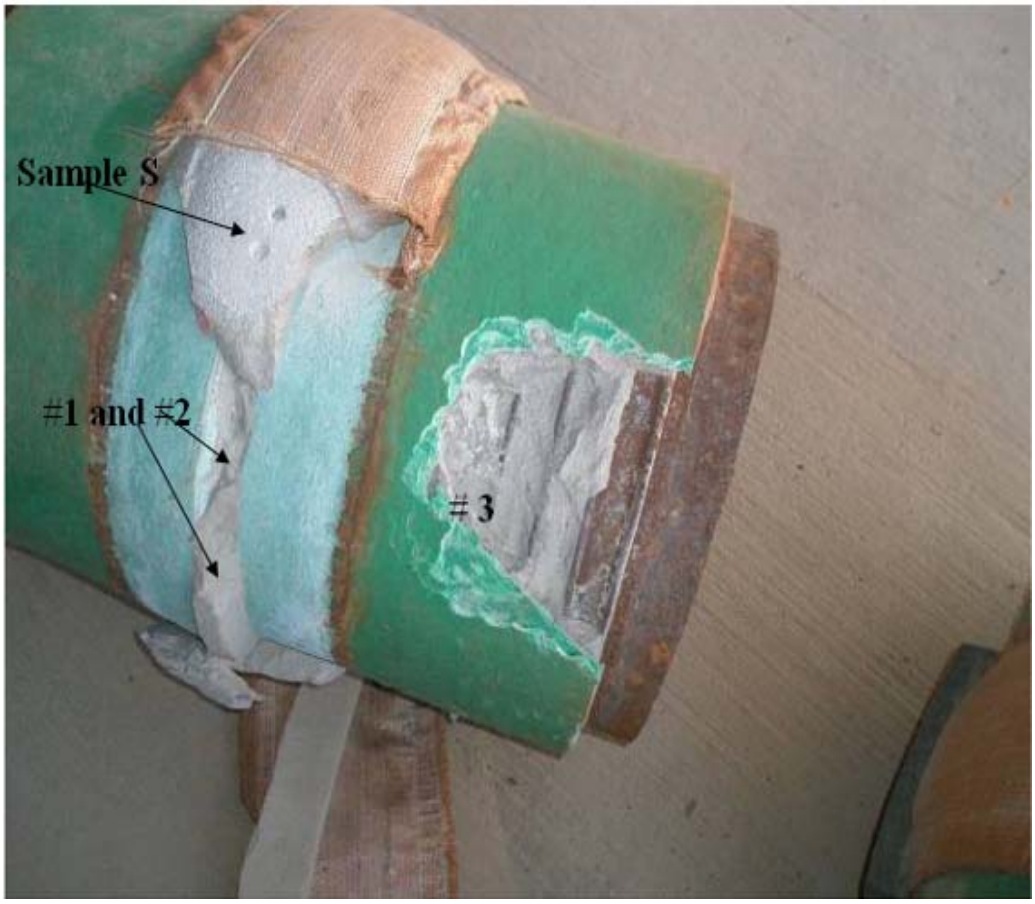

Figure 3.6 Powdered Samples Locations

Then the extracted powder samples were chemically analyzed for the water soluble chloride concentration Cl^- and sulfate concentration, % of the sample mass.

Then, the mortar and the diaper were removed from the joint assembly section to check the situation of the steel, coated and uncoated, whether they were corroded or not as shown in Figure 3.7.

Figure 3.7 the Steel at the Assembly Joint after Removing the Diaper and the Mortar to Check the Corrosion Signs.

3.1.2 TEST PROGRAM FOR LABORATORY SCALE MORTAR SPECIMENS

The small size laboratory specimens were prepared using embedded steel strips, coated with the three proposed coatings; epoxy paint, red oxide and zinc primer coating, and uncoated (bare steel) as control specimens, in concrete mortar simulating the FCCP assembled joint construction .

The concrete mortar consists of cement and sand with 1:2 ratios by mass and mixed using water cement ratio of 0.5. The mixing water consists of three types; free chloride (only pure water), NaCl solution with 3% of mortar mass and NaCl solution with 12% of mortar mass, based on the three proposed tests which were; high chloride exposure, accelerated corrosion and natural corrosion process test, respectively. In case of the high chloride exposure test, the concrete mortar was covered with the diaper for half of the specimens and was not for another half of the specimens.

These specimens were prepared with the following dimensions; 58*300*300 mm for the high chloride exposure test and 58∗75∗150 mm for both the accelerated corrosion test and the natural corrosion process test. The details of all the used laboratory specimens are in Table 3.5 and the drawing details in Figure 3.8 and Figure 3.9.

TABLE 3.5 Details of the Laboratory Specimens

Specimen Built-in-Mortar	**Specimens size**	**Coating on the Steel Strip**	**Number of Specimens**
12% NaCl-Admixed Mortar	58∗75∗150 mm	Red Oxide Primer	2
		Zinc Primer Dim Coat 6	2
		Epoxy Paint	2
		Bare Steel (uncoated)	2
Chloride Free Mortar *(with and without polyethylene diaper)*	58∗300*300 mm	Red Oxide Primer	4
		Zinc Primer Dim Coat 6	4
		Epoxy Paint	4
		Bare Steel (uncoated)	4
3% NaCl-Admixed Mortar	58∗75*150 mm	Red Oxide Primer	4
		Zinc Primer Dim Coat 6	4
		Epoxy Paint	4
		Bare Steel (uncoated)	4

Notes: (i) all strips were be centrally-embedded in the specimens, (ii) the strips were extended 50 mm on one side and (iii) the strips are 8 mm thickness and 20 mm wide.

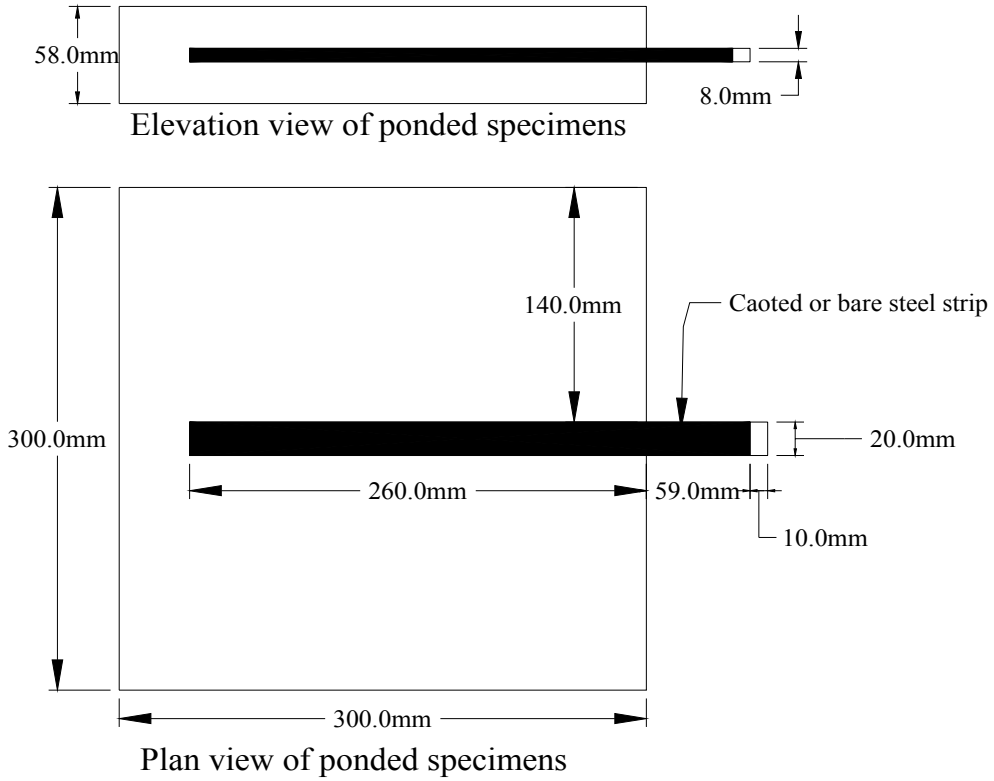

Figure 3.8 Ponded Specimens Details

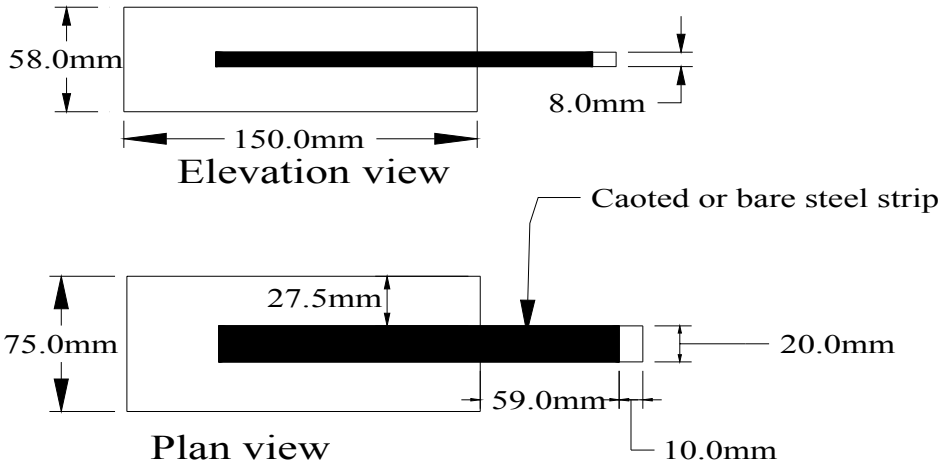

Figure 3.9 Accelerated And Natural Corrosion Specimens Details

After the above specimens were prepared, they were put for curing and the three types of tests were carried out which were:

a. Natural Corrosion Process Test.
b. High Chloride Exposure Test.
c. Accelerated Corrosion Test.

Here are the details of the above tests:

a. Natural Corrosion Process Test

The purpose of this test was to find out the relative corrosion resistance of the three coatings: epoxy paint, red oxide and zinc primer. Total of eight specimens were used with 58∗75∗150 mm dimensions and 12 % NaCl built in-mortar. The designations and all the other details of these specimens are in Table 3.6.

TABLE 3.6 Natural Corrosion Process Specimens

Specimen Dimensions	**Types of Coatings**	**No. of Specimens**	**Specimens designation**
58∗75∗150 mm	Red Oxide Primer	2	NCRP-1 to NCRP-2
58∗75∗150 mm	Zinc Primer Dim Coat 6	2	NCZP-1 to NCZP-2
58∗75∗150 mm	Epoxy Paint	2	NCEP-1 to NCEP-2
58∗75∗150 mm	Bare Steel (uncoated)	2	NCBS-1 to NCBS-2

For the purpose of measuring the corrosion current densities, Icorr (μA/cm2), the linear polarization resistance technique, LPR technique, was used [41 and 42].

The linear polarization resistance technique, LPR, has become a good method of finding the instantaneous corrosion rate measurement of reinforcing steel in concrete [35-39]. It is fast, non-destructive technique and requiring only connection to the reinforcing steel. It gives a curate data and more detailed information than a simple potential survey [35].

The LPR procedure is based on the Stern-Geary characterization of the typical polarization curve for the corroding metal. In this technique, a linear relationship is described mathematically for a region on the polarization curve in which slight change in the current applied to the corroding metal in an ionic solution causes corresponding change in the potential of the metal [43].

In the LPR method, the reinforcing steel is polarized by a small amount from its equilibrium potential [35], which can be satisfied either potentiostatically or galvanostatically. In this study, the steel reinforcing was polarized potentiostatically by changing its potential with a fixed amount, ΔE, and recording the corresponding current, ΔI, for a fixed duration.

The corrosion cell connection consisted of three references; reference electrode (Saturated Calomel with 242 mv potential), a working electrode which was the steel strip embedded in the concrete specimen, and a counter electrode (stainless steel), which were placed in the salt solution, 5% of NaCl solution, as shown in Figure 3.12.

The change in potential, ΔE, lies within the linear Stern-Geary range of 10-30 mv [40] and the steel strip was polarized by applying a small potential shift to it (ΔE = ±10 mV) and the resultant current (ΔI) between the working electrode and the counter electrode was measured[43].

The linear polarization resistance, Rp, was determined from the slope of the plot of applied potential versus the measured current. The corrosion current density was then calculated by using the Stern-Geary formula [44].

$$I_{corr} = \frac{\Delta E}{\Delta I} = \frac{B}{Rp} \quad , \qquad (3.1)$$

Where:

I_{corr} is the corrosion current density **(µA/cm^2)**,

R_p is the polarization resistance (**kΩ.cm^2**),

$$B = \frac{2.3*(\beta a*\beta c)}{(\beta a+\beta c)} \qquad (3.2)$$

β_a is the anodic Tafel constant,

β_c is the cathodic Tafel constant.

The values of βa and βc are determined from the Tafel plot. However, in case of insufficient data on βa and βc for steel in concrete, a value of B equal to 52 mV for steel in passive condition and a value equal to 26 mV for steel in active condition are normally used. For steel in aqueous media, values of βa and βc equal to 120 mV are normally used [43].

The area of the steel strip that is affected by the current flowing from the counter electrode is a main uncertainty in obtaining the polarization resistance. An apparent polarization resistance, differs from the true R_p value depending on the experimental conditions, is provided from $\Delta E/\Delta I$ measurements because of using a small counter electrode. Thus, when the metal is actively corroding, the current applied from a small counter electrode located on the concrete surface is 'drained' very efficiently by the rebar and it tends to confine itself on a small surface area as shown in Fig. 3.10. Conversely, when the metal is passive, Rp is high; the current applied tends to spread far away from the application point (right part on the rebar in Figure 3.10 [45].

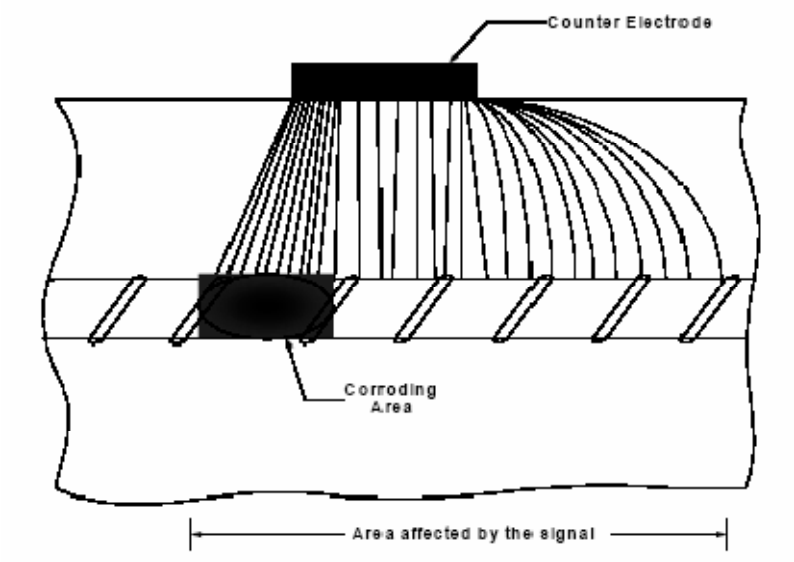

Figure 3.10 Spread of an Electrical Signal Applied From A Counter Electrode.

To overcome that problem, the counter electrode was prepared such that it covered both the sides of the specimen throughout the length and it is assumed while determining I_{corr} that corrosion is uniformly occurring over the whole steel area.

The eight specimens, two in each group of specimen as shown in Table 3.6, were kept in a purpose-built humidity chamber Figure3.11 fitted with temperature and humidity controls, maintaining 80% relative humidity and 40-45^{o}C temperature. This combination of hot and humid environment accelerated the natural corrosion process.

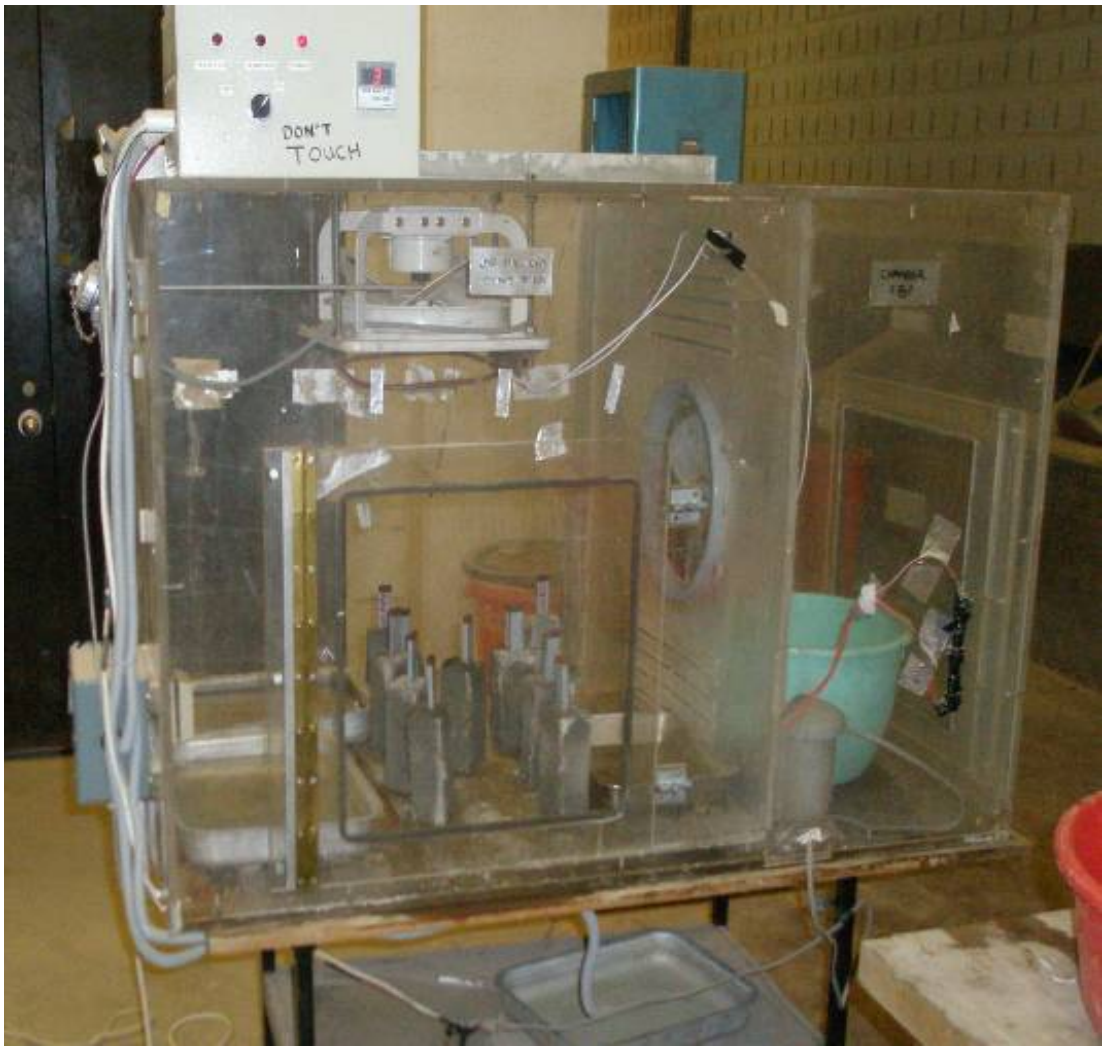

Figure 3.11 The Purpose-Built Humidity Chamber in Which the Natural Corrosion Process Specimens

Soon after ten days from the casting of the specimens, the curing duration, the first measurement of the current densities was taken using the LPR technique. Then the specimens were kept in the humidity chamber and the measurements of the corrosion current densities were taken periodically as shown in Figure 3.12.

Figure 3.12 Linear Polarization Resistance Technique Connection in Natural Corrosion Process Test.

b. High Chloride Exposure Test

A total of 16 samples of size 58*300∗300 mm were prepared, with no admixed chloride. All the samples were exposed to a high chloride simulation by ponding with a solution of 10% NaCl concentration for a period of 90 days Table 3.7.

TABLE 3.7 High Chloride Exposure Specimens

Specimen Dimensions	**Types of Coatings**	**No. of Specimens**	**Specimens designation**
58*300∗300 mm	Red Oxide Primer	2- With diaper	PDRP-1 to PDRP-2
		2- Without diaper	PRP-1 to PRP-2
58*300∗300 mm	Zinc Primer Dim Coat 6	2- With diaper	PDZP-1 to PDZP-2
		2- Without diaper	PZP-1 to PZP-2
58*300∗300 mm	Epoxy Paint	2- With diaper	PDEP-1 to PDEP-2
		2- Without diaper	PEP-1 to PEP-2
58*300∗300 mm	Bare Steel (uncoated)	2- With diaper	PDBS-1 to PDBS-2
		2- Without diaper	PBS-1 to PBS-2

Two sets of specimens were used: one set without using the polyethylene diaper and the other set using the polyethylene diaper to observe the effect of diaper, if any, on the chloride ingress. For each set, two specimens were cast for each of the following cases of coating on the embedded steel plate: (i) bare steel, (ii) epoxy-coating, (iii) red-oxide coating and (v) Zinc primer coating. The ponded specimens are shown in Figures 3.13 and 3.14.

The measurement of the amount of chloride penetration into the specimens was measured at four intervals of the ponding period t: t = 60 days, t = 74 days, t = 90 days, and t = 160 days. At each of the first three intervals, the powdered samples were extracted from each specimen by drilling at 5 mm and 10 mm depths from the top of the specimens (ponded face) for specimens without diaper, and 10 mm and 15 mm for specimens with diaper. At the fourth interval (t = 160 days), the powdered samples were extracted from one of the duplicated specimen by drilling at 5 mm, 10 mm, and 22 mm (at the steel strip surface) depths from the top of the specimens (ponded face) for specimens without diaper, and 10 mm, 15 mm, and 18 mm (at the steel strip surface) for specimens with diaper. The powdered samples were analyzed using chromatographic method.

The chromatography is defined terminologically as the collective term for a set of the laboratory methods for the mixtures separation. It is used mainly to separate the mixture components, purification form [46].

The analysis procedure was as following: weighing the extracted powder sample for one gram using a sensitive balance, 0.0001 gm, adding 100 ml distilled water, mixing the distilled water with the sample for a time of 24 hours using a specific machine as

shown in Fig. 3.15, filtering the mixture using a paper of filtration with (0.25 μm size) as shown in Fig.3.16 and then using the liquid chromatograph for the separation of the chloride ions.

Figure 3.13 Ponding Specimens (without diaper) During the Chloride Exposure.

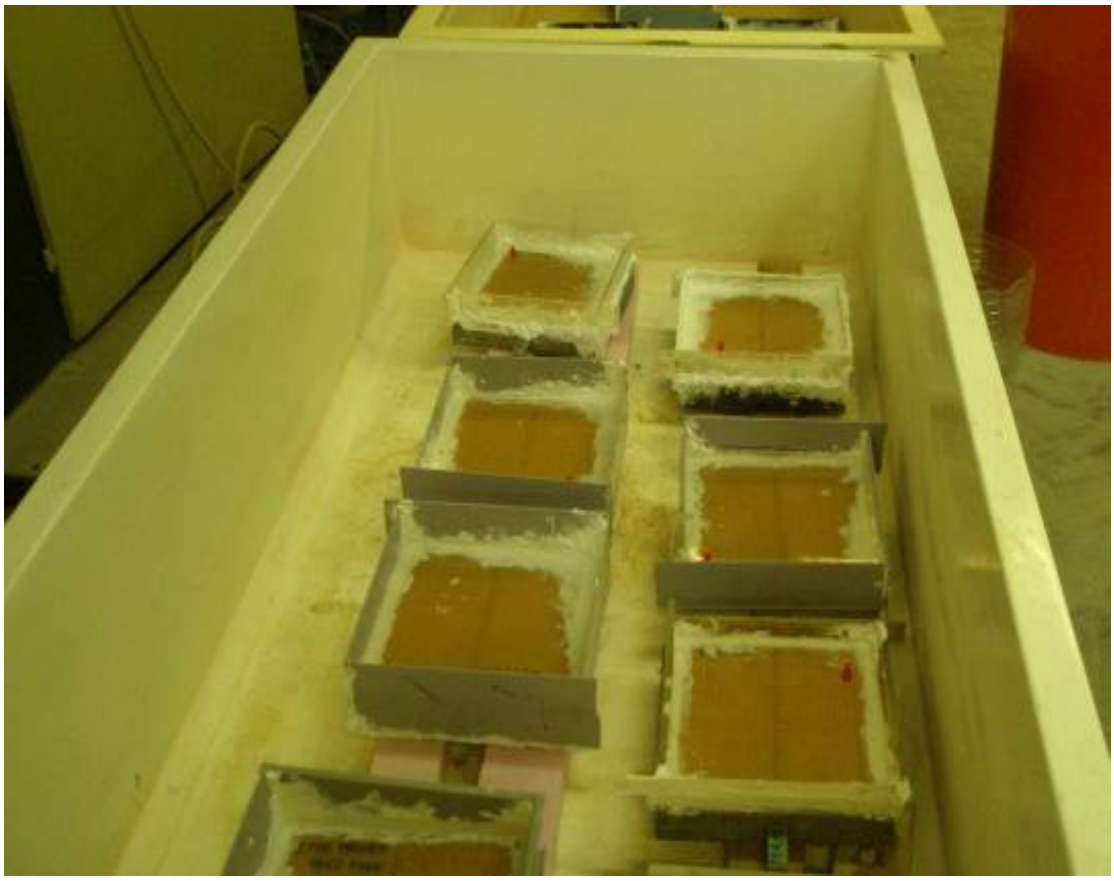

Figure3.14 Ponding Specimens (with Diaper) During the Chloride Exposure.

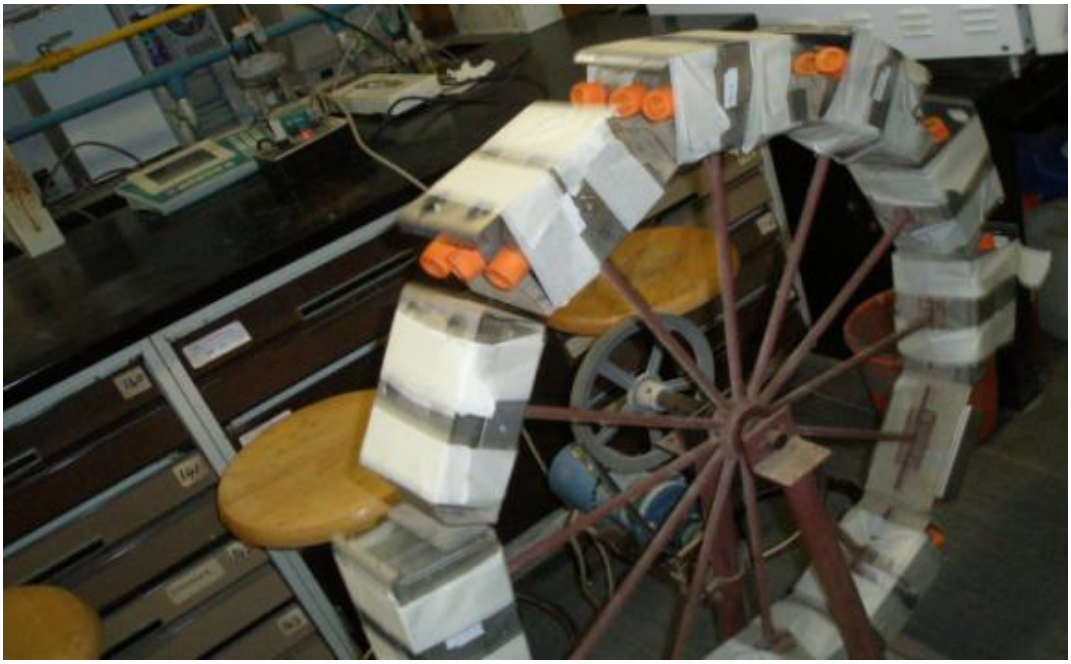

Figure3.15 The Mixing Machine of the Chloried Analysis.

Figure3.16 The Filetration of the Chloride Analysis Mixture.

Three different chloride contents are in the cement mortar; (i) total chloride content which is the total amount of the chloride ions in a sample of cement mortar, both bound in the solid phases and free in the pore solution, (ii) free chloride content, the amount of chloride ion in the pore solution extracted by squeezing the mortar sample at high pressure, and (iii) water soluble chloride which is the amount of the chloride ion in a mortar sample that can be obtained by leaching with water at room temperature.

In this study, the mortar samples were analyzed for the water soluble chloride, percent of the total sample mass. From the resulting values of the water soluble chloride concentrations, the diffusion coefficients of the cement mortar, in the specimens without diaper, and of the composite (cement mortar + polyethylene diaper) in the specimens with diaper, were calculated using the Fick's First and Second Laws.

The chloride diffusion into cement mortar, similar to any process of diffusion, is covered by Fick's First Law. In the one dimensional case, Fick's First Law says:

$$J = - D_e \frac{\partial C}{\partial x} \qquad (3.3)$$

Where;

J is the chloride ions flux

$\mathbf{D_e}$ is the effective diffusion coefficient.

C is the chloride ions concentration.

X is the distance from the penetrated surface.

$\frac{\partial C}{\partial x}$ is the concentration gradient in one dimension.

In the practical, this equation is useful after steady-state, no change in concentrations with time; conditions have been reached [47]. To cover the situation, when concentrations are changing, the Fick's Second Law is used which can be obtained by deriving the relevant equation for non-steady conditions [47] as follows:

$$\frac{\partial C}{\partial t} = - \frac{\partial J}{\partial x} \qquad (3.4)$$

Substituting for J from eq. 3.3;

$$\frac{\partial C}{\partial t} = D_e \frac{\partial^2 c}{\partial x^2} \qquad (3.5);$$

, Which considers the concentration changing with time (t), and De has been assumed to be constant.

Equation 3.5 has been solved using these boundary conditions for a semi-infinite domain which are as follows;

$C_x = C_i$ at $t = 0$ when $0 < x < \infty$

$C_x = C_s$ at $x = 0$ when $0 < t < \infty$

$C_x = C_i$ at $x = \infty$ when $0 < t < \infty$

By combination of variables, the solution for eq. 3.5 is;

$$\frac{C_x - C_i}{C_s - C_i} = 1 - erf\frac{x}{2\sqrt{De \cdot t}} \qquad (3.6)$$

Where;

C_i is the initial chloride concentration.

C_x is the chloride concentration at depth x.

C_s is the surface chloride concentration

erf is the error function.

D_e is the effective diffusion coefficient.

t is the time elapsed.

When the surface chloride concentration, the initial chloride concentration which was zero in this study, and the chloride concentration at a particular depth are known, the effective diffusion coefficient can be calculated using the above solution (3.6) [48].

The corrosion current densities were measured to track the corrosion initiation for all the specimens using the linear polarization resistance technique, LPR, as shown in the figure, Figure 3.17.

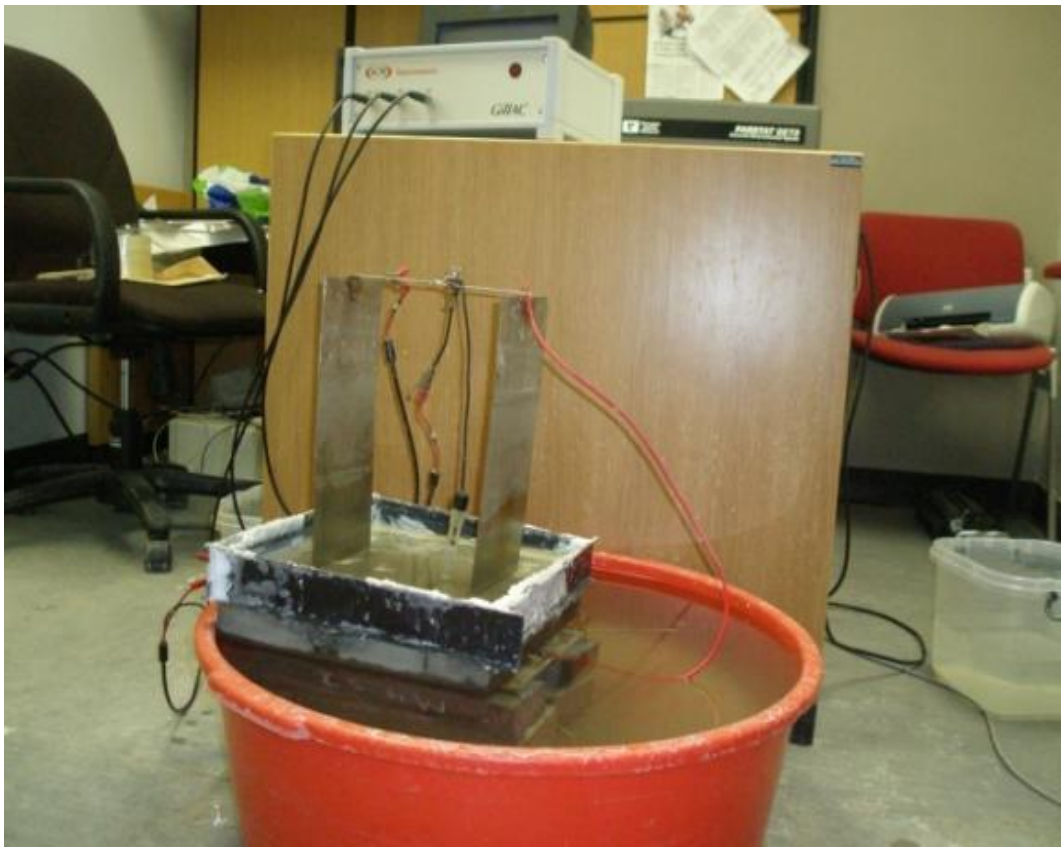

Figure 3.17 LPR Measurements for the Ponding Specimens Using ACM Equipment

c. Accelerated Corrosion Test

Sixteen coated and uncoated steel strips, (8 mm thick and 20 mm wide), embedded in mortar specimens of size 58∗75∗150 mm were prepared, with 3% premixed NaCl (by weight of mortar) added to the mortar, as shown in Figure 3.18 and detailed in Table 3.8.

Figure 3.18 The Specimens of the Accelerated Corrosion Test

TABLE 3.8 Accelerated Corrosion Specimens

Specimen Dimensions	**Types of Coatings**	**No. of Specimens**	**Specimen designation**
58∗75∗150 mm	Red Oxide Primer	4	ACRP-1 to ACRP-4
58∗75∗150 mm	Zinc Primer Dim Coat 6	4	ACZP-1 to ACZP-4
58∗75∗150 mm	Epoxy Paint	4	ACEP-1 to ACEP-4
58∗75∗150 mm	Bare Steel (uncoated)	4	ACBS-1 to ACBS-4

As shown in Figure 3.19, the strip in each specimen was centrally placed, partially embedded and partially extending outside. In both cases, uncoated and coated, a length of 70 mm of strip was allowed to be corroded under impressed current.

Impressed Current Application and Weight Loss Tests

First, all sixteen specimens were subjected to a constant potential of 4 volts for a period of four days and eight days by connecting the positive terminal of the DC source with the extended portion of the steel strip and negative terminal with the counter electrode. The drop in the potential was recorded by a data-logger during the entire period of the accelerated corrosion testing. Then, the corresponding currents were calculated using Ohm's law, using the constant basic resistance of the system as 10 Ω.

The set up of the accelerated corrosion test and the specimens during the test are as shown in Figures 3.19 and 3.20.

Figure 3.19 The Accelerated Corrosion Test Set Up

Figure 3.20 The Zinc Primer and the Bare Steel Specimens on the Second Day of the Accelerated Corrosion Test

The plots of the current (mA) versus the corresponding time (hours) were developed. After completion the accelerated corrosion test, the specimens were broken down and the embedded steel strips were taken out for gravimetric (weight loss) test as shown in Figures 3.21 and 3.22.

Figure 3.21 The Accelerated Corrosion Specimens After Completion of Test

Figure 3.22 Removed Steel Strips from Accelerated Corrosion Specimens

The steel strips were cleaned to remove all the rust products using Clarke's solution, hydrochloric acid (HCL, sp gr 1.91), 20 g antimony trioxide (Sb_2O_3) and 50 g stannous chloride ($SnCl_2$), as shown in Figures, 3.23 and 3.24.

Preparation of the Clarke's solution, cleaning and the evaluation of the corrosion test specimens were carried out in accordance with ASTM G-1-90-(1990).

The percentage weight loss was calculated as:

$$\text{Percentage weight loss} = \frac{W_i - W_f}{W_i} \times 100 \quad (3.7)$$

Where;

W_i = initial weight of the steel strips before corrosion.

W_f = weight after being cleaned of all rust products.

Figure 3.23 The Steel Strips of the Accelerated Corrosion Specimens in Clarke's Solution

Figure 3.24 The Steel Strips of the Accelerated Corrosion Test After Cleansing of Rust

From both the plots of current (mA) versus time (hours) and the gravimetric test analysis, the durability performance of the three used coatings; red oxide, zinc primer Dim Coat 6 and epoxy paint coating, was evaluated.

3.2 Electrical Resistance Assessments

The role of electrical resistance of the fiberglass resin coating, mortar lining and coating on steel plates in the overall effective electrical resistance of main concrete cylinder pipe (CCP) section and assembled joint section was assessed qualitatively based on the following:

1. The results of the accelerated corrosion test of the small scale specimens (as described above).
2. The results of the electrical resistivity test for the (chop fiber + resin) specimens in the past work [29].
3. The electrical resistance test as it is described in the following section.

3.2.1 Electrical Resistance Test

Total of twelve specimens consisting of uncoated (bare) and coated steel strips with the three different types of coating: epoxy paint, red oxide and zinc primer coating, were used in this test. The details of the test specimens are in Table 3.9.

TABLE 3.9 Electrical Resistance Specimens (Steel Strips Without Mortar)

Specimen Dimensions	Types of Coatings	No. of Specimens	Designation of Specimens
8*20*180 mm	Red Oxide Primer	3	RP-1 to RP-3
8*20*180 mm	Zinc Primer Dim Coat 6	3	ZP-1 to ZP-3
8*20*180 mm	Epoxy Paint	3	EP-1 to EP-3
8*20*180 mm	Bare Steel (uncoated)	3	BS-1 to BS-3

The LPR, linear polarization resistance, technique was used as an indirect method for measuring the electrical resistance of the coated and uncoated steel strips by applying a potential, -10 to +10 mv, gradually with a fixed value of ΔE and recording the corresponding current, ΔI. The set up of the LPR for this test is shown in Figure 3.25.

The plot of ΔE versus ΔI was developed and by taking the slope of the plot, the linear polarization resistance, R_p ($\Omega.cm^2$), was determined. From the determined Rp and knowing the subjected surface area of the steel strip to the polarization, the electrical resistances of the coated and uncoated steel strips were calculated.

Figure 3.25 The LPR Test Of The Electrical Resistance Test Set Up.

CHAPTER FOUR

RESULTS AND DISCUSSIONS

As mentioned earlier, two main parts of experimental work tests, the durability assessment and the electrical resistance assessment of the FCCP assembled joint components tests, were done and their results as following:

4.1 Durability Assessment Results

The durability assessment was based on testing two different types of specimens; prototype assembled joint section pipes and small scale specimens.

4.1.1 Tests Results of Assembled Joint Prototype Specimens

Two different tests for the prototypes assembled joint section pipes specimens; thermal cycling test and wet-dry cyclic test, were done and their results are as following:

a. Thermal Cycling Test Results

The visual inspection for the condition of the polyethylene diaper and its adhesion to the pipe was checked and it was noted to be very effective and no thermal cracks were observed in any of the specimens. Figures 4.1 and 4.2 show the diaper and the concrete underneath the diaper after thermal cycling. The diaper-assembly was found to be in excellent condition.

It may be noted that the open ended and short prototype specimens used in the test here do not have the indeterminacy to develop axial thermal stresses resulting from thermal cycling that would be expected under in-situ conditions for long pipes.

Figure 4.1 Thermal Cycling Test Specimens After Completion of Thermal Cycles

Figure 4.2 Thermally Cycled Test Specimens After Removal of the Diaper

b. Wet-Dry Cyclic Test Results

Eight specimens were used in this test and exposed to alternate wet and dry cycles, 48 hours in wet environment with Sabkha solution and 48 hours in dry condition, for a total period of six months. Then, powder samples were extracted from immediately underneath the diaper, from close to the diaper and from under the FRP in the main body (Figure 4.3) and were chemically analyzed for water soluble chloride and sulfate concentrations.

The results of the water soluble chloride and the sulfate concentration (percent by weight of mortar) are shown in Table 4.1. The concentration results of the chloride and the sulfate show that the diaper gives reasonable protection against penetration of the

aggressive ions, but not as effective as the fiber resin coating (FRC) which is virtually impenetrable.

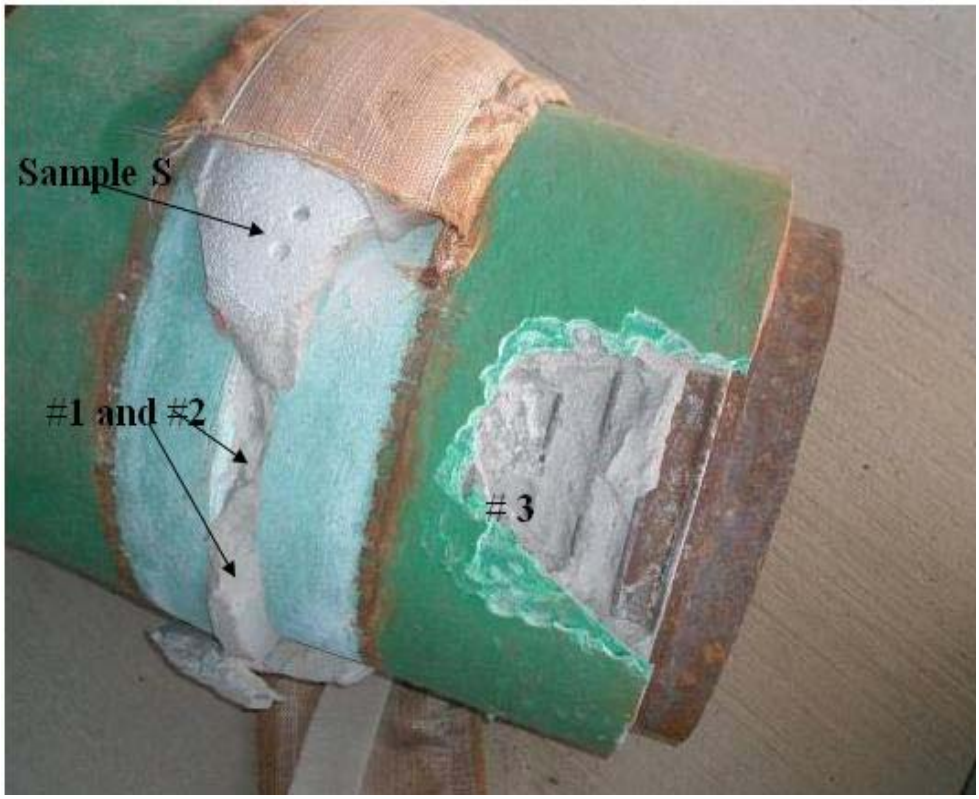

Figure 4.3 Locations of the Extracted Powder Sample

TABLE 4.1 Water Soluble Chloride and Sulfate Concentration in Wet-Dry Cyclic Test

Prototype Specimen	Powder Sample	Location of Sample	Chloride Concentration cl%	Sulfate Concentration%
BS1W	BS1WS	A	0.184	0.092
	BS1W1	B	0.072	0.016
	BS1W2		0.023	0.014
	BS1W3	C	0.023	0.014
BS2W	BS2WS	A	0.075	0.093
	BS2W1	B	0.017	0.019
	BS2W2		0.006	0.012
	BS2W3	C	0.002	0.014
EP1W	EP1WS	A	0.317	0.052
	EP1W1	B	0.009	0.015
	EP1W2		0.005	0.018
	EP1W3	C	0.005	0.014
EP2W	EP2WS	A	0.084	0.072
	EP2W1	B	0.015	0.025
	EP2W2		0.005	0.02
	EP2W3	C	0.011	0.013

TABLE 4.1 Water Soluble Chloride and Sulfate Concentration in Wet-Dry Cyclic Test Cont'd

Prototype Specimen	Powder Sample	Location of Sample	Chloride Concentration cl%	Sulfate Concentration%
RP1W	RP1WS	A	0.089	0.032
	RP1W1	B	0.006	0.015
	RP1W2		0.016	0.014
	RP1W3	C	0.005	0.017
RP2W	RP2WS	A	0.04	0.065
	RP2W1	B	0.005	0.017
	RP2W2		0.01	0.018
	RP2W3	C	0.012	0.01
ZP1W	ZP1WS	A	0.129	0.02
	ZP1W1	B	0.01	0.012
	ZP1W2		0.014	0.013
	ZP1W3	C	0.002	0.011
ZP2W	ZP2WS	A	0.028	0.094
	ZP2W1	B	0.01	0.019
	ZP2W2		0.006	0.018
	ZP2W3	C	0.004	0.013

Note: A: 0.5 cm underneath the diaper at the joint, **B**: 1-2 cm underneath the diaper at the joint, and **C**: 1-2 cm underneath the FRC at main body of pipe

Visual inspection was carried out to check the steel plate's condition at the joint and no trace of corrosion was seen on any of the specimens, as shown in Figure 4.4.

This is a significant result in view of the fact that the prototype assembled joint sections were subjected to a highly aggressive sabkha solution for a period of six months under alternate wet-dry cycling but no signs of corrosion were noted.

Figure 4.4 Steel at the Joint (No Trace of Corrosion) after Completion of Wet-Dry Cyclic Test

It may be concluded that the chloride penetration in mortar is minimal in the six months of mortar wet/dry cyclic test. However, the chloride penetration at the joint is relatively higher than in the main glass fiber coated pipe section.

4.1.2 TESTS RESULTS OF LABORATORY SCALE MORTAR SPECIMENS

Three different tests on the small scale specimens, natural corrosion process, high exposure chloride and accelerated corrosion test, were done and their results as following:

a. Natural Corrosion Process test results

The measured values of corrosion current densities using linear polarization resistance technique at different periods, six periods, of exposure to hot and humid environment are shown collectively in Table 4.2 for all test specimens. The average of the two values recorded for duplicates of each specimen type was taken as the representative value for that specimen.

Table 4.3 [50], gives the values of the level of corrosion activity which are known as the theoretical benchmarks for the rate of corrosion. These standard values can be used as a point to find out the degree of corrosion taking place in a corroding specimen. Based on the criteria shown in Table 4.3[50], it was observed that all specimens, exclusive of NCEP which had steel plates coated with epoxy, were in the state of active corrosion on the first day of measurement (ten days from casting), as the corrosion current density far exceeded the passive limit of 0.1 $\mu A/cm^2$.

TABLE 4.2 Measured Corrosion Current Densities I_{corr} for Specimens Under Natural Corrosion

Specimens	**t = 10 days**	**t = 15 days**	**t = 20 days**	**t = 25 days**	**t = 30 days**	**t = 35 days**
	I_{corr} ($\mu A/cm^2$)	I_{corr} ($\mu A/cm^2$)	I_{corr} ($\mu A/cm^2$)	I_{corr} ($\mu A/cm^2$)	I_{corr} ($\mu A/cm^2$)	I_{corr} ($\mu A/cm^2$)
NCBS	3.15	3.33	1.68	4.31	3.38	3.18
NCEP	0.12	0.17	0.16	0.21	0.25	0.27
NCRP	1.35	3.86	1.68	4.05	2.29	1.90
NCZP	1.26	2.16	1.14	2.26	1.78	1.14

NCBS (bare steel); NCEP (epoxy-coating); NCRP (red oxide); NCZP (zinc primer)

*'t' is time from casting

TABLE 4.3 Typical Corrosion Rates of Steel in Concrete [50]

Rate of Corrosion	Corrosion current density (I_{corr}) in $\mu A/cm^2$	Corrosion penetration rate in μm/year
High	10 to 100	100 to 1000
Medium	1 to 10	10 to 100
Low	0.1 to 1	1 to 10
Passive	Less than 0.1	< 1

A variety of factors affect the measured values of corrosion current densities in Table 4.2 such as number of localized pitting corrosion, test and physical conditions. Because of such effects, there is variation in the measured values of corrosion rate for a specimen with time as shown in Table 4.2. Once steady-state corrosion is reached, test specimens under unchanged environmental conditions generally show more or less steady readings with small fluctuations. The last two readings (t = 30 and 35 days) represent steady-state conditions for all specimens with the exception of ones with epoxy-coated plates. It is well-known from Table 4.2 that data for the last two sets of measurements (t = 30, 35) are reasonably consistent. Based on this, it is likely to assign a steady-state value of I_{corr} as follows:

Bare plate (NCBS): I_{corr} = 3.28 μA/cm^2

Epoxy-coated plate (NCEP): I_{corr} = 0.26 μA/cm^2

Red-oxide coated plate (NCRP): I_{corr} = 2.10 μA/cm^2

Zinc primer coated plate (NCZP): I_{corr} = 1.46 μA/cm^2

It should be noted that NCEP specimens had negligible or no corrosion, and therefore steady-state corrosion was not reached in over 30 days from the time of casting.

Comparing the results of I_{corr} in Table 4.2 to the standard ranges of I_{corr} shown in Table 4.3, it is clear that epoxy-coated specimens have performed remarkably well compared with the rest of the specimens. The I_{corr} magnitudes were less than 0.3 μA/cm^2 after 35 days, in place of practically passive corrosion state, because a value of I_{corr} less than 0.3 μA/cm^2 is viewed by most as the limiting value of I_{corr} for the passive state.

All other three types of steel plate (bare, red-oxide and zinc primer) reached active corrosion of medium intensity right from the first day of measurement (ten days from casting). The corrosion rate in bare steel was highest, as expected. In terms of relative performance, both red-oxide and zinc primer can be rated about the same as both exhibited similar I_{corr} values after 35 days. Considering the results of the bare steel (control specimen), it can be proved that coating reduces rate of corrosion, as it provides protection to the parts of steel other than those where localized pitting corrosion takes place.

It is clear from the test results given in Table 4.2, that the chloride bearing mortar containing 12% admixed sodium chloride by percentage weight of mortar is extremely violent in promoting corrosion. For bare steel, the corrosion was expected to occur almost immediately, as the threshold value of water-soluble Cl^- to promote corrosion is about 0.3% by weight of cement content, and the used Cl^- content in the mortar with 2:1 sand-cement ratio far exceeded the limit. The coating of red oxide and zinc primer did not seem to delay much the initiation of corrosion because both showed signs of corrosion at the first measurement.

It was not possible to pick up the exact time of corrosion initiation for the two types of coatings and therefore it is difficult to point out which one of the two coatings would have longer initiation period under the adopted test conditions. Nevertheless, it is clear that neither red oxide nor zinc primer would perform well for a longer time in a highly corrosive environment.

The test was stopped after 35 days from casting, the last measurement time, for all the three specimens types: red oxide, zinc primer and bare steel, and continued for the epoxy paint coating specimens 38 days more (73 days from casting). The measurement of the I_{corr} was taken at that time for the epoxy paint coating specimens and the average of the two values recorded for these specimens was taken as the representative value which equals to 1.303 $\mu A/cm^2$.

From a comparison of the relative performances of the three types of coating, it is clear that the epoxy coating has much longer corrosion initiation time in a given corrosive environment than those for the red oxide and zinc primer coatings. Under test conditions,

epoxy coating has exhibited much superior corrosion-resistance property than the two other coatings by delaying the corrosion initiation time.

b. High Chloride Exposure

For this test in which chloride-free specimens were ponded with 10% NaCl solution, two sets of specimens were used: one set without using the polyethylene diaper and the other set using diaper to observe the effect of diaper, if any, on the chloride ingress. For each set, two specimens were cast for each of the following cases of coating on the embedded steel plate: (i) bare steel, (ii) epoxy-coating, (iii) red-oxide coating and (iv) zinc-primer coating.

- **Chloride Penetration**

The measurement of the amount of chloride penetration into the specimens was measured at four intervals of the ponding period t: t = 60 days, t = 74 days, t = 90 days and t = 160 days. At each interval, the powdered samples were extracted from each specimen by drilling at 5 mm and 10 mm depths from the top of the specimens (ponded face) for specimens without diaper, and 10 mm and 15 mm for specimens with diaper. For the forth interval, at t = 160 days, the powdered samples were extracted from each specimen by drilling at 5 mm, 10 mm and 22 mm (on the steel strips surfaces) depths from the top of the specimens (ponded face) for specimens without diaper, and 10 mm, 15 mm and 18 mm (on the steel strips surfaces) for specimens with diaper. The powdered samples were analyzed using chromatographic method.

The measured values of water-soluble chloride content at the first three time intervals are collectively shown in Tables 4.4 and 4.5 for specimens without and with

diapers, respectively, using average values for the duplicate specimens for each group and in Tables 4.6 and 4.7 for specimens without and with diapers at the fourth interval (t = 160 days) . The chloride build-up increases with increase in exposure time as expected, and this is evidenced in data presented in Tables 4.4, 4.5, 4.6 and 4.7 for all samples.

As all the specimens were cast using the same mortar mix, it is expected that all specimens without diaper should show similar chloride concentration. From the data in Tables 4.4 and 4.6, it is observed that all values of chloride content for a particular exposure period are reasonably close. To observe the variation from a mean value, the calculated average values for the four specimens are shown in Tables 4.4 and 4.6 for each time period, t. It can be seen that the variation of individual values of chloride content from this mean value is small, and therefore the mean values can be taken as the chloride content at the depths of 5 mm and 10 mm for each value of time 't' and at depth of 22 mm for the forth interval.

Similar observations can be made for specimens cast with diaper. Although the values of measured chloride content in Tables 4.5 and 4.7 are somewhat more scattered than the values in Tables 4.4 and 4.6, reasonable range-bound limits can be seen. The variability in values is partly attributed to the difficulty in maintaining more exact depths for the diaper-wrapped specimens. Again, the individual readings for different specimens for a given, t are in reasonable agreement with the average values shown in Tables 4.5 and 4.7.

TABLE 4.4 Water Soluble Chloride Contents in Ponded Specimens without Diaper

Test Specimens	Chloride Content as Percentage Weight of Mortar					
	Depth from exposed face = 5 mm			Depth from exposed face = 10 mm		
	t = 60 days	t = 74 days	t = 90 days	t = 60 days	t = 74 days	t = 90 days
PBS	0.148	1.080	1.253	0.088	0.871	1.070
PEP	0.118	0.861	0.988	0.094	0.595	0.757
PRP	0.132	0.883	1.232	0.109	0.765	1.132
PZP	0.295	1.035	1.257	0.142	0.810	0.937
Average for all specimens	**0.173**	**0.965**	**1.183**	**0.108**	**0.760**	**0.974**

Note: PBS (bare steel); PEP (epoxy paint); PRP (red oxide); PZP (zinc primer)

TABLE 4.5 Water Soluble Chloride Contents in Ponded Specimens with Diaper

Test Specimens	Chloride Content as Percentage Weight of Mortar					
	Depth from exposed face = 10 mm			Depth from exposed face = 15 mm		
	t = 60 days	t = 74 days	t = 90 days	t = 60 days	t = 74 days	t = 90 days
PDBS	0.060	0.099	0.988	0.031	0.098	0.541
PDEP	0.115	0.359	0.531	0.047	0.288	0.384
PDRP	0.059	0.187	0.298	0.025	0.091	0.210
PDZP	0.041	0.267	0.792	0.033	0.142	0.488
Average for all specimens	**0.069**	**0.228**	**0.652**	**0.034**	**0.155**	**0.406**

Note: PDBS (bare steel); PDEP (epoxy paint); PDRP (red oxide); PDZP (zinc primer)

TABLE 4.6 Water Soluble Chloride Contents in Ponded Specimens without Diaper: t= 160days

Test Specimens	Chloride Content as Percentage Weight of Mortar at t = 160days		
	At depth = 5mm	At depth = 10mm	At depth = 22 mm (Corresponds to Steel Surface)
PBS	2.106	1.779	1.211
PEP	1.589	1.382	1.072
PRP	1.931	1.672	1.261
PZP	1.790	1.567	1.270
Average for all specimens	**1.854**	**1.600**	**1.204**

Note: PBS (bare steel); PEP (epoxy paint); PRP (red oxide); PZP (zinc primer)

TABLE 4.7 Water Soluble Chloride Contents in Ponded Specimens with Diaper: t= 160days

Test Specimens	Chloride Content as Percentage Weight of Mortar at t = 160days		
	At depth = 10mm	At depth = 15mm	At depth = 18 mm (Corresponds to Steel Surface)
PDBS	1.299	1.072	1.011
PDEP	0.624	0.501	0.468
PDRP	0.888	0.711	0.736
PDZP	1.120	0.906	0.812
Average for all specimens	**0.983**	**0.797**	**0.757**

Note: PDBS (bare steel); PDEP (epoxy paint); PDRP (red oxide); PDZP (zinc primer)

A comparison of the chloride content data at the depth of 10 mm from the ponded surface for the specimens with diaper (Tables 4.5 and 4.7) and without diaper (Tables 4.4 and 4.6), shows that the diaper-wrapped specimens had smaller chloride concentration in all specimens for all three chloride exposure periods. On the basis of average values, the measured chloride content in specimens with diaper at the depth of 10 mm were 0.069% for t = 60 days, 0.228% for t = 74 days, 0.652% for t = 90 days, and 0.983% for t = 160days, compared with the corresponding values of 0.108%, 0.760%, 0.974%, and

1.600% in specimens without diaper. This revelation indicates that the diapers as used, slows down chloride ingress, at least in the early stages of exposure. This is a positive attribute of the diaper, as it provides some resistance to chloride ingress from external sources.

- **Chloride Penetration Rate**

Of the several known processes for chloride penetration into a cementitious body from an outside source, the most dominant mode of chloride transport processes are diffusion and absorption. In a moist cementitious body, diffusion is the flow of ions from a higher concentration to lower concentration through the pore water. Diffusion of chloride in concrete is a complex process, particularly in view of the binding effect of chloride in which part of the moving chloride is chemically bound with C_3A (tricalcium aluminate) in cement, reducing in effect the amount of free flowing chloride. Many researchers have noted that for normal concrete, the chemical binding of chloride is not high and therefore, for a simple mathematical modeling of chloride transport, binding effect can be neglected. This has encouraged researchers to use Fick's second law of diffusion to model the chloride penetration into concrete.

Fick's second law of diffusion for specimens with no initial chloride content is

$$C_x = C_s \left[1 - erf \frac{x}{2\sqrt{D_e t}} \right] \tag{4.1}$$

in which C_x = chloride concentration at a depth x from exposed surface.

C_s = chloride concentration at the surface

erf = error function

D_e = effective diffusion coefficient

t = exposure time (elapsed time)

In the case of sand-cement mortar mix used in this experiment, the amount of cement by the weight of the sample was high as the mix proportion was 2:1 (sand: cement). Thus, a considerable amount of chemical binding of chloride is possible and consequently this may raise the question of validity of Eq. (4.1) for chloride transport in sand-cement mortars with high cement content.

However, an attempt has been made to calculate D_e using Eq. (4.1). To avoid conversion of salt concentration to a percentage weight of mortar (which requires information about mortar porosity), an indirect approach is used. From two data points, one can determine D_e from:

$$C_{x1} = C_{x2}\left[\frac{\left(1 - erf\,\frac{x_1}{2\sqrt{D_e t}}\right)}{\left(1 - erf\,\frac{x_2}{2\sqrt{D_e t}}\right)}\right] \qquad (4.2)$$

When C_{x1} = measured chloride concentration at distance x_1

C_{x2} = measured chloride concentration at distance x_2

In Eq. (4.2), x_1 is 5 mm and x_2 is 10 mm for specimens without diaper and x_1 is 10 mm and x_2 is 15 mm for specimens with diaper.

As the values of C_{x1} and C_{x2} are known (Tables 4.4, 4.5, 4.6 and 4.7), the D_e can be calculated for each t. Using Eq. (4.2), the values of D_e were calculated using the average values of chloride contents in Tables 4.4, 4.5, 4.6 and 4.7, and are shown in Table 4.8.

TABLE 4.8 Values of Apparent Diffusion Coefficient, D_e

Specimens	Diffusion Coefficient De in cm2/sec			
	t= 60 days	t= 74 days	t=90 days	t=160days
Without diaper	15.85E-08	36.85E-08	41.877E-08	37.543E-08
With diaper	12.78E-08	22.99E-08	13.987E-08	25.977E-08

Past research on diffusion in chloride in concrete has pointed out that D_e is expected to vary with time, as the pore structure of concrete changes with chloride-binding. Other researchers assume chloride diffusivity to be a function of chloride levels. On the basis of Eqs. (4.1 and 4.2), the values of the D_e calculated can only be used as indicated values, and not true values. The average of D_e is about 33.03×10^{-8} cm^2/s for the mortar without diaper and 18.93×10^{-8} cm^2/s for the diaper-wrapped mortar. The chloride penetration in diaper-wrapped specimens is expected to be less than that for specimens without diaper in view of the lower value of D_e. This is confirmed from the observed data.

- **Corrosion Initiation Time**

Using linear polarization resistance technique measurements, the measured average values of duplicate specimens of the corrosion current densities, I_{corr} (μA/cm2), for specimens without diaper are in Table 4.9 and for specimens with diaper are in Table 4.10.

TABLE 4.9 Values of I_{corr} ($\mu A/cm^2$) For Ponded Specimens without Diaper

Specimen #	t = 90 days	t = 157 days	t = 160 days
PBS	1.144	6.982	4.704
PEP	0.036	0.152	0.115
PRP	0.012	0.475	0.461
PZP	0.358	2.090	1.511

TABLE 4.10 Values of I_{corr} ($\mu A/cm^2$) for Ponded Specimens with Diaper

Specimen #	t = 90 days	t = 157 days	t = 160 days
PDBS	0.433	1.900	1.051
PDEP	0.002	0.063	0.051
PDRP	0.0024	0.276	0.287
PDZP	0.261	0.768	0.680

For specimens without diaper, Table 4.9, the average value of the duplicate uncoated (bare) specimens at time t = 90 days from starting the chloride exposure is 1.144 μA/cm^2, epoxy coated specimens is 0.036 μA/cm^2, red oxide coated specimens is 0,012 μA/cm^2, and for zinc primer coated specimen is 0.358 μA/cm^2. However, the average value of I_{corr} for red oxide coated specimens at t = 160 days is 0.461 μA/cm^2 and for epoxy coated specimens at t = 160 days is 0.115 μA/cm^2.

Comparing these results in Table 4.9 with the typical corrosion rates of steel in concrete, Table 4.3 [50], it can be observed that the zinc primer coated specimens were in active corrosion (low level from t = 90days and medium level from t = 160 days) because it exceeded 0.1 μA/cm^2 whereas the uncoated (bare steel) specimens were in active corrosion (medium level from t = 90 days onward).

Nevertheless, both epoxy paint coated specimens and red oxide coated specimens were in passive case (no corrosion) at t = 90 days as their I_{corr}'s didn't exceed the border level of corrosion, 0.1 μA/cm^2. At t = 160 days, the red oxide coated specimens were in active corrosion (low level) but the epoxy paint coated specimen cannot be seen that it is in the active corrosion case as the value of I_{corr} (0.115 μA/cm^2) is still close to the border corrosion value, 0.1 μA/cm^2.

Based on the measured corrosion current densities by which the corrosion initiation time for each type of specimens was determined, the corresponding chloride concentration can be calculated using the values of diffusion coefficients (Table 4.8), average values of the chloride concentration Table 4.4 and applying Equation 4.2, in both uncoated specimens and zinc primer coated specimens. The values of chloride

concentrations at depth 22 mm at the first three time intervals t = 60, 74, and 90 days are calculated and given in Table 4.11 using the average values of the diffusion coefficient De (3.156E-07 cm2/s) and the average calculated surface chloride concentrations Cs, 1.29% of total mass of mortar. In case of the forth interval, t = 160 days, the measured values of the chloride concentration at 22 mm depth is shown in Table 4.6 and again in Table 4.11.

TABLE 4.11 Values of Cl% at the Steel Strip Surface for Ponded Specimens Without Diaper

Time From Starting the Test	Cl Content at 22 mm (Corresponding to Steel Strip Surface)	
	% Weight of Mortar	% Weight of Cement
t = 60 days	0.289	0.578
t = 74 days	0.353	0.706
t = 90 days	0.414	0.828
t = 160 days	1.204	2.408

From Table 4.11, the chloride concentration at the steel strip surface for t = 90 days is 0.289% of the mortar mass, approximately 0.578% of cement mass, which exceeded the threshold chloride value (0.3% of cement mass) that induce corrosion for steel. For the zinc primer coated specimens, the value of the chloride concentration at t = 90 days (the initiation corrosion time based on I_{corr} measurements) is 0.414% of mass

mortar which approximately equals to 0.828% of cement mass, and may therefore be considered as the threshold chloride value for such coated specimen type.

For the red oxide coated specimens, the average value of the measured chloride concentration at depth 22 mm (Table 4.11) is 1.204% of total mass of mortar (2.408% of cement mass) which can be considered as the chloride threshold value induced corrosion for this type of coated specimen. However, the epoxy coated specimens were not considered to be in the active corrosion based on the value of Icorr (0.115 $\mu A/cm^2$) Table 4.9 up to time t = 160 days. This means that, the threshold chloride concentration value of this coating specimen type is more than 2.408% of cement mass. Such observation was satisfied from the natural corrosion process test in which the high chloride built-in mortar (14.4% of cement mass) was used and the corrosion initiation time for epoxy paint coated specimens was delayed more than 35 days. The values of the approximate corrosion initiation time and corresponding chloride concentration values of each type of coated specimen are in Table 4.12.

TABLE 4.12 Approximate Threshold Chloride Concentration Values and Corresponding Corrosion Initiation Times of Ponded Specimens without Diaper

Specimen Type	Approximate Time Of Initiation Corrosion From Starting The Test (Days)	Approximate Threshold Chloride Concentration Percentage Weight of Cement
PBS	Less than 60	Less than 0.6
PEP	More than 160	More than 2.4
PRP	160	2.4
PZP	90	0.8

The results in Table 4.12 are satisfied qualitatively by visual inspection after broken down the ponded specimens and taken out the coated and uncoated steel strips as shown in Figures 4.5 and 4.6.

Figure 4.5 Bare, Red Oxide, and Zinc Primer Coated Steel Strips of Ponded Specimens after the Completion of the High Exposure Chloride Test

Figure 4.6 Epoxy Paint Coated Steel Strips of Ponded Specimen after the Completion of the High Exposure Chloride Test

Using the chloride data for t = 160 days, the average water soluble chloride concentration Cl% of mortar mass versus depth (cm) from the ponded face of the ponded specimens without and with diaper plots of high chloride exposure test are in Figures 4.7.

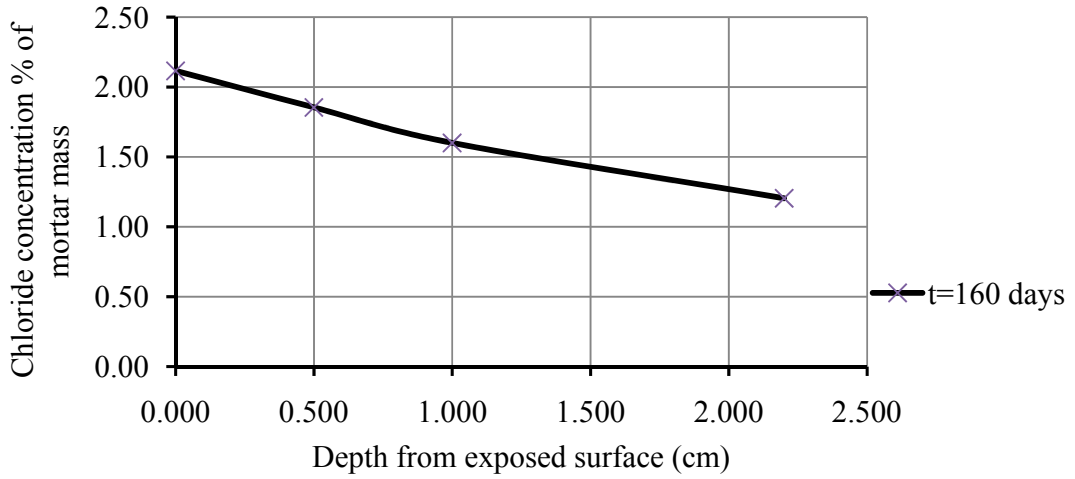

(a) Ponded Specimens without Diaper

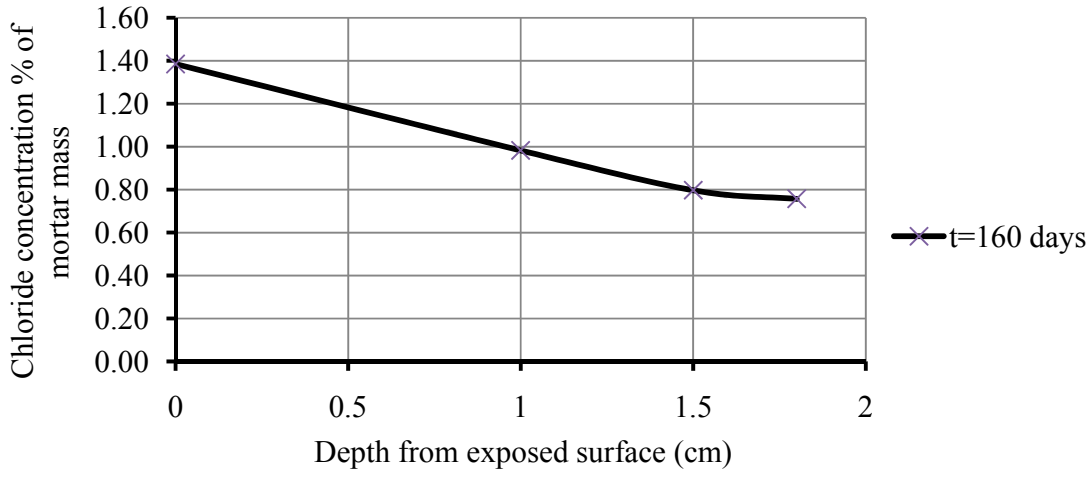

(b) Ponded Specimens with Diaper

Figure 4.7 Chloride Concentrations Cl% Of Mortar Mass Versus Depth From The Exposed Face Of Ponded Specimen at the Forth Interval.

c. Accelerated Corrosion Test Results

In this test, a total of sixteen specimens were subjected to accelerated corrosion by impressing a constant potential of 4 volts for two durations, 4 and 8 days.

Current versus time data

For all specimens with bare and coated steel plates, the values of current passing in the accelerated corrosion circuitry as a result of the applied voltage, recorded for a period of 4 and 8 days, are typically plotted in Figures 4.8 through 4.15.

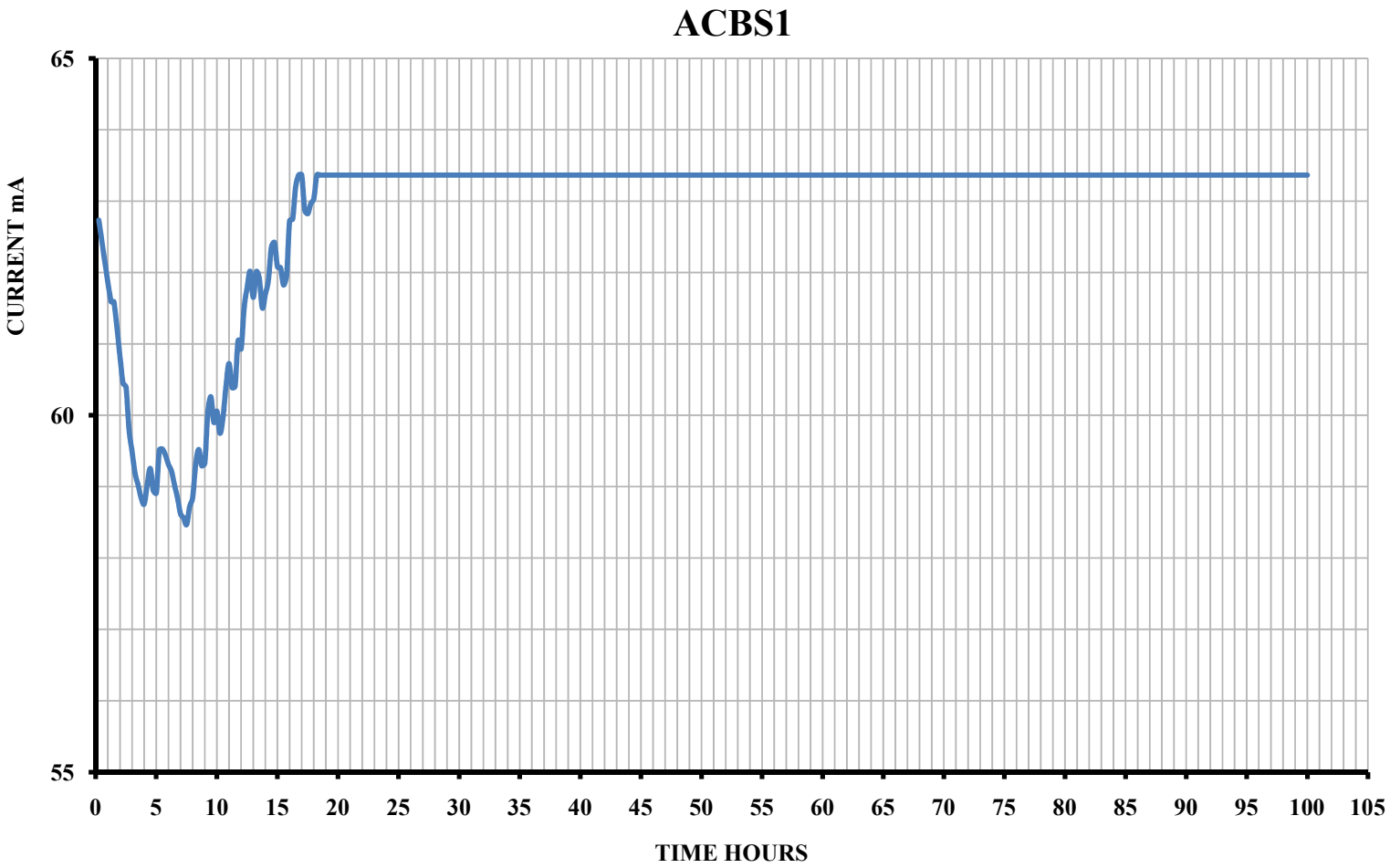

Figure 4.8 Current versus Time Plot for Uncoated Specimen Subjected To Accelerated Corrosion for a *Duration of 4 Days*

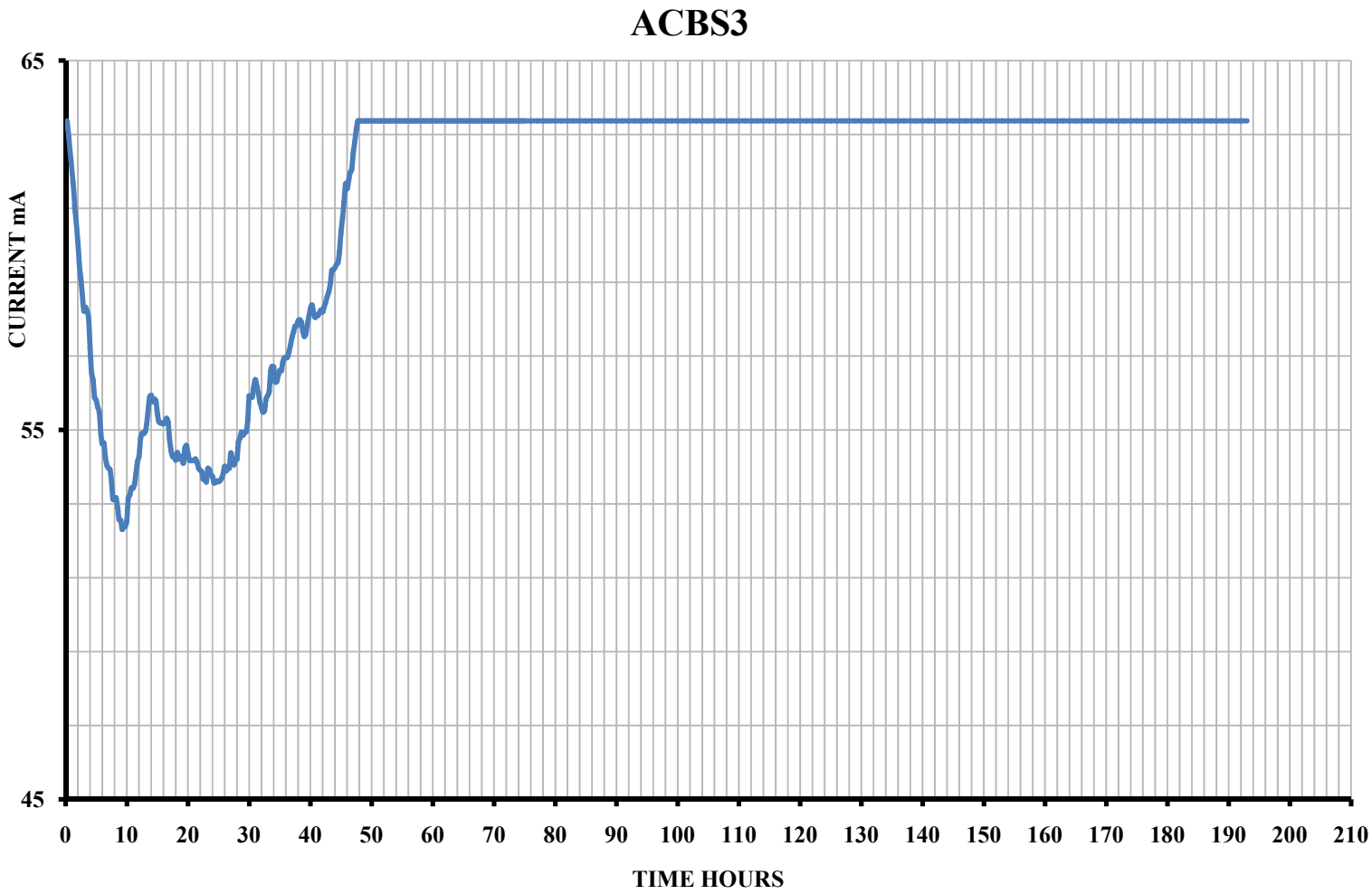

Figure 4.9 Current versus Time Plot for Uncoated Specimen Subjected To Accelerated Corrosion for a *Duration of 8 Days*

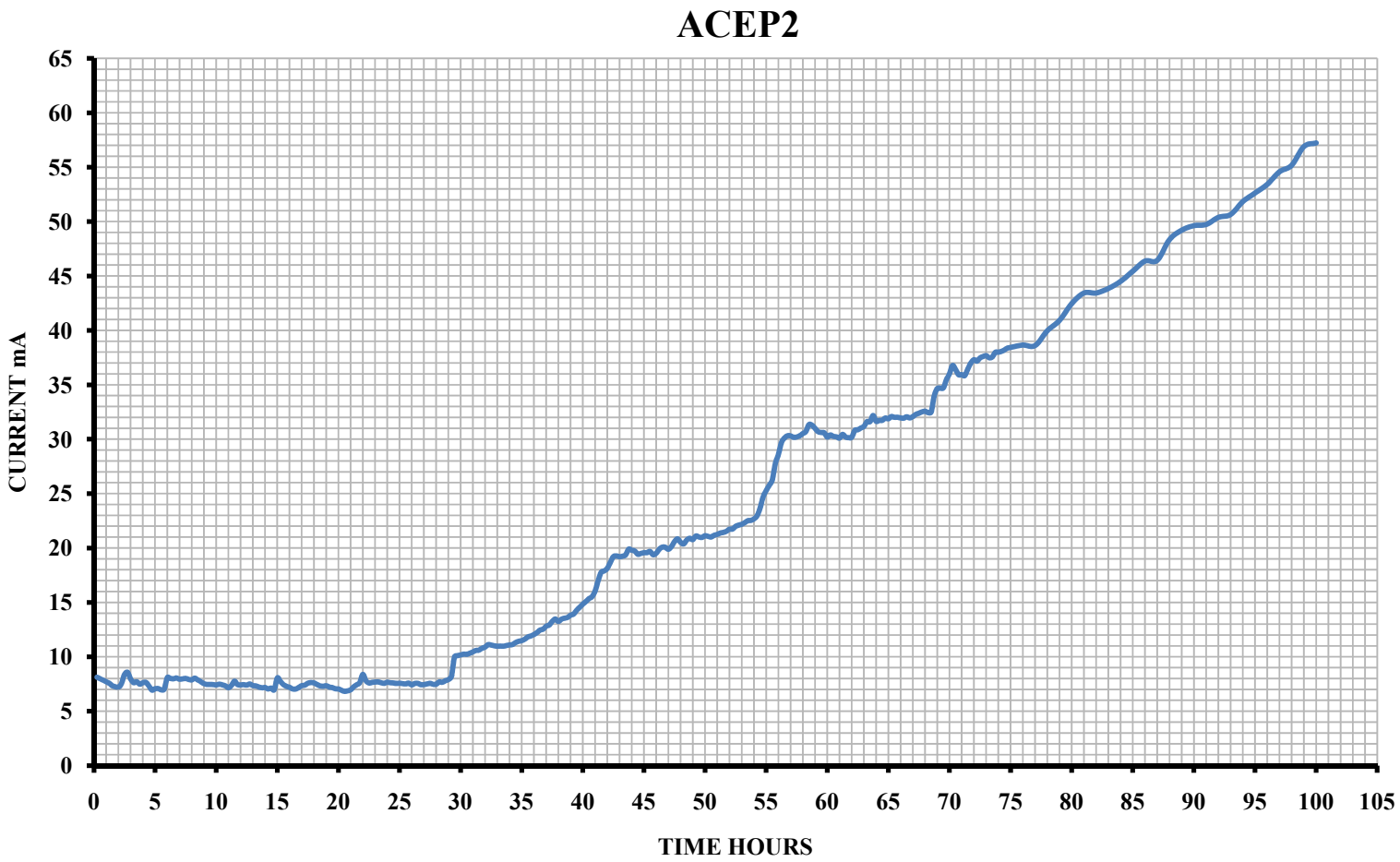

Figure 4.10 Current versus Time Plot for Epoxy-Coated Specimen Subjected To Accelerated Corrosion for a *Duration of 4 Days*

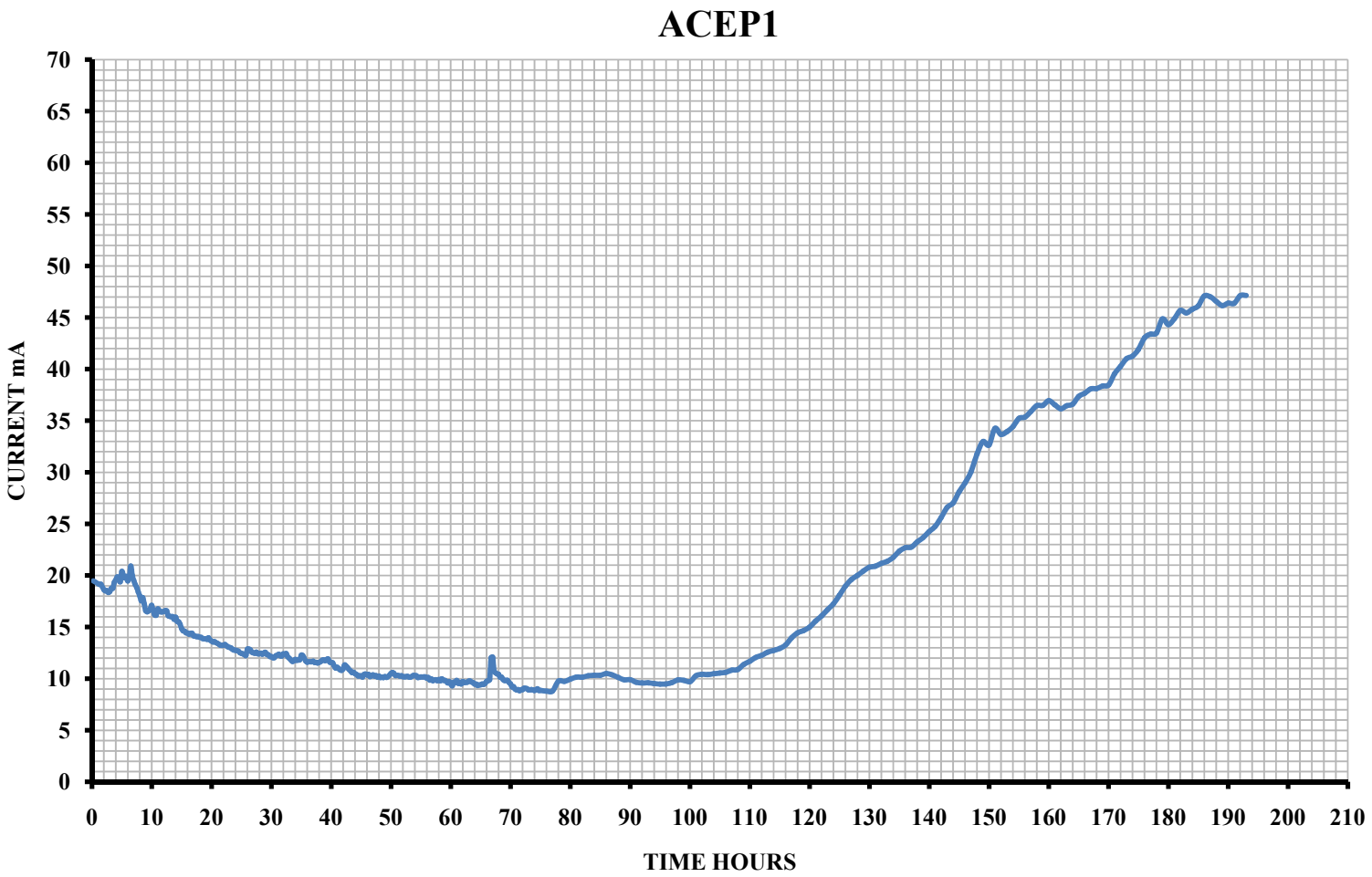

Figure 4.11 Current versus Time Plot for Epoxy-Coated Specimen Subjected To Accelerated Corrosion for a *Duration of 8 Days*

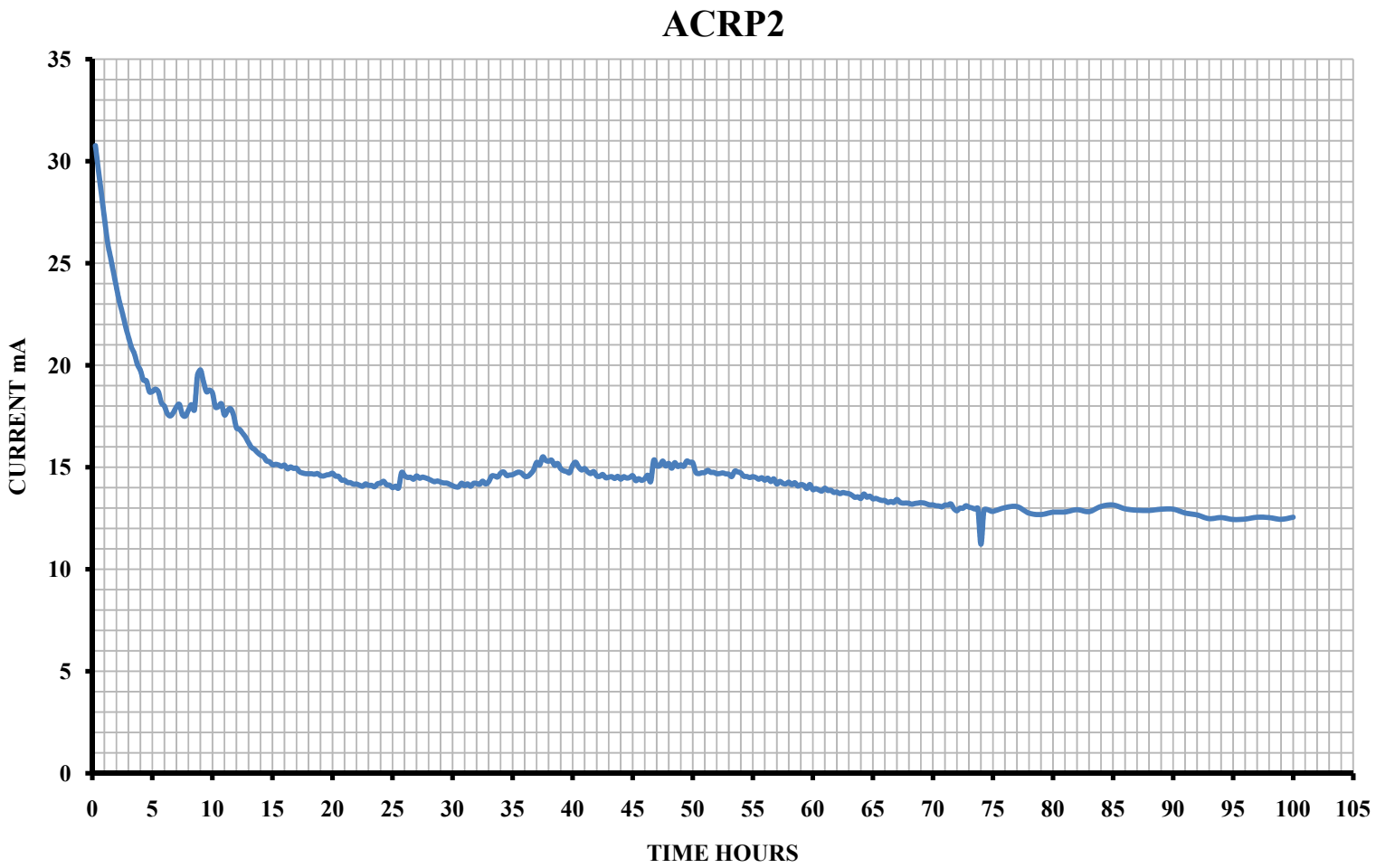

Figure 4.12 Current versus Time Plot for Red Oxide-Coated Specimen Subjected To Accelerated Corrosion for a *Duration of 4 Days*

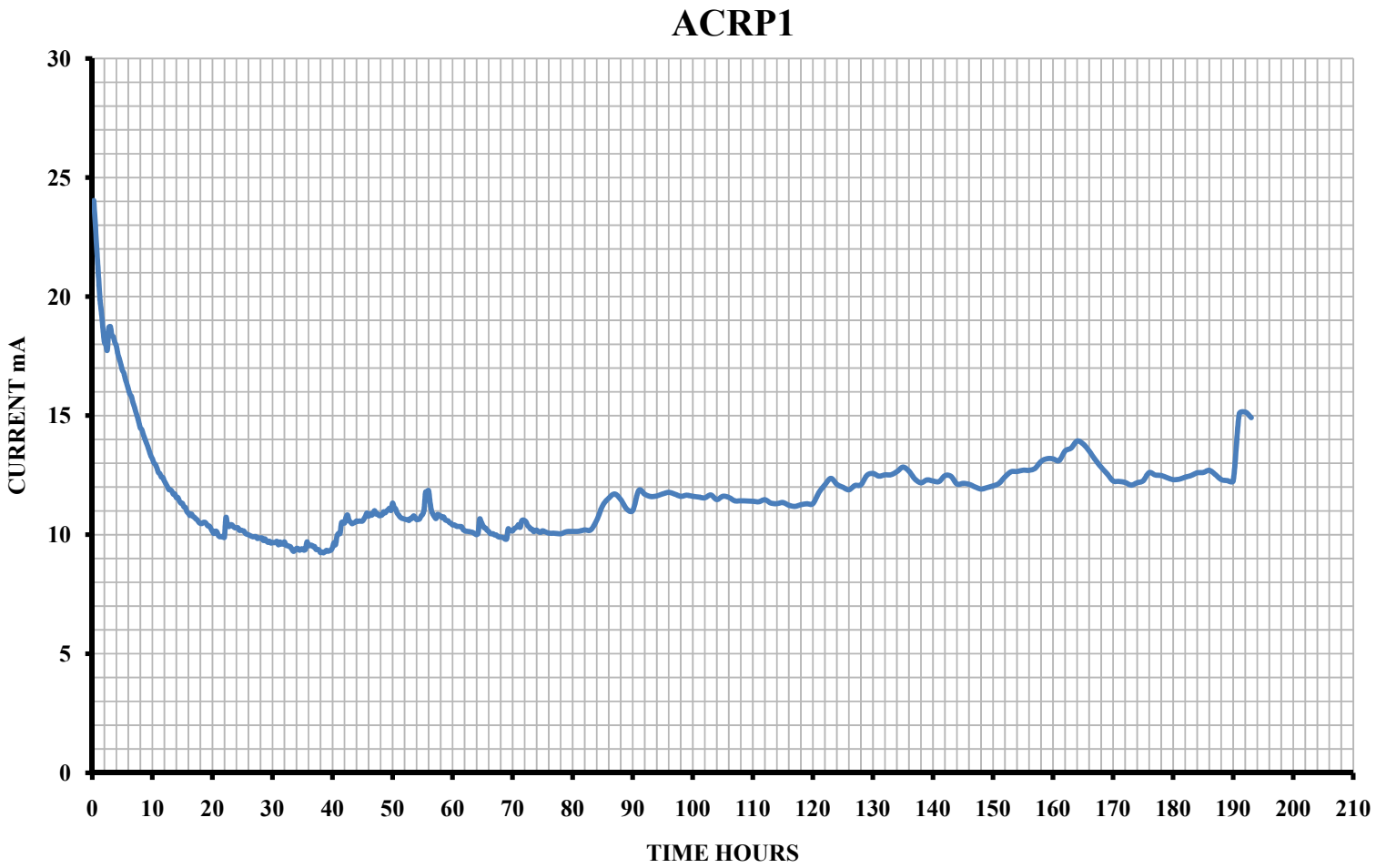

Figure 4.13 Current versus Time Plot for Red Oxide-Coated Specimen Subjected To Accelerated Corrosion for a *Duration of 8 Days*

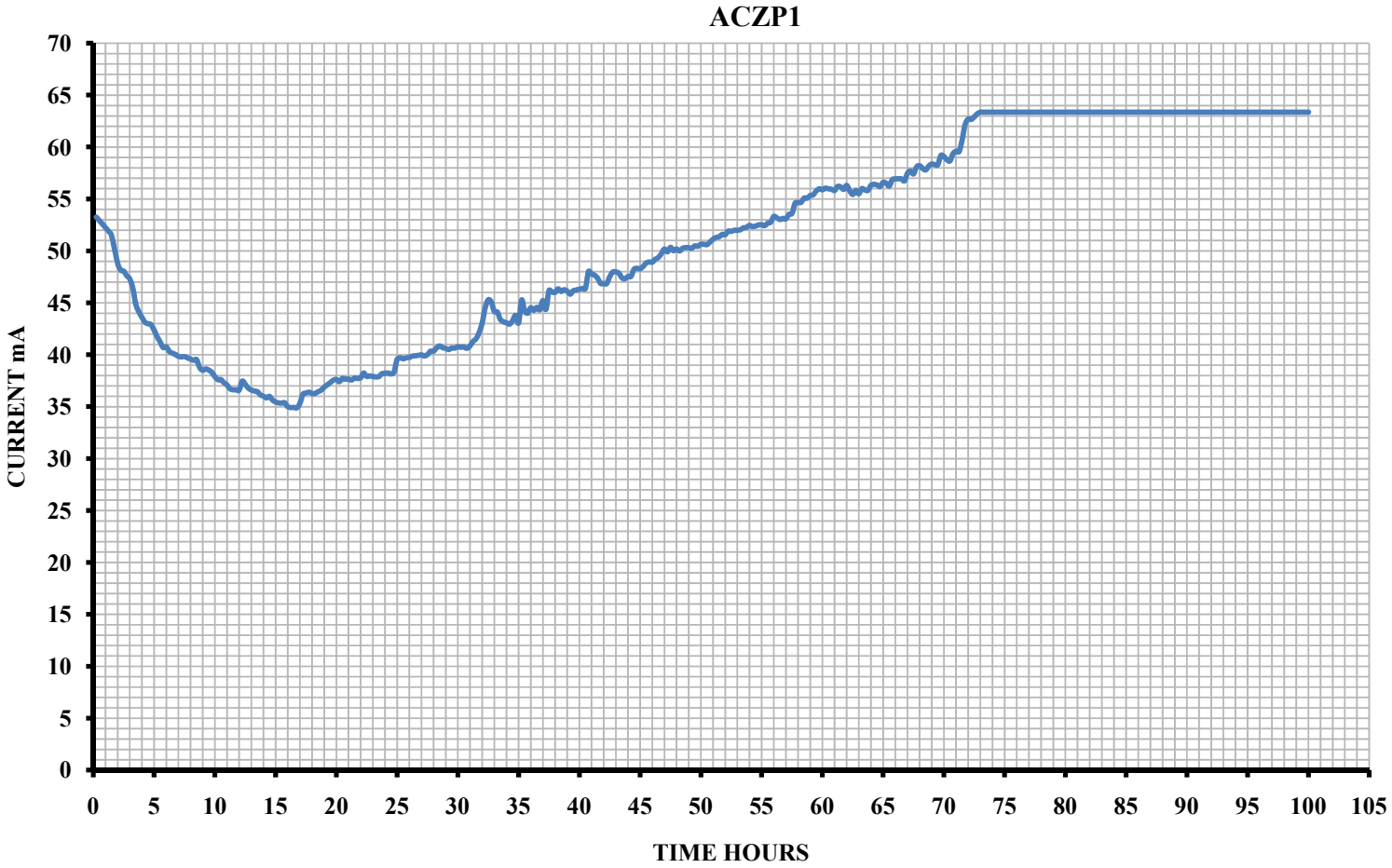

Figure 4.14 Current versus Time Plot for Zinc Primer-Coated Specimen Subjected To Accelerated Corrosion for a *Duration of 4 Days*

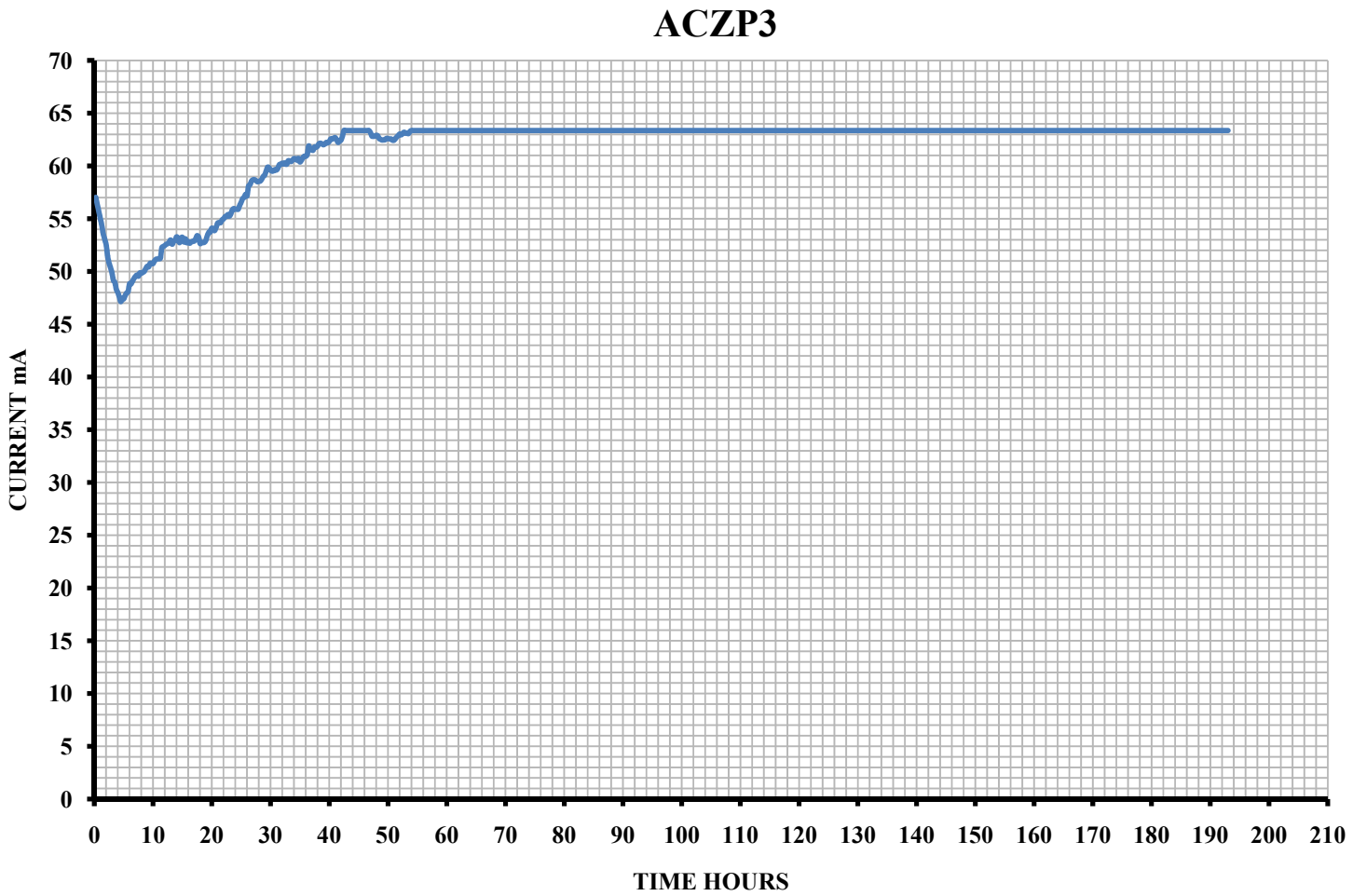

Figure 4.15 Current versus Time Plot for Zinc Primer-Coated Specimen Subjected To Accelerated Corrosion for a *Duration of 8 Days*

From the above accelerated corrosion test result plots, three important indices can be used to evaluate the relative performance of the coatings as following:

(i) Initial circuit current, I_i

(ii) Corrosion initiation time, t_i

(iii) Steady-state circuit current, I_s

The initial circuit current, I_i, is the recorded current in mA flowing into the circuit at 4.0 V when the power is switched on. In Figs. 4.8-4.15, I_i correspond to zero hour. Corrosion initiation time, t_i, is the observed time consumed in initiating corrosion of steel plate. Whenever corrosion occurs, the coating at the location of corrosion cells breaks out and becomes less resistant, resulting into increased flow of current. Thus an ideal plot of time versus circuit current at a fixed impressed voltage would show a noticeable sharp change in the magnitude of current. The time at which this change in current occurs is taken as the time t_i. Because of the small fluctuations that are normally observed in current versus time plots, the corrosion initiation would be approximate in most cases.

Once the corrosion rate is more or less constant, the corresponding current reaches a steady state (I_s), the value of which can be determined from the current-time plots.

The average values of I_i, t_i and I_s are shown in Table 4.13 for all four types of specimens.

TABLE 4.13 Values I_i, t_i and I_s

Type of Coating	Initial Circuit Current, I_i (mA)	Corrosion Initiation Time, t_i (Hours)	Steady-State Circuit Current, I_s (mA)
Uncoated	63	10	64
Epoxy-Coated	14	29	52
Coated with Red Oxide Primer	28	14*	14
Coated with Zinc Primer	56	11	60

* See explanation in the text.

With regard to I_i, the initial circuit current, it is observed that the bare steel plate had the highest value of 63 mA, confirming the fact that the bare steel has the least resistance and therefore it had the highest current. Of the three coatings, epoxy coating resulted in higher resistivity that led to lowest current. Plates with zinc primer also showed higher current, indicating that effective resistivity of the specimens is not much higher than the specimens with bare steel.

On the basis of the initial resistivity of the specimen with embedded coated and uncoated steel plates, it can be concluded that both epoxy coating and red oxide primer coating offers higher circuit resistance compared to bare steel and zinc primer coating.

From the indicative values of corrosion initiation time t_i, in Table 4.13, it is seen that t_i for uncoated and zinc primer coated steel plates is smaller than t_i observed in the case of epoxy-coated and red-oxide coated plates. It should be noted that in the case of red-oxide coating, the current-time plots did not show any clear shift in current magnitude like others. As the steady-state current is reached after some hours of current

application, the time taken to reach steady-state is considered as the time for corrosion initiation. The epoxy-coated plates appear to have the highest value of corrosion initiation time at t_1 = 29 hours. Comparatively, the bare steel plate showed active corrosion after only about 10 hours. It can be concluded that all coatings delayed the onset of active corrosion, but the delay is more evident in the case of epoxy coating and red oxide primer coating.

With regard to steady-state circuit current, I_s, data in Table 4.9 show some interesting results. Both epoxy coating and zinc primer coating showed similar I_s values which are close to the steady state current for the bare plate. This suggests that once steady-state corrosion in epoxy coated steel is reached, the resistivity of specimens falls to a level similar to that of specimens with bare steel. In other words, high corrosion-resistance of epoxy coated plate which is visible at earlier stage of accelerated corrosion breaks down with the onset of steady-state corrosion. However, that was not the case with red oxide primer, which showed much lesser value of I_s, apparently by maintaining a relatively higher level of resistivity.

Both bare steel and zinc primer coated steel have similar characteristics in terms of the three indices, I_i, t_i and I_s.

- **Gravimetric (weight loss) test data**

The results of the gravimetric test conducted on the strips extracted from the mortar after allowing them to corrode for 4 and 8 days under a constant voltage of 4 V are presented in Table 4.14.

TABLE 4.14 Gravimetric Test Results

Type of Coating	**Average Loss of Weight after 4 Days (% by mass)**	**Average Loss of Weight after 8 Days (% by Mass)**
Uncoated	6.9	9.4
Epoxy-Coated	1.8	3.5
Coated with Red Oxide Primer	2.5	3.7
Coated with Zinc Primer	5.5	11.6

From Table 4.14, it can be observed that epoxy-coated plate shows lowest metal loss after both 4 and 8 days of accelerated corrosion. The next lower metal loss was observed in red oxide coated plates. Both uncoated and zinc primer coated plates showed similar metal loss, an observation that is consistent with one made earlier while comparing the results of I_i, t_i and I_s (Table 4.13).

Table 4.14 also shows that the present increase in metal loss for epoxy coated plates in 8 days from 4 days was higher than red oxide coated plates (about 95% versus about 50%). This observation again in line with the conclusion made earlier that once the epoxy-coated plate reaches steady state corrosion, the coating loses its effectiveness as corrosion inhibitor. While after 4 days of corrosion, there was a noticeable difference between the metal loss percentages for epoxy coated and red oxide coated plates, the metal loss after 8 days of corrosion for both types of coated plates was found to be similar. This observation can be explained as follows:

After the onset of corrosion, the metal loss rate is directly proportional to the product of current and time duration ($I_{corr}t$), when I_{corr} = corrosion current density and t = active corrosion period. I_{corr} is calculated as I_s divided by the surface area of steel subjected to corrosion. The product $I_{corr}t$, known as corrosion activity index, is simply the area under the current-time plot divided by the surface area of the plate. In the case of epoxy-coated plates, after steady-state of corrosion, I_{corr} is higher but t is smaller due to delayed start of corrosion. Compared to this, red oxide primer coating has lower I_{corr} but higher t.

In accelerated corrosion, data presented in Tables 4.13 and 4.14 show that zinc primer has little effect on corrosion. It may perform better in natural corrosion process where the corrosion current is considerably small, but in this study the coating was found to be virtually ineffective in providing some resistance to corrosion.

4.2 **Electrical Resistance Assessment**

As mentioned in chapter three, the results of the accelerated corrosion test of the small scale specimens, the results of the electrical resistivity test of the (chop fiber + resin) from the past work [29] and the results of the electrical resistance test of the steel strips (coated and uncoated), were used for the electrical resistance assessment of the fiberglass resin coating, the mortar lining, and the coatings on steel plates.

The accelerated corrosion test results particularly the initial current (mA), I_i, were used for determining the electrical resistance of each specimen by applying Ohm's law and the circuit potential, 4 volts.

The values of the calculated resistances, R's, and the corresponding initial currents, I_i's, are shown in Table 4.15. Data presented in Table 4.15 show that the epoxy paint specimens have the highest resistance with average value of 349 Ω and the uncoated (bare) specimens have the lowest resistance value with 63.4 Ω as expected. The red oxide specimens have average electrical resistance of 148 Ω more than the average value of the zinc primer resistance, 73 Ω. Thus, the three coatings can be ranked in terms of their electrical resistance from highest to lowest as: epoxy paint, red-oxide and zinc primer.

TABLE 4.15 I_i and R of the Accelerated Corrosion Specimens

Specimen Type	I_i (mA)	R (Ω)
Uncoated (Bare)	63	63.4
Epoxy Paint	14	349
Red Oxide	28	148
Zinc Primer	56	73

The results shown in Table 4.15 are for the specimens consisting of cement mortar, 2.5 cm thickness, and coated and uncoated steel strips which mean that the calculated values of the electrical resistance can be considered as combined electrical resistance for each specimen. However, the composition of the cement mortar, it should be noted, was identical for all specimens.

It is known from the previous work [49] that the mortar lining (w/c = 0.5) resistance ranges between 100 Ω.m and 3900 Ω.m for 100% and 60% relative humidity, respectively. In this study, the relative humidity was 100% because the specimens were immersed in the solution during the test which means that the 100 Ω.m resistance is considered for the mortar lining.

The combined resistance includes three parts; mortar lining, steel strips and the coatings. The resistance of the uncoated specimens can be considered as the combined resistance of the steel strips and the mortar lining in order that the electrical resistance of

the coating equals to the combined resistance of the corresponding specimen reducing the resistance of the uncoated specimens. The net resistances, coatings resistances, are shown in Table 4.16.

TABLE 4.16 Net Resistances of the Accelerated Corrosion Specimens

Coating Type	Net Resistance (Ω)
Bare	0
Epoxy Paint	285.6
Red Oxide	84.6
Zinc Primer	9.6

The values of the linear polarization resistances (LPR's) and the corresponding resistances of the electrical resistance specimens are shown in Table 4.17

TABLE 4.17 LPR and the resistances of the Electrical Resistance Specimens

Specimen #	Type of Coating	Dimensions	Linear polarization Resistance LPR (Ω.cm2) Area=52 cm^2	Resistance (Ω)	Average Resistance (Ω)
BS1	BARE STEEL	175*20*8 mm	88	1.69	**1.50**
BS2			97	1.87	
BS3			49	0.94	
EP1	EPOXY PAINT	175*20*8 mm	105090	2020.96	**905.53**
EP2			15128	290.92	
EP3			21045	404.71	
RP1	RED OXIDE	175*20*8 mm	23352	449.08	**761.59**
RP2			79196	1523.00	
RP3			16260	312.69	
ZP1	ZINC PRIMER	175*20*8 mm	147	2.83	**2.51**
ZP2			113	2.17	
ZP3			132	2.54	

From Table 4.17, the values of the resistances of the specimens are somewhat different than the values in Table 4.15 because of the different techniques being used for each. However, the trend is similar; the epoxy paint specimens have the highest value followed by the red oxide and the lowest value of the zinc primer which is more than the bare steel specimens.

The results of the electrical resistivity test from the past work [29] are shown in Table 4.18. The used specimens in this test were (chop fiber + resin) with 75*150 mm in dimensions. As it is shown in Table 4.18, the average value of the two specimens (close to each other) after dividing by the specimen lengths (15 cm), 2.667 KΩ, can be considered as the electrical resistance of the fiberglass resin coating (FRC).

TABLE 4.18 Electrical Resistances of Fiberglass Resin Coating

Specimens #	**Resistance (KΩ.cm)**	**Resistance (KΩ)**
1	39.2	2.613
2	86.5	5.767
3	40.9	2.727

CHAPTER FIVE

CONCLUSION AND RECOMMENDATIONS

5.1 Conclusions

1. Prototype testing of the assembled Bell and Spigot joint section under Thermal Cycling and Wet-Dry Cycling, both for periods of six months, showed no ill effects in either of the two accelerated durability tests.

2. No cracks in the mortar or debonding of the polyethylene diaper from the mortar were noted in the Thermal Cycling test. The latter indicates thermal compatibility of the polyethylene diaper with the mortar. Absence of cracks indicates that thermal stress build up, mostly in the circumferential direction, was not enough to cause cracking or other distress of the mortar.

3. Absence of any visual evidence of corrosion in the intensive six months wet-dry cycling test in a highly aggressor Sabkha environment and low measured levels of pore chloride and sulfate reflect the effectiveness of the diaper/mortar protection system for the steel elements located in the Bell and Spigot joint. However, as expected, the diaper/mortar barrier is not as effective as the FRP coating is in the main section of the pipe.

4. In natural corrosion induced by high level of admixed chloride, epoxy-coated steel plates performed best, showing virtually a passive state of

corrosion after 35 days of casting. Both red oxide and zinc primer coated specimens showed active corrosion soon after casting.

5. From a comparison of the test data for the amount on chloride penetration into mortar specimens with and without diapers, it can be concluded that the diapers slows down chloride penetration to some extent acting as barrier. However, the joint reflects a vulnerability to chloride penetration in contrast to the main section of the pipe with its "impenetrable" FRP casting.

6. The apparent chloride diffusion coefficient for the mortar is expected to be around 33.03×10^{-8} cm^2/sec which is indicative of the mortar being more porous than sound concrete.

7. Among the three types of coatings, epoxy coating shows the longest corrosion initiation time. Initially, it provides effective corrosion resistance. However, once the steady-state corrosion is reached it performs no better than plates without coating.

8. In accelerated corrosion tests, zinc primer coating appears to have negligible corrosion resistance. Its performance is similar to that of bare steel plate.

9. Red oxide primer seems to reach low-level steady-state corrosion current soon. However, under active corrosion state its performance with regard

to metal loss is encouraging in the sense that metal loss rate is not worse than epoxy coating under active corrosion.

10. The threshold chloride values induced corrosion for the epoxy paint coated specimens was higher than for the red oxide coated specimens whereas the threshold chloride concentration induced corrosion for the zinc primer coated specimens was the smallest value among the three coatings and close to bare steel threshold value.

11. Among the three coating types, the electrical resistance of the epoxy paint coating was the highest followed by the electrical resistance of the red oxide coating but the zinc primer coated specimens had the smallest electrical resistance.

12. Fiberglass resin coating had the highest electrical resistance comparing to all used coating types and the main pipe body mortar lining where it plays the main effective role in such property.

13. Because of the nature of both the red oxide coating and the zinc primer coating as sacrificial coatings, the coating thickness plays an important role for making these coatings as effective barriers against corrosion whereas the proper application of the epoxy paint coating on the steel surface is more important factor to avoid and permeability in epoxy coated specimens.

14. Among the three coating types; epoxy paint, red oxide, and zinc primer dim coat6, the epoxy paint coating can be selected as the best performance one in such study conditions and proposed tests.

5.2 **Recommendations**

1. For zinc and red oxide coating, the coating thickness plays an important role for making these coatings as effective barriers against corrosion.

2. The proper application of the epoxy paint coating on the steel surface is an important factor to avoid any poor performance in epoxy coated specimens.

3. It is recommended that the epoxy paint coating should be used for protection against the ions penetration at the Bell and Spigot assembled joint.

4. Using the polyethylene diaper to band the sand cement mortar at the assembled joint is highly recommended as it gives barrier action against aggressive materials attack.

REFERENCES

1. Fiber Glast, Developments Corporation, "Fundamentals of Fiberglass". WWW.fiberglast.com

2. Fiber Glast Evercoat, A division of Illinois Tool Works Inc., ITW Evercoat. "Choosing the Right Resin-Epoxy Resin".

3. Wicks, Z. W. JR., Jones, F. N., Pappes,S.P, Wicks,D.A. "Organic Coatings Science and Technology ". 3rd edition, 2007.

4. Schweitezer, P.A., P.E. "Paint and Coatings, Applications and Corrosion Resistance ".2006.

5. AUCSC. "Corrosion Protection by Coatings for Water and Wastewater Pipelines".

6. http:/en.wikipedia.org/wiki/fiberglass

7. Loewenstein, K.L. "The Manufacturing Technology of Continuous Glass Fibers", New York: Elsevier Scientific. pp. 2–94. ISBN 0-444-41109-7, 1973.

8. Gupta, V.B., Kothari, V.K. "Manufactured Fibre Technology", London: Chapman and Hall. pp. 544–546. ISBN 0-412-54030-4, 1997

9. Volf, M.B. "Technical Approach to Glass", New York: Elsevier. ISBN 0-444-98805-X, 1990.

10. http://www.engineersedge.com/finishing/epoxy_coatings.htm

11. Lee, H., Neville,K. ,"Handbook of epoxy resins", 1st, 1967.

12. http:/en.wikipedia.org/wiki/epoxy

13. May, C. A. "Epoxy Resins: Chemistry and Technology", 2nd, New York: Marcel Dekker Inc. pp. 794. ISBN 0824776909,1987.

14. Morena, J. J. Advanced Composite Mold Making, New York: Van Nostrand Reinhold Co. Inc. pp. 124–125. ISBN 0-442-26414-3, 1988.

15. McCreight, T., Bsullak, N, "Color on Metal: 50 Artists Share Insights and Techniques", Madison, WI: Guild. pp. 74. ISBN 1893164063.

16. Raychaudhury, R. "Fusion Bonded Epoxy".

17. AWWA C213-96, “Fusion-Bonded Epoxy Coating for the Interior and Exterior of Steel Water Pipeline”, AWWA, Denver, CO., 1996.

18. AWWA 210-97, “Liquid-Epoxy Coating Systems for the Interior and Exterior of Steel Water Pipelines”, AWWA, Denver, CO., 2000.

19. AWWA Manual M41, “Ductile Iron Pipe and Fittings”, AWWA,, Denver, CO., 1996.

20. NACE T-6A TPC 2 Publication, “Coatings and Linings for Immersion Service”, NACE International, Second edition, 1998.

21. http://en.wikipedia.org/wiki/Iron(III)_oxide

22. http://www.zinc.org/Documents/Communications/Publications/ZincGuide2004.pdf

23. http://www.zinc.org/Documents/Communications/Publications/Coatings-A4.pdf.

24. Guan, S.W. “100% Solids Polyurethane Coatings Technology for Corrosion Protection in Water and Wastewater Systems”, the 9th Middle East Corrosion Conference, Bahrain, February, 2001.

25. AWWA C222-99, "Polyurethane Coatings for the Interior and Exterior of Steel Pipelines and Fittings", AWWA, Denver, CO., 1999.

26. ISO 8179, “Ductile iron pipes -- External zinc coating -- Part 1: Metallic zinc with finishing layer”, 1995.

27. AWWA C209-00, “Cold-Applied Tape Coatings for the Exterior of Special Sections, Connections, and Fittings for Steel Water Pipelines”, AWWA, Denver, CO., 2000.

28. AWWA C216, “Heat-Shrinkable Cross-Linked Polyolefin Coatings for the Exterior of Special Sections, Connections, and Fittings for Steel Water Pipelines”, AWWA, Denver, CO., 2000.

29. "Development of an Improved Protection System for CCP Construction (Fiberglass Resin Coating as an Alternative Form of Coating)", Final Report, RI Project CER2264, January, 2007 G.

30. Schutze, M., Malessa , M. "Standardization of Thermal Cycling Exposure Testing ", European Federation of Corrosion, Publication Number 53, 2007.

31. Schweitzer, P.A. "Fundamental of Metallic Corrosion ", Atmospheric and Media Corrosion of Metals, Corrosion Engineering Handbook, 2nd edition 2007.

32. Johnson, W.S. "Adhesively Bonded Joints Testing", Analysis and Design, 1988.

33. Al-Kurdi,S.M.A." Durability Assessment Criterion for Concrete and Reinforcement Exposed to Simulated Environmental Conditions of Saudi Arabia", MS thesis, August, 1984.

34. AMERON, "FCPP-Fiberglass-Coated Concrete Pressure Pipes", Product Guide, Amiantit Pipe Systems.

35. Ha-Won Song, Velu Saraswathy," Corrosion Monitoring Of Reinforced Concrete Structures-A Review", Int. J. Electrochem.Sci.,Vol.2, (2007).

36. J.P.Broomfield, Techniques To Assess The Corrosion Activity Of Steel Reinforced Concrete Structures. In: N. S. Berke, E. Escalante, C. K. Nmai And D. Whiting Editor, ASTM STP 1276 (1996), P.91-106.

37. K. R. Gowers, S. G. Milard, J. S. Gill And R. P. Gill. Brit Corr J 29 (1994) 25.

38. K. R. Gowers, S. G. Milard, J. S. Gill. NACE, Corrosion 92, Paper 205.

39. K. C. Clear. Transport Res Record 1211 (1989) 28.

40. M. Stern And A. L. Geary. J. Electrochem Soc 104 (1957) 56.

41. Escalante, E., Ito, S., and Cohen, M., "Measuring the Rate of Corrosion of Steel in Concrete", Annual Report NBSIR 80-2012, National Bureau of Standards, Gaithersburg, Md., March 1980, pp. 1-26.

42. Escalante, E., Whitenton, E., and Qui, F., "Measuring the Rate of Corrosion of Reinforcing Steel in Concrete", Final Report NBSIR 86-3456, National Bureau of Standards, Gaithersburg, Md., Oct. 1986, pp. 1-27.

43. Al-Gohi, Basheer Hsan Ali," Time-Dependent Modeling of Loss of Flexural Strength of Corroding RC Beams", MS Thesis, May 2008.

44. Stern, M., and Geary, A. L., "Electrochemical polarization, theoretical analysis of the shape of polarization curves", Journal of Electrochemical Society, Vol. 104, No. 1, 1957, pp. 56-63.

45. Andrade, C., and Alonso, C., "On-Site Measurements of Corrosion Rate of Reinforcements", Construction and Building Materials, March, 2001, pp. 171-183.

46. http://en.wikipedia.org/wiki/Chromatography.

47. K.D. Stanish, R. D. Hooton And M. D. A. Thomas, Department Of Civil Engineering, University Of Toronto, Toronto, Ontario, Canada." Prediction of Chloride Penetration In Concrete". FHWA Contract DTFH61-97-R-00022.

48. Crank, J., The Mathematics of Diffusion, 2nd ed., Oxford University Press, (1975).

49. Luca Bertolini, Bernhard Elsener, Pietro Pedeferri, Rob Polder. “Corrosion of Steel In Concrete”. Prevention, Diagnosis, Repair. November 2003.

50. Millard, S.G. Corrosion Rate Measurement of in-situ Reinforced Concrete Structures. Proc. ICE, Structs. & Bldgs, 99, Feb. 1993, 84-88.

APPENDICES

APPENDIX A

NATURAL CORROSION PROCESS TEST DATA

TABLE A.1 I_{corr} Measurements

Specimen #	t = 10 Days		t = 15 Days	
	Current Density i_{corr} (μA/cm2)	Average i_{corr} (μA/cm2)	Current Density i_{corr} (μA/cm2)	Average i_{corr} (μA/cm2)
NCBS1	3.15	3.68	2.43	3.33
NCBS2	4.21		4.23	
NCEP1	0.13	0.12	0.19	0.17
NCEP2	0.11		0.15	
NCRP1	1.51	1.35	4.70	4.28
NCRP2	1.20		3.86	
NCZP1	0.77	1.26	2.13	2.16
NCZP2	1.75		2.19	

TABLE A.1 I_{corr} Measurements (cont')

Specimen #	t = 20 Days		t = 25 Days	
	Current Density i_{corr} (μA/cm2)	Average i_{corr} (μA/cm2)	Current Density i_{corr} (μA/cm2)	Average i_{corr} (μA/cm2)
NCBS1	1.34	*1.68*	*3.99*	*4.31*
NCBS2	2.02		*4.62*	
NCEP1	0.18	*0.16*	*0.23*	*0.21*
NCEP2	0.14		*0.18*	
NCRP1	1.55	*1.68*	*4.05*	*4.85*
NCRP2	1.80		*5.65*	
NCZP1	0.93	*1.14*	*1.91*	*2.26*
NCZP2	1.34		*2.61*	

Specimen #	t = 30 Days		t = 35 Days	
	Current Density i_{corr} (μA/cm2)	Average i_{corr} (μA/cm2)	Current Density i_{corr} (μA/cm2)	Average i_{corr} (μA/cm2)
NCBS1	3.30	3.38	3.34	3.18
NCBS2	3.46		3.02	
NCEP1	0.22	0.25	0.25	0.27
NCEP2	0.27		0.29	
NCRP1	2.13	2.29	1.50	1.90
NCRP2	2.46		2.30	
NCZP1	1.36	1.78	0.59	0.86
NCZP2	2.20		1.14	

APPENDIX B

HIGH CHLORIDE EXPOSURE TEST DATA

TABLE B.1 Chloride Content Cl% of Mortar Mass

Ponding Specimen #	Extracted Sample	Description (Distance From The Exposed Face)	24-Dec-2009 t=5184000 sec	7-Jan-2010 t= 6393600 sec	21-Jan-2010 t= 7603200 sec
PBS1	PBS1S	X1=0.5 cm	0.148	1.191	1.142
	PBS1C	X2=1.0 cm	0.116	0.986	0.943
PBS2	PBS2S	0.5 cm	0.147	0.968	1.364
	PBS2C	1.0 cm	0.06	0.756	1.196
PEP1	PEP1S	0.5 cm	0.118	0.78	0.958
	PEP1C	1.0 cm	0.083	0.447	0.697
PEP2	PEP2S	0.5 cm	0.118	0.942	1.017
	PEP2C	1.0 cm	0.104	0.742	0.816
PRP1	PRP1S	0.5 cm	0.126	0.737	1.231
	PRP1C	1.0 cm	0.093	0.576	1.052
PRP2	PRP2S	0.5 cm	0.138	1.029	1.233
	PRP2C	1.0 cm	0.125	0.954	1.212
PZP1	PZP1S	0.5 cm	0.261	1.113	1.291
	PZP1C	1.0 cm	0.168	0.728	0.763
PZP2	PZP2S	0.5 cm	0.33	0.958	1.223
	PZP2C	1.0 cm	0.115	0.891	1.11

TABLE B.1 Chloride Content Cl% of Mortar Mass (cont')

Ponding Specimen #	Extracted Sample	Description (Distance From The Exposed Face)	24-Dec-2009 t=5184000 sec	7-Jan-2010 t= 6393600 sec	21-Jan-2010 t= 7603200 sec
PDBS1	PDBS1S	1.0 cm	0.06	0.16	1.243
	PDBS1C	1.5 cm	0.034	0.098	0.439
PDBS2	PDBS2S	1.0 cm	0.059	0.038	0.732
	PDBS2C	1.5 cm	0.027	0.032	0.643
PDEP1	PDEP1S	1.0 cm	0.183	0.508	0.781
	PDEP1C	1.5 cm	0.059	0.431	0.557
PDEP2	PDEP2S	1.0 cm	0.047	0.209	0.28
	PDEP2C	1.5 cm	0.035	0.144	0.211
PDRP1	PDRP1S	1.0 cm	0.047	0.041	0.177
	PDRP1C	1.5 cm	0.009	0.037	0.1
PDRP2	PDRP2S	1.0 cm	0.072	0.332	0.419
	PDRP2C	1.5 cm	0.041	0.091	0.21
PDZP1	PDZP1S	1.0 cm	0.039	0.283	1.023
	PDZP1C	1.5 cm	0.033	0.197	0.645
PDZP2	PDZP2S	1.0 cm	0.044	0.251	0.561
	PDZP2C	1.5 cm	0.032	0.087	0.332

TABLE B.2 Chloride Contents at t = 160 Days of Ponded Specimens

Test Specimens	Chloride Content as Percentage Weight of Mortar for the Time Interval t = 160Days		
	At Depth = 5mm	At Depth = 10mm	At Depth = 22 mm (Corresponding to Steel Strips Surfaces)
PBS	2.106	1.779	1.211
PEP	1.589	1.382	1.072
PRP	1.931	1.672	1.261
PZP	1.790	1.567	1.270

Test Specimens	At Depth = 10mm	At Depth = 15mm	At Depth = 18 mm (Corresponding to Steel Strips Surfaces)
PDBS	1.299	1.072	1.011
PDEP	0.624	0.501	0.468
PDRP	0.888	0.711	0.736
PDZP	1.120	0.906	0.812

TABLE B.3 I_{corr} Values of the Ponded Specimens

Specimen #	t = 90 days	t = 157 days	t = 160 days
PBS1	0.800	6.55	4.094
PBS2	1.487	7.413	5.313
PEP1	0.000219	0.026	0.00000557
PEP2	0.0709	0.278	0.2291
PRP1	0.0238	0.434	0.4273
PRP2	0.000374	0.515	0.4956
PZP1	0.2762	1.104	0.7463
PZP2	0.44	3.075	2.276
PDBS1	0.2693	1.69	0.8074
PDBS2	0.5976	2.11	1.294
PDEP1	0.00161	0.00176	0.00002678
PDEP2	0.001731	0.124	0.1024
PDRP1	0.00212	0.32	0.2599
PDRP2	0.00265	0.232	0.3148
PDZP1	0.2702	0.823	0.771
PDZP2	0.2519	0.712	0.588

APPENDIX C

ACCELERATED CORROSION TEST DATA AND PLOTS

TABLE C.1 Weight Loss of the Accelerated Corrosion Test Specimens

Specimen #	Weight loss %	Average Weight loss %	Remarks
NACBS1	5.28	6.93	4-Days Duration
NACBS2	8.59		4-Days Duration
NACBS3	10.07	9.41	8-Days Duration
NACBS4	8.75		8-Days Duration
NACEP1	3.48	3.52	8-Days Duration
NACEP4	3.56		8-Days Duration
NACEP2	2.63	1.81	4-Days Duration
NACEP3	0.99		4-Days Duration
NACRP1	4.48	3.70	8-Days Duration
NACRP4	2.92		8-Days Duration
NACRP2	2.37	2.49	4-Days Duration
NACRP3	2.61		4-Days Duration
NACZP1	4.91	5.50	4-Days Duration
NACZP2	6.08		4-Days Duration
NACZP3	12.72	11.62	8-Days Duration
NACZP4	10.53		8-Days Duration

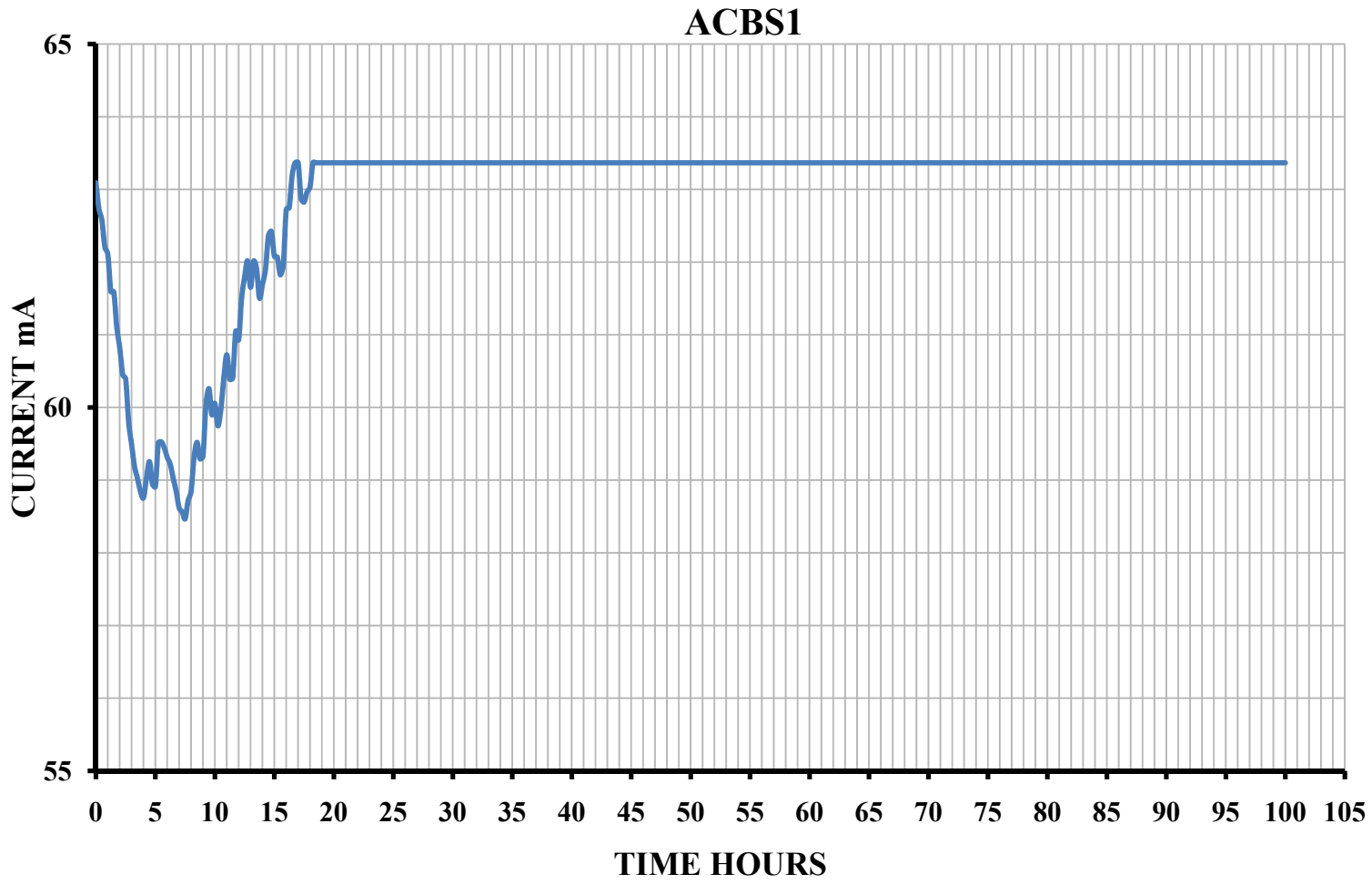

Figure C.1 Current versus Time Plot for Uncoated Specimen Subjected To Accelerated Corrosion for a *Duration of 4 Days*

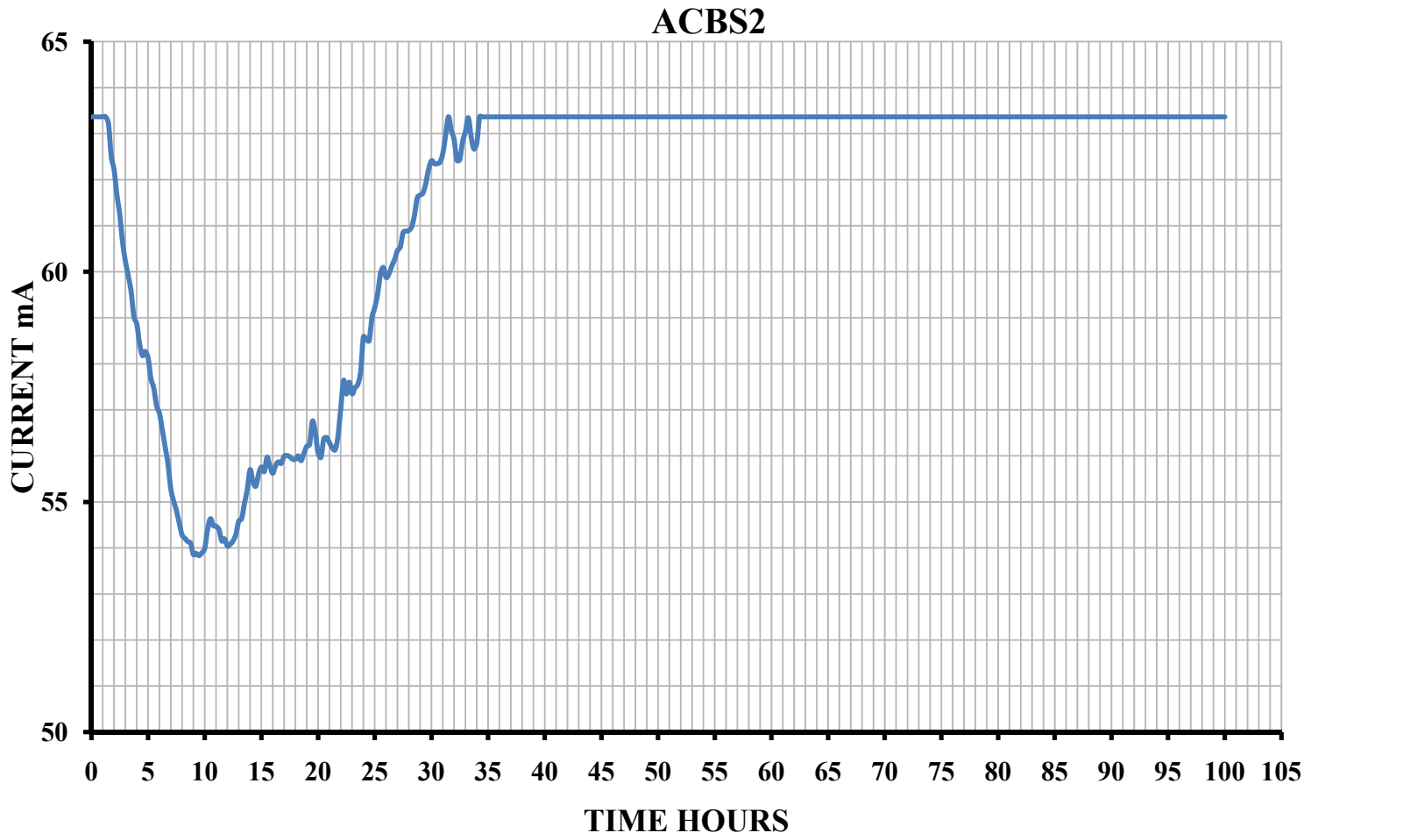

Figure C.2 Current versus Time Plot for Uncoated Specimen Subjected To Accelerated Corrosion for a *Duration of 4 Days*

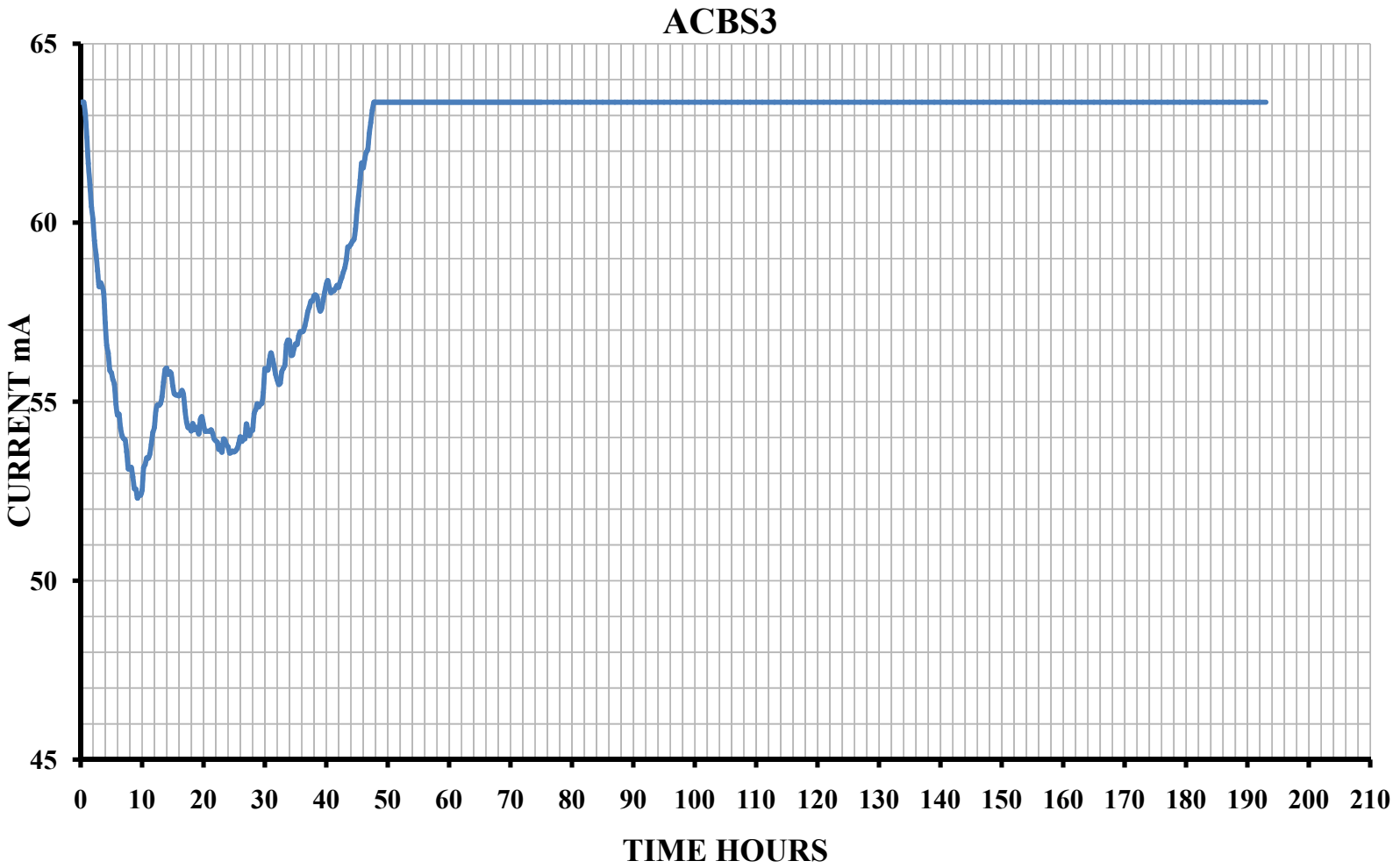

Figure C.3 Current versus Time Plot for Uncoated Specimen Subjected to Accelerated Corrosion for a *Duration of 8 Days*

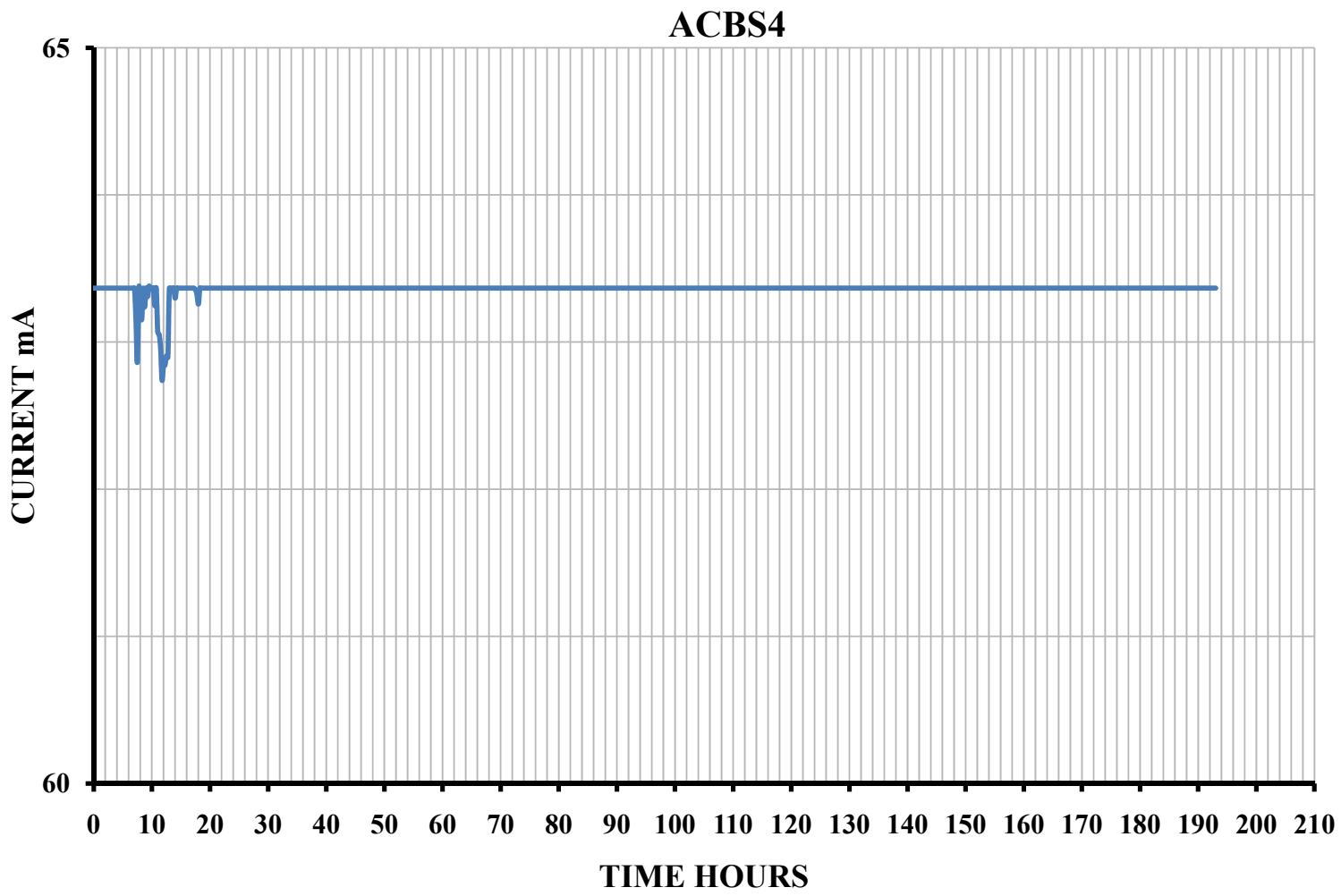

Figure C.4 Current versus Time Plot for Uncoated Specimen Subjected to Accelerated Corrosion for a *Duration of 8 Days*

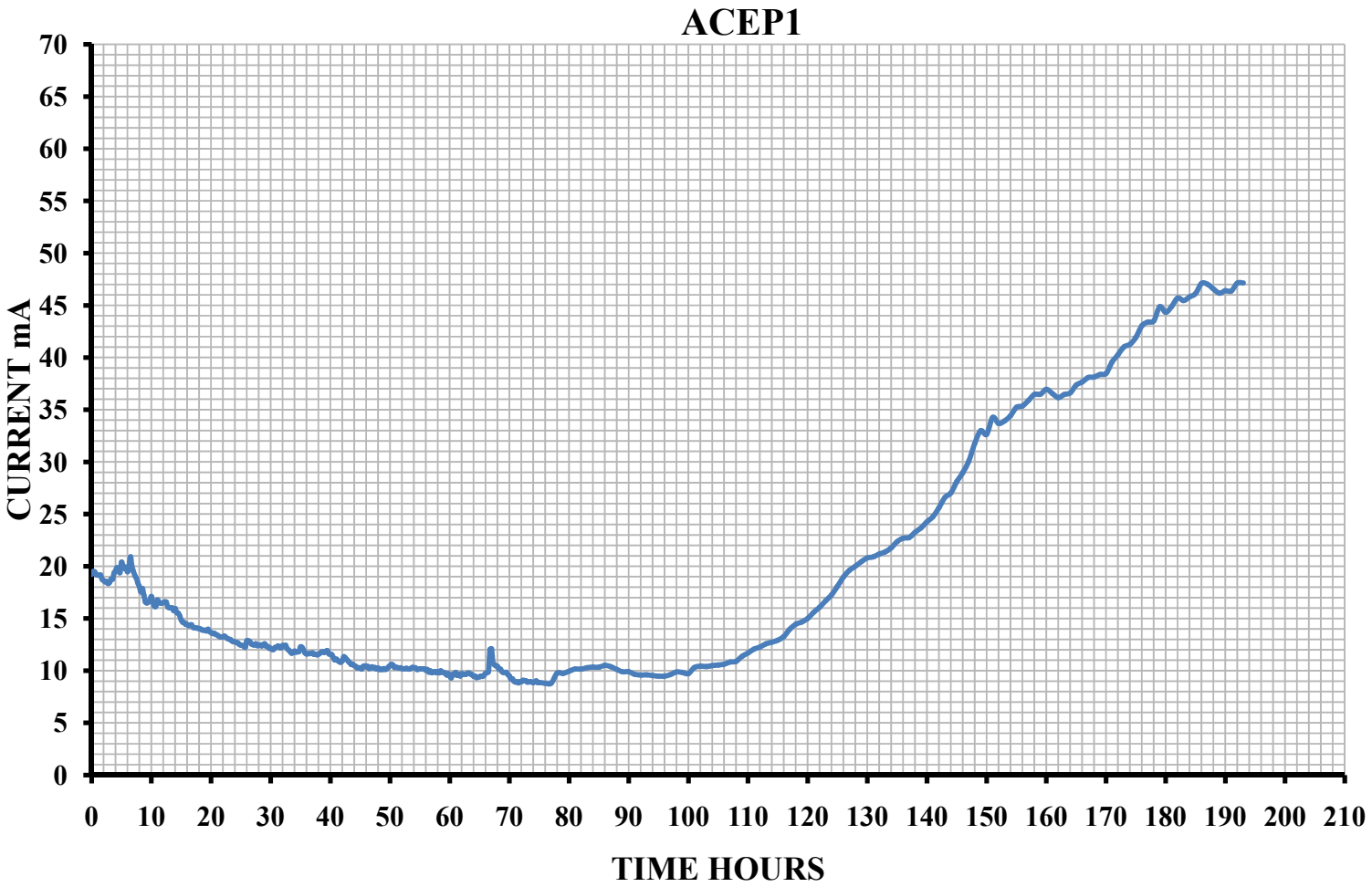

Figure C.5 Current versus Time Plot for Epoxy-Coated Specimen Subjected to Accelerated Corrosion for a *Duration of 8 Days*

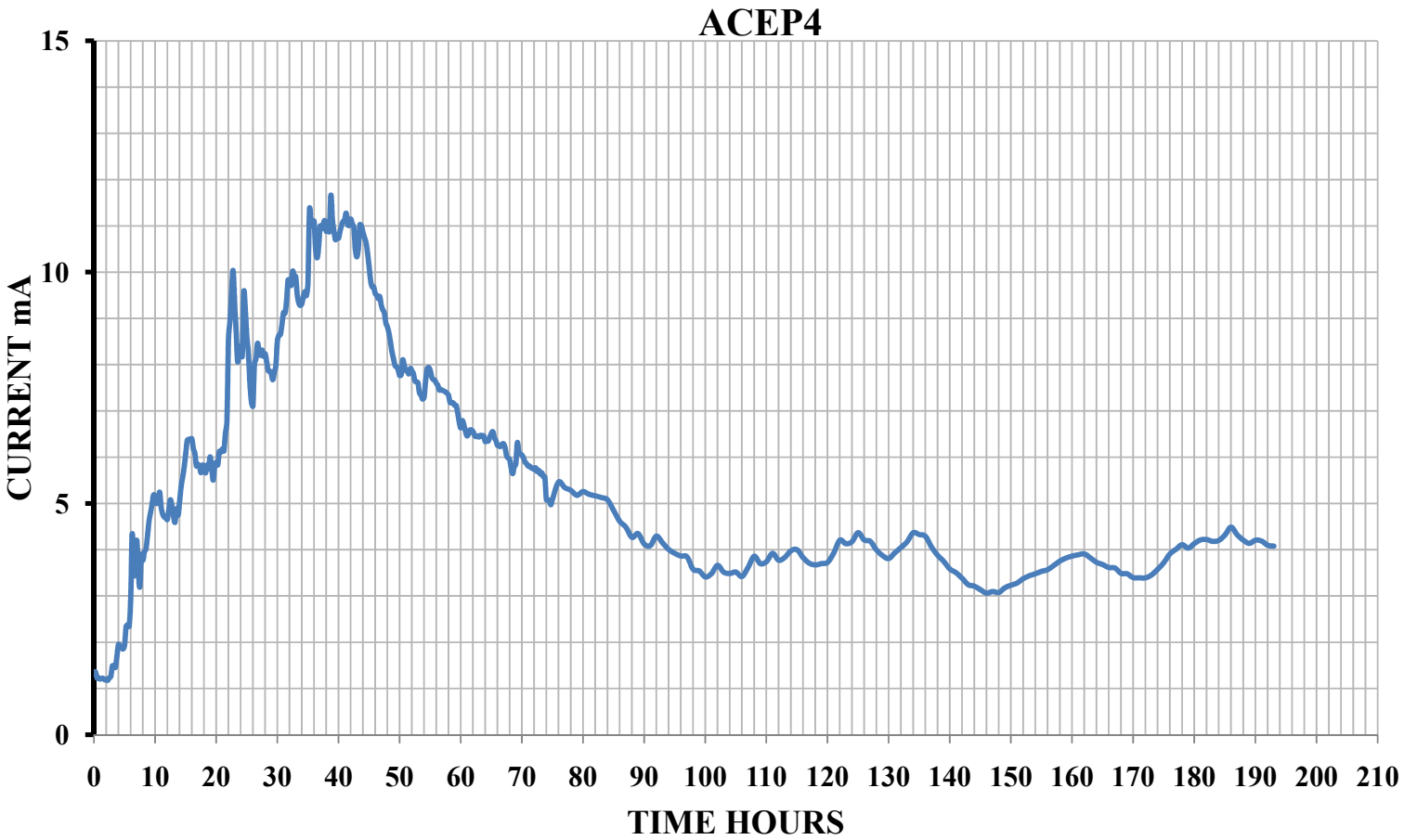

Figure C.6 Current versus Time Plot for Epoxy-Coated Specimen Subjected to Accelerated Corrosion for a *Duration of 8 Days*

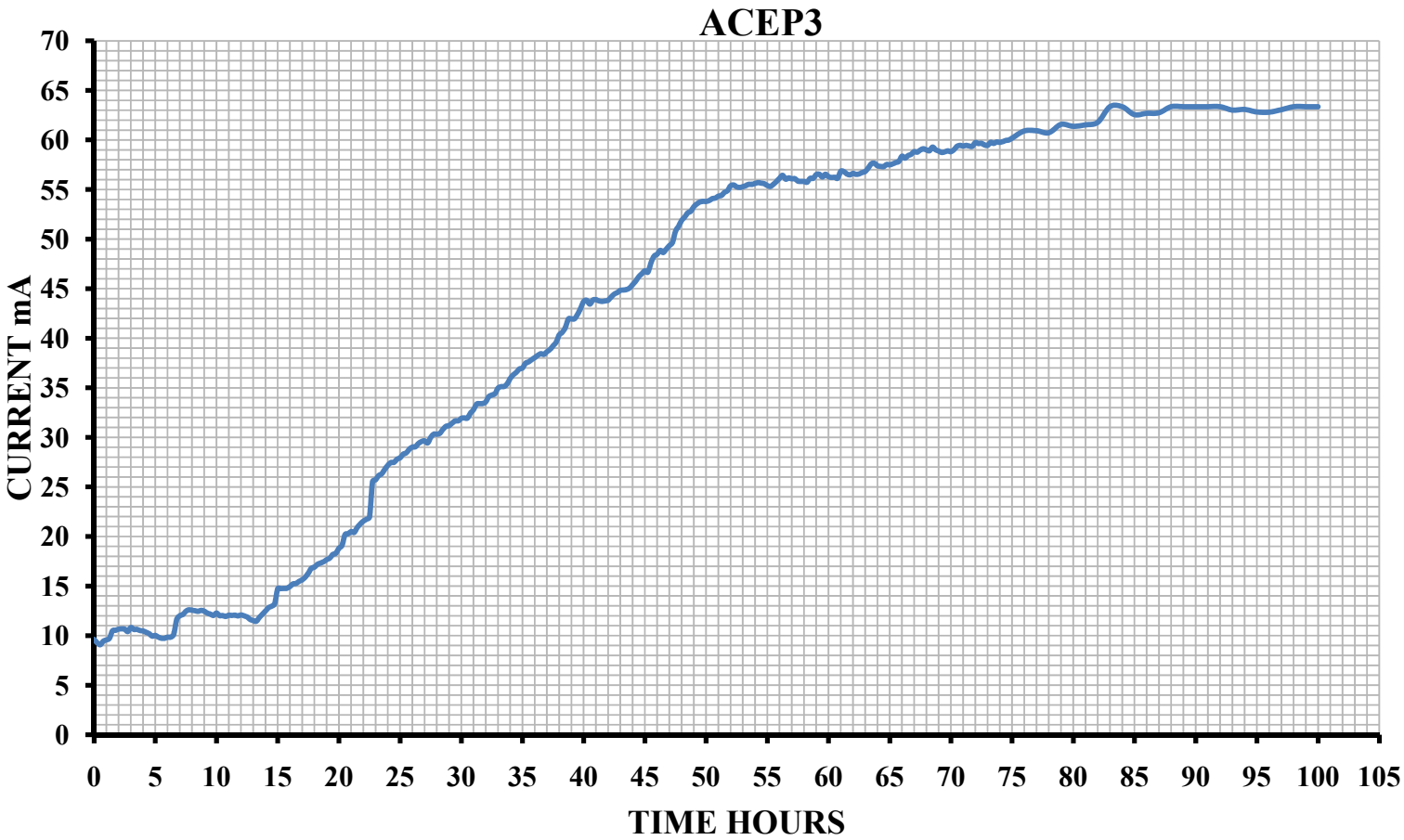

Figure C.7 Current versus Time Plot for Epoxy-Coated Specimen Subjected to Accelerated Corrosion for a *Duration of 4 Days*

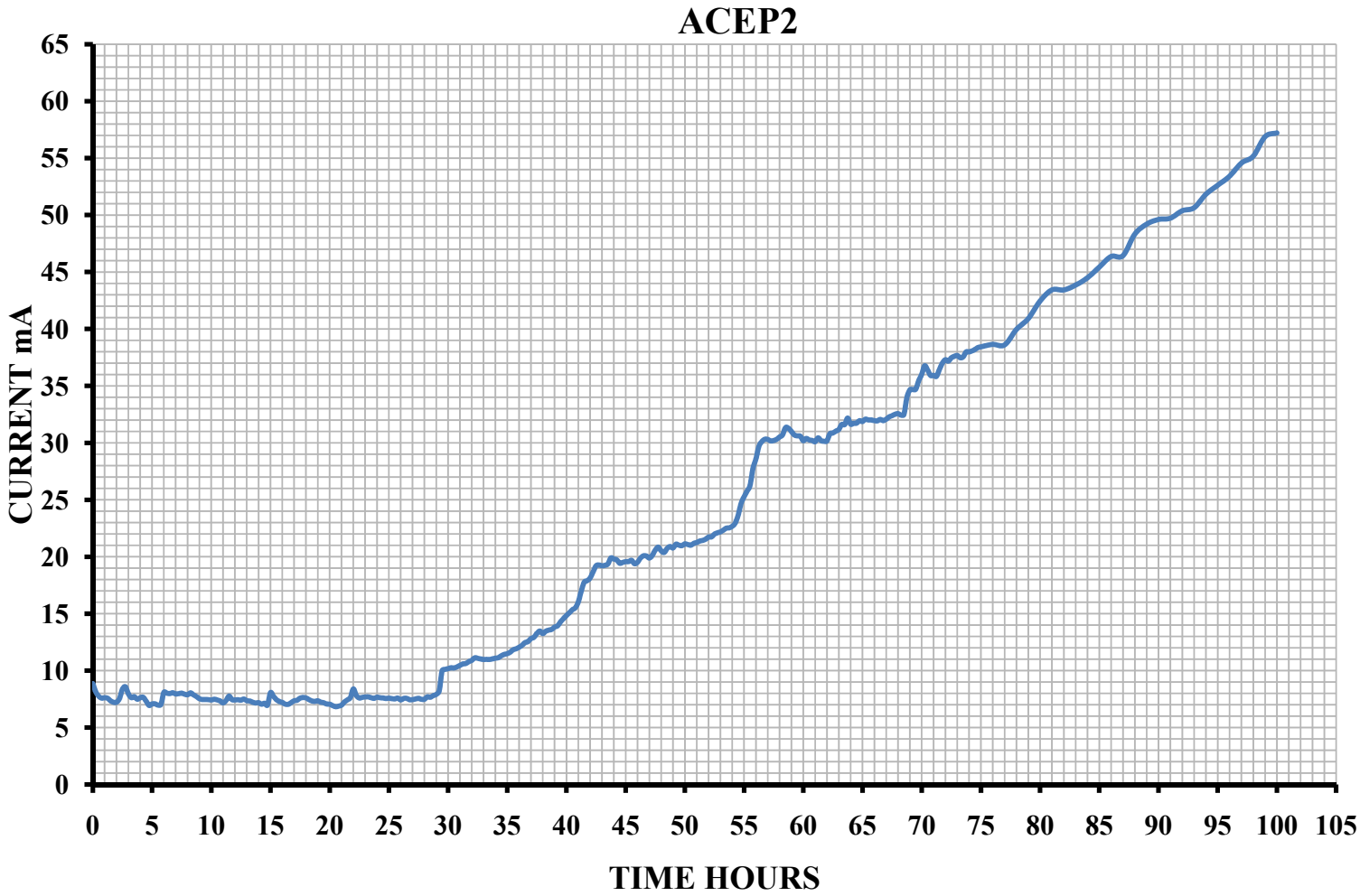

Figure C.8 Current versus Time Plot for Epoxy-Coated Specimen Subjected to Accelerated Corrosion for a *Duration of 4 Days*

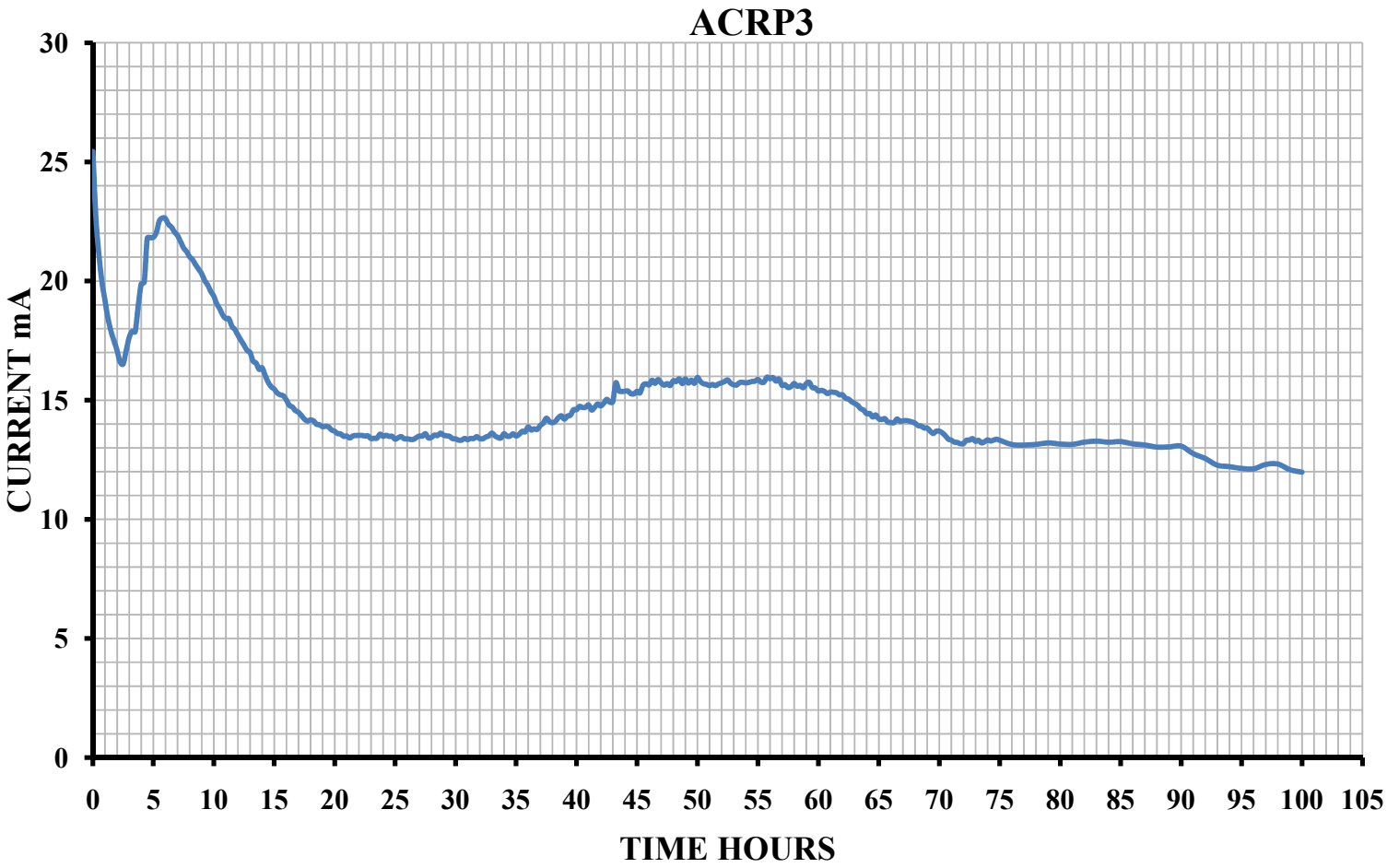

Figure C.9 Current versus Time Plot for Red Oxide-Coated Specimen Subjected to Accelerated Corrosion for a *Duration of 4 Days*

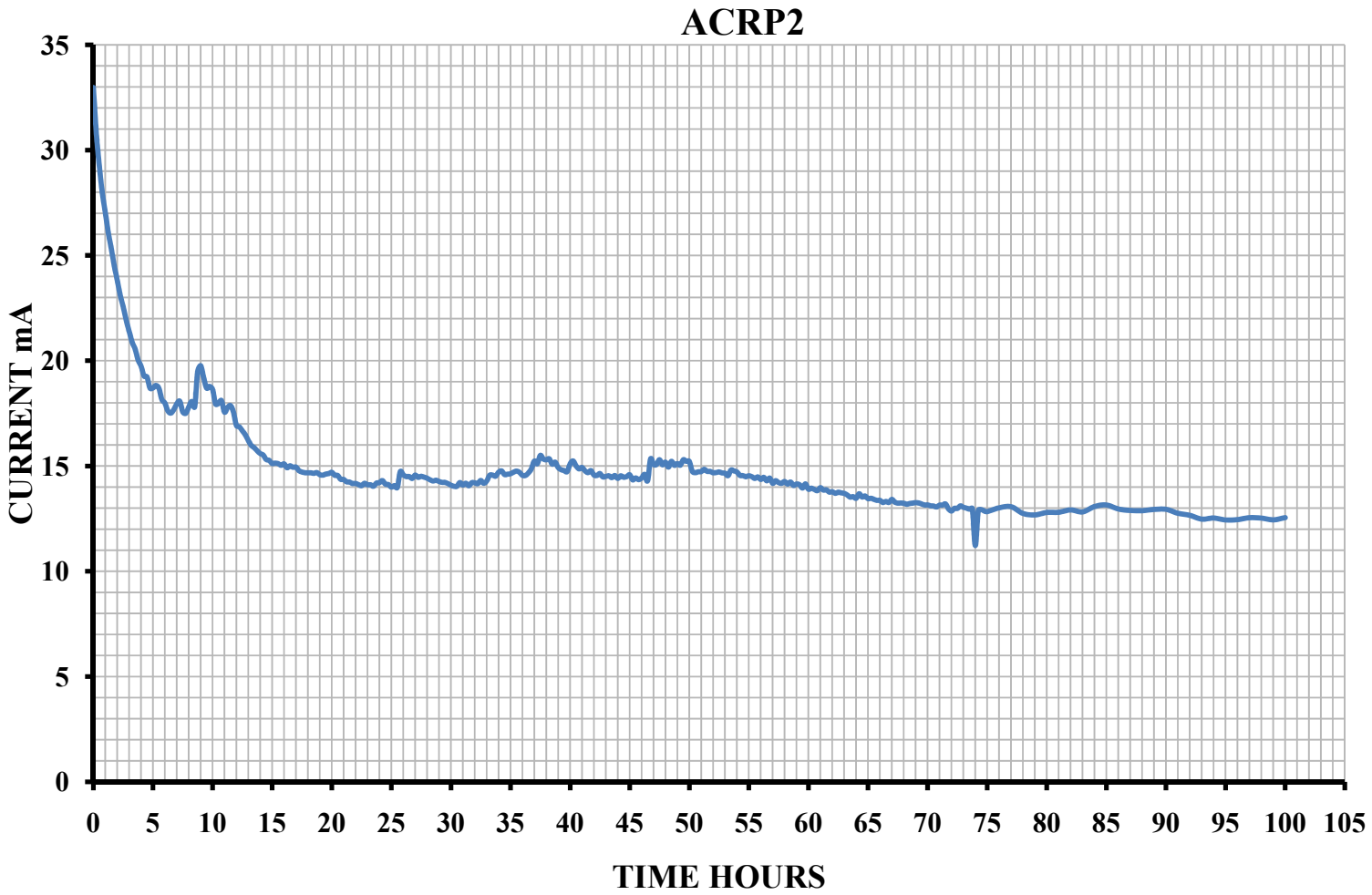

Figure C.10 Current versus Time Plot for Red Oxide-Coated Specimen Subjected to Accelerated Corrosion for a *Duration of 4 Days*

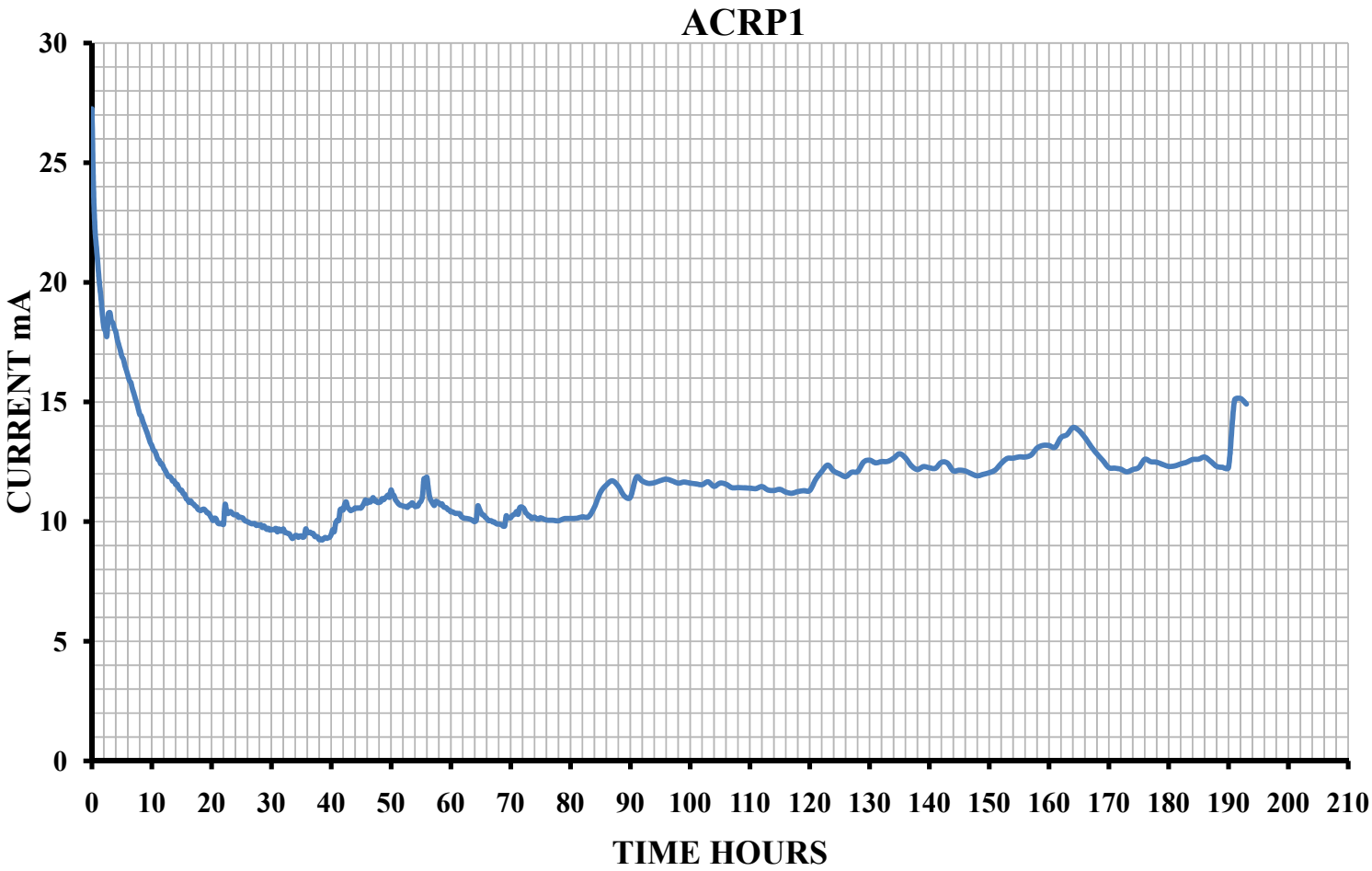

Figure C.11 Current versus Time Plot for Red Oxide-Coated Specimen Subjected to Accelerated Corrosion for a *Duration of 8 Days*

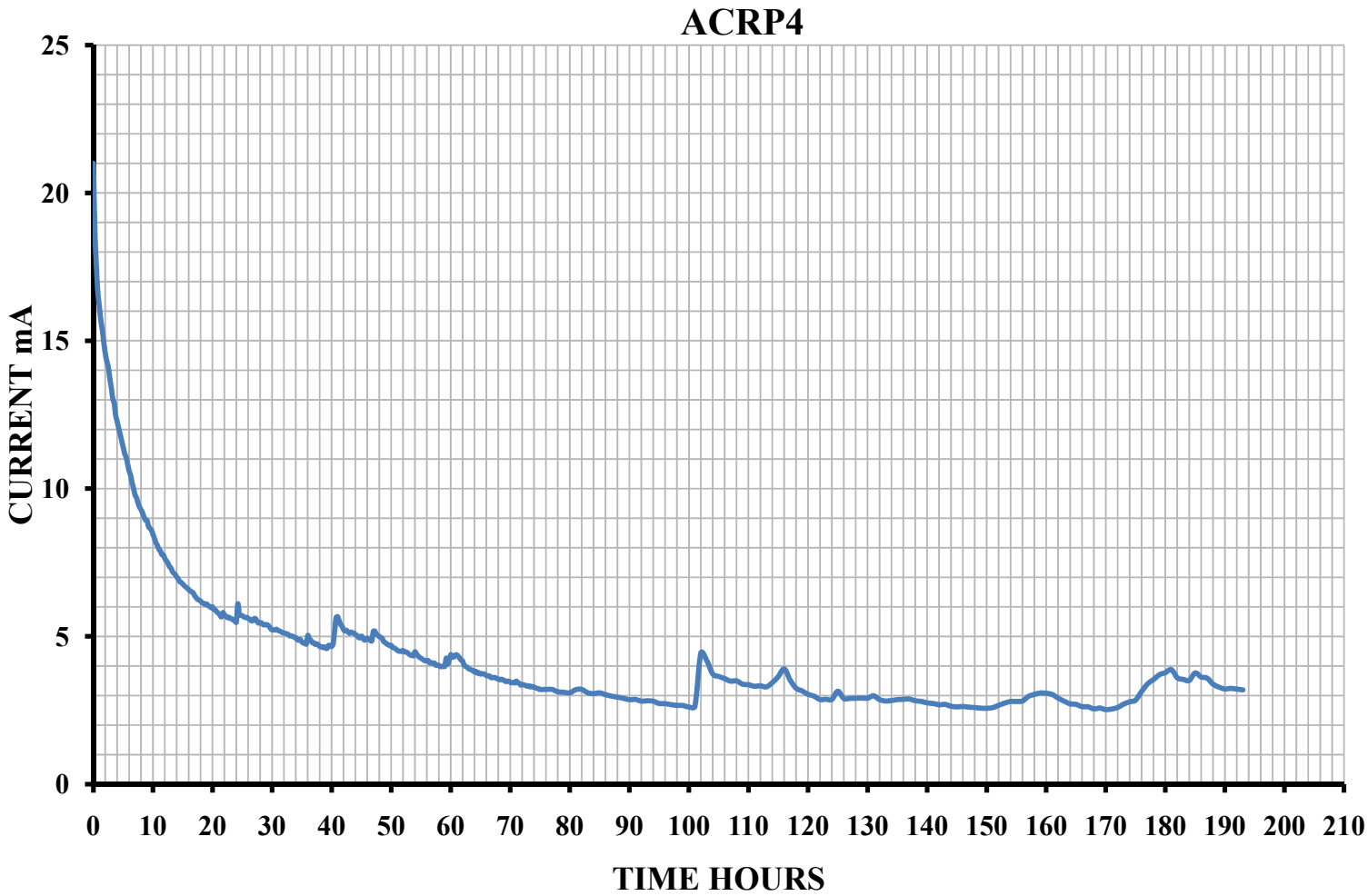

Figure C.12 Current versus Time Plot for Red Oxide-Coated Specimen Subjected to Accelerated Corrosion for a *Duration of 8 D*

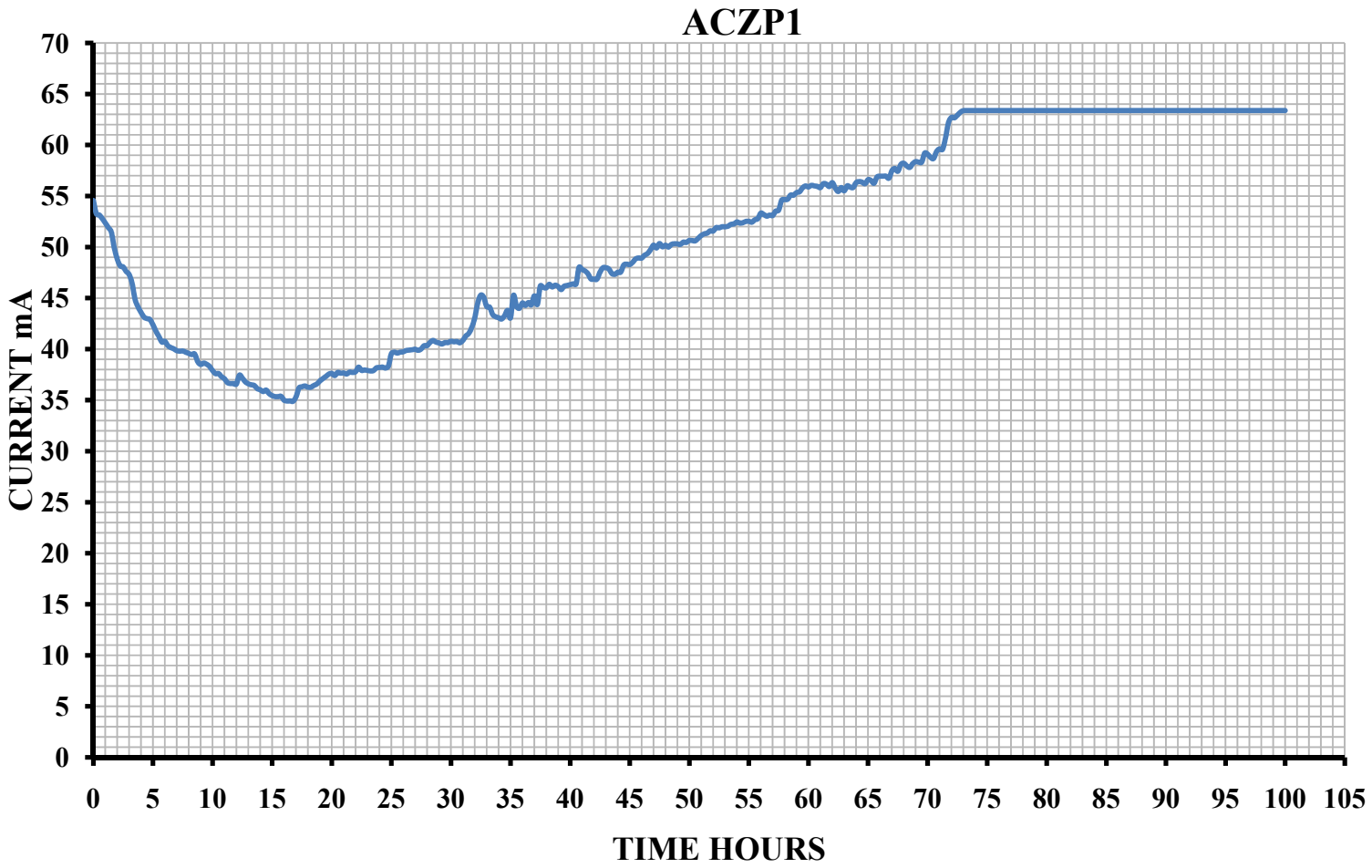

Figure C.13 Current versus Time Plot for Zinc Primer-Coated Specimen Subjected to Accelerated Corrosion for a *Duration of 4 Days*

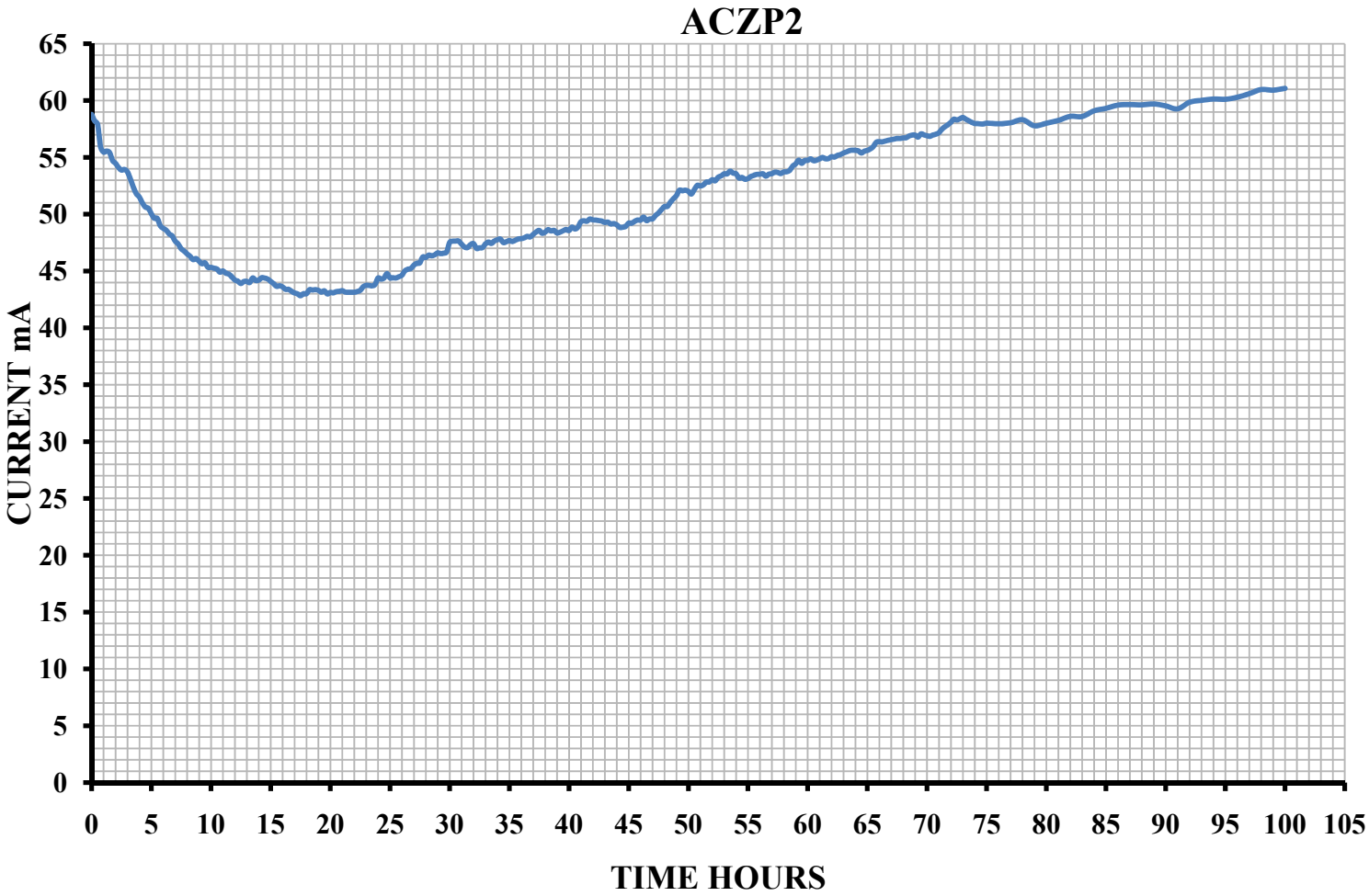

Figure C.14 Current versus Time Plot for Zinc Primer-Coated Specimen Subjected to Accelerated Corrosion for a *Duration of 4 Days*

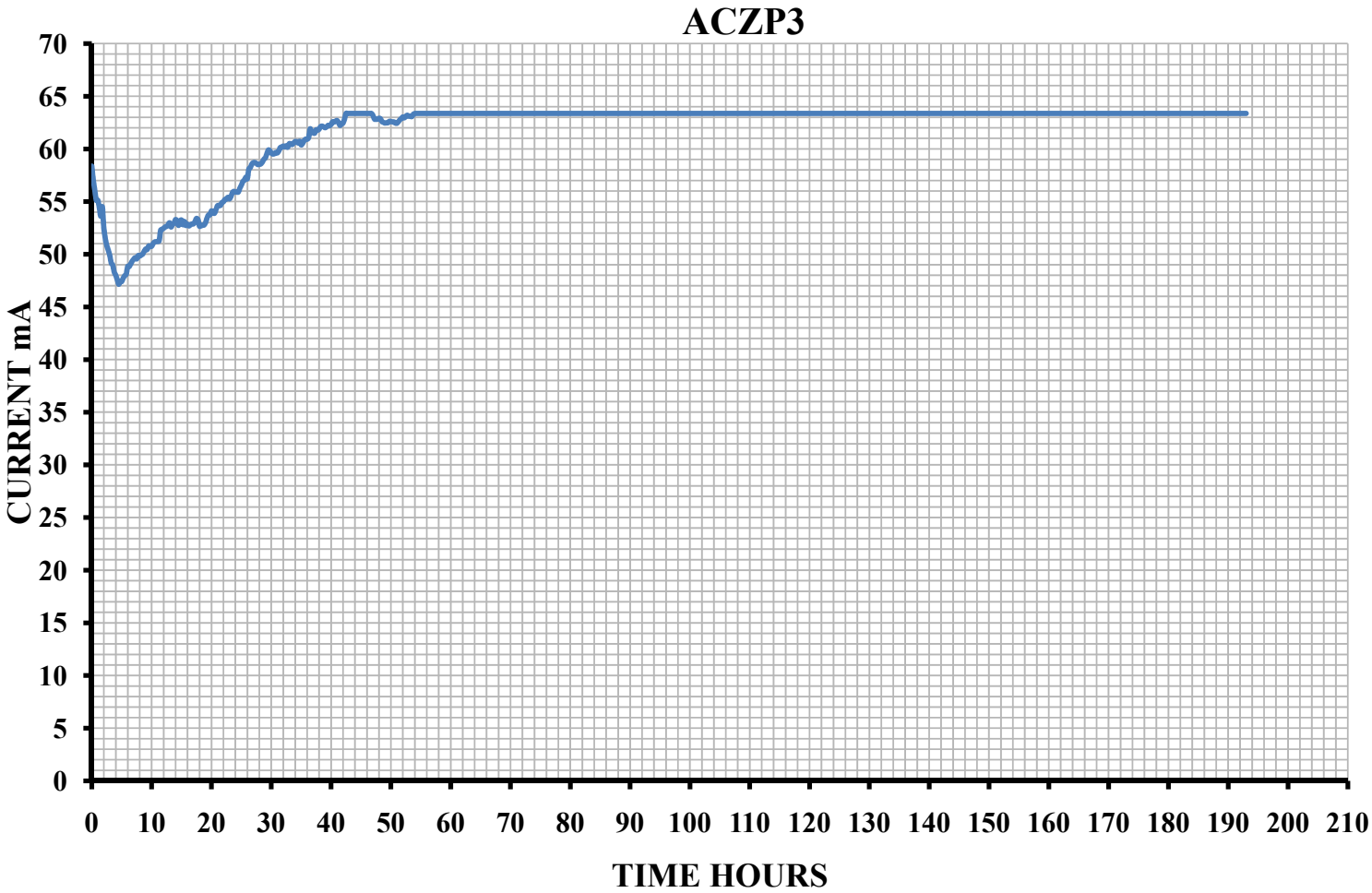

Figure C.15 Current versus Time Plot for Zinc Primer-Coated Specimen Subjected to Accelerated Corrosion for a *Duration of 8 Days*

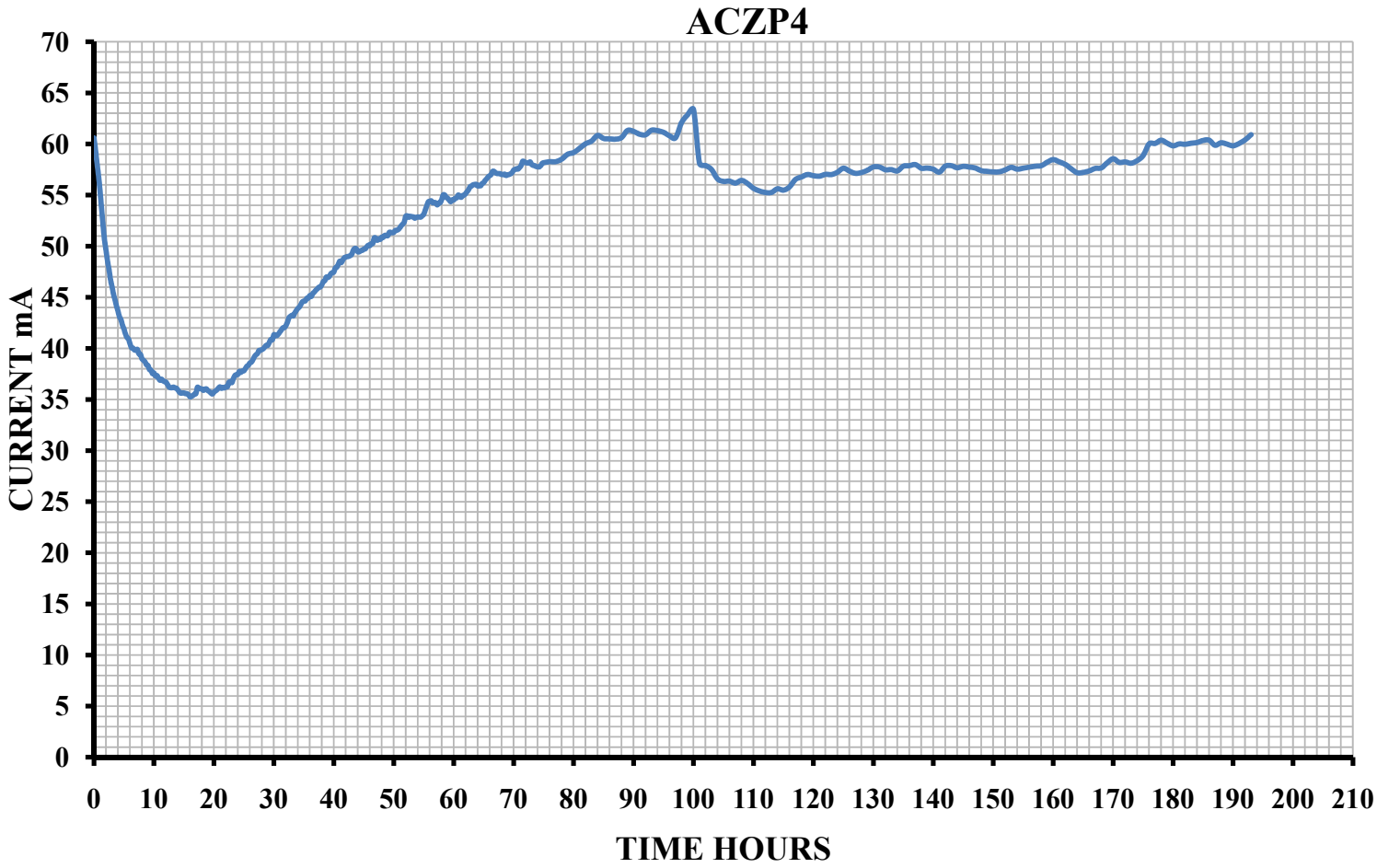

Figure C.15 Current versus Time Plot for Zinc Primer-Coated Specimen Subjected to Accelerated Corrosion for a *Duration of 8 Days*

APPENDIX D

ELECTRICAL RESISTANCE TEST DATA

TABLE D.1 Electrical Resistances From The Accelerated Corrosion Test

Specimens #	Type of Coating	$I_{initial}$ (mA)	Resistance (Ω)	Average Resistance (Ω)
ACBS1	BARE STEEL	62.70	63.80	63.29
ACBS2		63.40	63.09	
ACBS3		63.30	63.19	
ACBS4		63.40	63.09	
ACEP1	EPOXY PAINT	19.50	205.13	996.10
ACEP2		8.13	492.00	
ACEP3		9.30	430.11	
ACEP4		1.40	2857.14	
ACRP1	RED OXIDE	24.10	165.98	171.49
ACRP2		30.80	129.87	
ACRP3		22.70	176.21	
ACRP4		18.70	213.90	
ACZP1	ZINC PRIMER	53.30	75.05	70.32
ACZP2		58.20	68.73	
ACZP3		57.00	70.18	
ACZP4		59.40	67.34	

TABLE D.2 Electrical Resistances of the Electrical Resitance Test Specimens Using LPR Technique

Length Immersed = 9.3 cm with Surface Area = 52cm^2

Specimen #	Type of Coating	Dimensions	Linear polarization Resistance LPR (Ω.cm2) Area=52 cm^2	Rest Potential Rp (mv)	Resistance (Ω)	Average Resistance (Ω)
BS1	BARE STEEL	175*20*8 mm	88	-503	1.69	1.50
BS2			97	-577	1.87	
BS3			49	-453	0.94	
EP1	EPOXY PAINT	175*20*8 mm	105090	-485	2020.96	958.25
EP2			23352	-404	449.08	
EP3			21045	-380	404.71	
RP1	RED OXIDE	175*20*8 mm	15128	-486	290.92	708.87
RP2			79196	-513	1523.00	
RP3			16260	-475	312.69	
ZP1	ZINC PRIMER	175*20*8 mm	147	-1068	2.83	2.51
ZP2			113	-1053	2.17	
ZP3			132	-1063	2.54	

VITA

Name : Mohammed Mohammed Hussein Al-Tholaia

Nationality : Yemeni.

Date of Birth : 4th March 1979

Education :

- Graduated from high school in 1996 with grade of 92.63%, scientific section, Thamar, Yemen.
- Received a scholarship from the Ministry of Higher Education to study B.Sc. at Ain Shams University, Egypt, in 1997.
- Graduated from Ain Shams University with B.Sc. degree in the civil engineering, structural section in 2002 with accumulative grade of very good.
- Received a scholarship from the Ministry of Higher Education and Thamar University to study MS degree at KFUPM in 2007.
- Received a ward as one of the top ten graduate students in MS program at KFUPM on June 1, 2010, for achieving high GPA (3.94/4).

Work and Experience:

In 2003, appointed as a graduate assistant at Thamar University, college of engineering and I am still working there as a faculty member.

During the period from 2002 right 2007, I worked as a supervisor and engineer designer for a lot of reinforced concrete projects in both the national and private sectors in Yemen.

Present Address: KFUPM, Dhahran, Saudi Arabia, T.L: 0530059084
Permanent Address: Thamar, Yemen.
E-mail : al_tholaia1978@yahoo.com
T.L : 00967-6-517566.